

**AUGUST 2015**

**M.Sc. in Mechanical Engineering**

**ÖZKAN ÖZBEK**

**UNIVERSITY OF GAZİANTEP  
GRADUATE SCHOOL OF  
NATURAL & APPLIED SCIENCES**

**BENDING ANALYSIS OF COMPOSITE PLATES  
USING MESHFREE METHODS**

**M.Sc. THESIS  
IN  
MECHANICAL ENGINEERING**

**BY  
ÖZKAN ÖZBEK  
AUGUST 2015**

**Bending Analysis of Composite Plates  
Using Meshfree Methods**

**M.Sc. Thesis**

**in**

**Mechanical Engineering  
University of Gaziantep**

**Supervisor**

**Assist. Prof. Dr. Ömer Yavuz BOZKURT**

**By**

**Özkan ÖZBEK**

**August 2015**

© 2015 [Özkan ÖZBEK]


REPUBLIC OF TURKEY  
UNIVERSITY OF GAZİANTEP  
GRADUATE SCHOOL OF NATURAL & APPLIED SCIENCES  
MECHANICAL ENGINEERING

Name of the thesis: Bending Analysis of Composite Plates Using Meshfree Methods


Name of student : Özkan ÖZBEK

Exam Date : 20.08.2015


Approval of the Graduate School of Natural and Applied Sciences

  
Prof. Dr. Motin BEDİR  
Director

I certify that this thesis satisfies all the requirements as a thesis for the degree of Master of Science.

  
Prof. Dr. M. Sait SOYLEMEZ  
Head of Department

This is to certify that we have read this thesis and that in our opinion it is fully adequate, in scope and quality, as a thesis for the degree of Master of Science.

  
Assist. Prof. Dr. Ömer Yavuz BOZKURT  
Supervisor




Examining Committee Members

Assist. Prof. Dr. Ömer Yavuz BOZKURT

Assist. Prof. Dr. İbrahim GÖV

Assist. Prof. Dr. Eyüp YETER

Signature

  
.....  
  
.....  
  
.....

**I hereby declare that all information in this document has been obtained and presented in accordance with academic rules and ethical conduct. I also declare that, as required by these rules and conduct, I have cited and referenced all material and results that are not original to this work.**

**Özkan ÖZBEK**

## **ABSTRACT**

# **BENDING ANALYSIS OF COMPOSITE PLATES USING MESHFREE METHODS**

ÖZBEK, Özkan

M.Sc. in Mechanical Eng.

Supervisor: Assist. Prof. Dr. Ömer Yavuz BOZKURT

August 2015, 109 pages

In this study, bending problems of isotropic and layered orthotropic plates are presented using Element-Free Galerkin Method (EFGM). In the first section; the effects of selectable parameters of EFGM such as type of weight function, support domain size, number of Gauss integration point in a background cell, number of monomials and value of penalty coefficient are investigated on the solution accuracy of EFGM solutions and optimum values of them are determined for related examples of isotropic plates. In the second section; the reliability of EFGM solutions are examined by considering various number of layers, fiber orientation and thickness to span ratio for layered orthotropic plate bending problems.

EFGM algorithms have been developed on MATLAB programming environment for both sections. Examples are solved by using developed algorithms and obtained results are compared with analytical results or reference study results in the literature.

**Keywords:** Meshfree methods, Element-free Galerkin method, isotropic and layered orthotropic plate bending

## ÖZET

### AĞSIZ YÖNTEMLER İLE KOMPOZİT PLAKALARIN EĞİLME ANALİZİ

ÖZBEK, Özkan

Yüksek Lisans Tezi, Mak Müh. Bölümü

Tez Yöneticisi: Yrd. Doç. Dr. Ömer Yavuz BOZKURT

Ağustos 2015, 109 sayfa

Bu çalışmada, izotropik ve tabakalı ortotropik plaka eğilme problemleri, Eleman Bağımsız Galerkin Yöntemi (EFGM) kullanılarak çözümlenmiştir. İlk kısımda izotropik plakalar için Eleman Bağımsız Galerkin Yönteminin sahip olduğu ağırlık fonksiyonu türü, destek etki büyüklüğü, arka plan hücrelerindeki entegrasyon nokta sayısı, monomiyallerin derecesi ve ceza katsayısı gibi seçilebilir parametrelerinin çözüm doğruluğuna etkisi araştırılmış ve ilgili problemlere göre parametrelerin optimum değerleri belirlenmiştir. İkinci kısımda ise tabakalı ortotropik plaka eğilme problemlerinde çeşitli tabaka sayısı, fiber yönelmesi ve kalınlık/uzunluk oranına göre EFGM çözümlerinin güvenilirliği incelenmiştir.

Her iki kısım için MATLAB programı üzerinde EFGM algoritmaları geliştirilmiştir. Problemler geliştirilen algoritmalara göre çözülmüş ve elde edilen sonuçlar literatürdeki analitik sonuçları veya analitik sonucu bulunmayan problemler için referans sonuçları ile karşılaştırılmıştır.

**Anahtar Kelimeler:** Ağsız yöntemler, Eleman Bağımsız Galerkin Yöntemi, izotropik ve ortotropik plaka bükme

*To my family...*



## **ACKNOWLEDGEMENTS**

I want to express my honest respect to my supervisor Assist. Prof. Dr. Ömer Yavuz BOZKURT for his guidance, suggestions and encouragement during master education and preparation of this thesis.

Also, I want to thank my friends for their reassurance and support. Finally, I would like to thank my fiance for the unwavering moral and emotional support.

## CONTENT

	<b>Page</b>
ABSTRACT .....	v
ÖZET.....	vi
ACKNOWLEDGEMENTS .....	viii
CONTENT .....	ix
LIST OF FIGURES .....	xi
LIST OF TABLES .....	xiv
CHAPTER 1 .....	1
INTRODUCTION .....	1
1.1. General Introduction .....	1
1.2. Research Objectives and Tasks .....	2
1.3. Layout of Thesis.....	2
CHAPTER 2 .....	4
LITERATURE SURVEY .....	4
2.1. Introduction .....	4
2.2. General Review of Some Mesh-free Methods .....	4
2.2.1. Smoothed Particle Hydrodynamics Method .....	4
2.2.2. Diffuse Element Method .....	5
2.2.3. Point Interpolation Method .....	5
2.2.4. Meshless Local-Petrov Galerkin .....	6
2.2.5. Reproducing Kernel Particle Method .....	6
2.3. Element-Free Galerkin Method.....	7
2.4. Element-Free Galerkin Method in the Solution of Plate Bending Problems.....	8
2.5. Element-Free Galerkin Method in the Solution of Composite Plate Problems.....	9
2.6. Conclusions on Literature Survey .....	9
CHAPTER 3 .....	10
PLATE THEORIES .....	10
3.1. Introduction .....	10
3.2. Review of The Plate Theories .....	11
3.2.1. Higher-Order Sher Deformation Theory.....	11

3.2.2. Kirchhoff Plate Theory .....	11
3.2.3. Reissner-Mindlin Plate Theory .....	13
CHAPTER 4 .....	17
ELEMENT FREE GALERKIN METHOD FOR MINDLIN-REISSNER PLATE BENDING PROBLEMS .....	17
4.1. Introduction .....	17
4.2. Short Description of Implementation Procedure for Galerkin Meshfree Methods.....	17
4.2.1. Basic Definitions for Meshfree Methods .....	18
4.2.1.1. Local Domains (Support and Influence Domains) .....	18
4.2.1.2. Background cells.....	19
4.3. First-Order Shear Deformation Theory (FSDT) for composite plates.....	19
4.4. Element-Free Galerkin Method.....	23
4.4.1. Moving-Least Square (MLS) Apprximation .....	23
4.4.2. Galerkin Weak Form and Enforcement Boundary Conditions .....	26
CHAPTER 5 .....	28
NUMERICAL RESULTS AND DISCUSSIONS FOR BENDING ANALYSIS OF NON-LAYERED ISOTROPIC PLATES .....	28
5.1. Introduction .....	28
5.2. Clamped square plate under transverse centric point load.....	28
5.3. Clamped square plate under uniform load. ....	39
5.4. Simply supported circular plate under uniform load.....	49
5.5. Simply supported Morley's skew plate under uniform load. ....	58
CHAPTER 6 .....	72
NUMERICAL RESULTS AND DISCUSSIONS FOR BENDING ANALYSIS OF LAMINATED COMPOSITE PLATES.....	72
6.1. Introduction .....	72
6.2. Clamped square plate angle-ply orientation.....	73
6.3. Clamped square plate cross-ply orientation .....	75
6.4. Simply supported square plate angle-ply orientation.....	79
6.5. Simply supported square plate cross-ply orientation .....	81
6.6. Simply supported square plate asymmetric angle-ply orientation .....	91
6.7. Clamped circular orthotropic plate.....	93
6.8. Simply supported skew plate cross-ply and angle-ply orientation.....	95
CHAPTER 7 .....	98
CONCLUSIONS.....	98
REFERENCES.....	100
PUBLICATIONS.....	109

## LIST OF FIGURES

	Page
Figure 3.1. Plate subjected to transverse lateral loads .....	10
Figure 3.2. Deformed geometries of an edge according to Kirchhoff theory in plate cross-section a) y-z plane b) x-z plane .....	11
Figure 3.3. Free body diagram of the plate element .....	13
Figure 3.4. A typical Reissner-Mindlin plate .....	14
Figure 3.5. Deformed geometries of an edge according to Reissner-Mindlin in plate theory in plate cross-section a) y-z plane b) x-z plane .....	14
Figure 4.1. Support Domain; the centre is a quadrature point .....	19
Figure 4.2. A typical laminate plate .....	21
Figure 5.1. Clamped square plate under transverse centric point load .....	29
Figure 5.2. The EFGM models for a) regular node distributions, b) irregular node distributions .....	29
Figure 5.3. Variations of normalized central deflections $w_c / \left( \frac{pL^4}{100D} \right)$ against $n_g$ for clamped square plate under transverse centric point load and regular node distribution with $\alpha_p = 6$ .....	32
Figure 5.4. Variations of normalized central deflections $w_c / \left( \frac{pL^4}{100D} \right)$ against $n_g$ for clamped square plate under transverse centric point load and irregular node distribution with $\alpha_p = 6$ .....	34
Figure 5.5. Variations of normalized central deflections $w_c / \left( \frac{pL^4}{100D} \right)$ against $\alpha_p$ for clamped square plate under transverse centric point load and regular node distribution with $n_g = 5$ .....	36

Figure 5.6. Variations of normalized central deflections $w_c/\left(\frac{pL^4}{100D}\right)$ against $\alpha_p$ for clamped square plate under transverse centric point load and irregular node distribution with $n_g = 5$ .....	38
Figure 5.7. Clamped square plate under uniform load.....	39
Figure 5.8. The EFGM models for a) regular node distributions, b) irregular node distributions.....	39
Figure 5.9. Simply supported circular plate under uniform load.....	49
Figure 5.10. The EFGM models for a) regular node distributions, b) irregular node distributions.....	49
Figure 5.11. Simply supported Morley's skew plate under uniform load .....	58
Figure 5.12. The EFGM models for a) regular node distributions, b) irregular node distributions.....	58
Figure 5.13. Variations of normalized central deflections $w_c/\left(\frac{pL^4}{100D}\right)$ against $n_g$ for simply supported skew plate subjected to uniform load and regular node distribution with $\alpha_p = 6$ .....	60
Figure 5.14. Variations of normalized central maximum moments $M_c/\left(\frac{pL^2}{10}\right)$ against $n_g$ for simply supported skew plate subjected to uniform load and regular node distribution with $\alpha_p = 6$ .....	61
Figure 5.15. Variations of normalized central minimum moments $M_c/\left(\frac{pL^2}{10}\right)$ against $n_g$ for simply supported skew plate subjected to uniform load and regular node distribution with $\alpha_p = 6$ .....	62
Figure 5.16. Variations of normalized central deflections $w_c/\left(\frac{pL^4}{100D}\right)$ against $n_g$ for simply supported skew plate subjected to uniform load and irregular node distribution with $\alpha_p = 6$ .....	63
Figure 5.17. Variations of normalized central maximum moments $M_c/\left(\frac{pL^2}{10}\right)$ against $n_g$ for simply supported skew plate subjected to uniform load and irregular node distribution with $\alpha_p = 6$ .....	64
Figure 5.18. Variations of normalized central minimum moments $M_c/\left(\frac{pL^2}{10}\right)$ against $n_g$ for simply supported skew plate subjected to uniform load and irregular node distribution with $\alpha_p = 6$ .....	65
Figure 5.19. Variations of normalized central deflections $w_c/\left(\frac{pL^4}{100D}\right)$ against $\alpha_p$ for simply supported skew plate subjected to uniform load and	

regular node distribution with $n_g = 5$ .....	66
Figure 5.20. Variations of normalized central maximum moments $M_c / \left(\frac{pL^2}{10}\right)$ against $\alpha_p$ for simply supported skew plate subjected to uniform load and regular node distribution with $n_g = 5$ .....	67
Figure 5.21. Variations of normalized central minimum moments $M_c / \left(\frac{pL^2}{10}\right)$ against $\alpha_p$ for simply supported skew plate subjected to uniform load and regular node distribution with $n_g = 5$ .....	68
Figure 5.22. Variations of normalized central deflections $w_c / \left(\frac{pL^4}{100D}\right)$ against $\alpha_p$ for simply supported skew plate subjected to uniform load and irregular node distribution with $n_g = 5$ .....	69
Figure 5.23. Variations of normalized central maximum moments $M_c / \left(\frac{pL^2}{10}\right)$ against $\alpha_p$ for simply supported skew plate subjected to uniform load and irregular node distribution with $n_g = 5$ .....	70
Figure 5.24. Variations of normalized central minimum moments $M_c / \left(\frac{pL^2}{10}\right)$ against $\alpha_p$ for simply supported skew plate subjected to uniform load and irregular node distribution with $n_g = 5$ .....	71

## LIST OF TABLES

	Page
Table 5.1. Normalized central deflections $w_c / \left( \frac{pL^4}{100D} \right)$ of clamped square plate under transverse centric point load for regular node distribution with $\alpha_p = 6$ .....	31
Table 5.2. Normalized central deflections $w_c / \left( \frac{pL^4}{100D} \right)$ of clamped square plate under transverse centric point load for irregular node distribution with $\alpha_p = 6$ .....	33
Table 5.3. Normalized central deflections $w_c / \left( \frac{pL^4}{100D} \right)$ of clamped square plate under transverse centric point load using regular node distribution with $n_g = 5$ .....	35
Table 5.4. Normalized central deflections $w_c / \left( \frac{pL^4}{100D} \right)$ of clamped square plate under transverse centric point load using irregular node distribution with $n_g = 5$ ...	37
Table 5.5. Normalized central deflections $w_c / \left( \frac{pL^4}{100D} \right)$ of clamped square plate subjected to uniform load for regular node distribution with $\alpha_p = 6$ .....	41
Table 5.6. Normalized central moments $M_c / \left( \frac{pL^2}{10} \right)$ of clamped square plate subjected to uniform load for regular node distribution using with $\alpha_p = 6$ .....	42
Table 5.7. Normalized central deflections $w_c / \left( \frac{pL^4}{100D} \right)$ of clamped square plate subjected to uniform load for irregular node distribution with $\alpha_p = 6$ .....	43
Table 5.8. Normalized central moments $M_c / \left( \frac{pL^2}{10} \right)$ of clamped square plate subjected to uniform load for irregular node distribution with $\alpha_p = 6$ .....	44
Table 5.9. Normalized central deflections $w_c / \left( \frac{pL^4}{100D} \right)$ of clamped square plate subjected to uniform load using regular node distribution with $n_g = 5$ .....	45
Table 5.10. Normalized central moments $M_c / \left( \frac{pL^2}{10} \right)$ of clamped square plate subjected to uniform load using regular node distribution with $n_g = 5$ .....	46
Table 5.11. Normalized central deflections $w_c / \left( \frac{pL^4}{100D} \right)$ of clamped square plate subjected to uniform load using irregular node distribution with $n_g = 5$ .....	47
Table 5.12. Normalized central moments $M_c / \left( \frac{pL^2}{10} \right)$ of clamped square plate	

subjected to uniform load using irregular node distribution with $n_g = 5$ .....	48
Table 5.13. Normalized central deflections $w_c / \left( \frac{pL^4}{100D} \right)$ of simply supported circular plate subjected to uniform load for regular node distribution with $\alpha_p = 6$ ..	50
Table 5.14. Normalized central moments $M_c / \left( \frac{pL^2}{10} \right)$ of simply supported circular plate subjected to uniform load for regular node distribution with $\alpha_p = 6$ .....	51
Table 5.15. Normalized central deflections $w_c / \left( \frac{pL^4}{100D} \right)$ of simply supported circular plate subjected to uniform load for irregular node distribution with $\alpha_p = 6$	52
Table 5.16. Normalized central moments $M_c / \left( \frac{pL^2}{10} \right)$ of simply supported circular plate subjected to uniform load for irregular node distribution with $\alpha_p = 6$ .....	53
Table 5.17. Normalized central deflections $w_c / \left( \frac{pL^4}{100D} \right)$ of simply supported circular plate subjected to uniform load using regular node distribution with $n_g = 5$ .....	54
Table 5.18. Normalized central moments $M_c / \left( \frac{pL^2}{10} \right)$ of simply supported circular plate subjected to uniform load using regular node distribution with $n_g = 5$ .....	55
Table 5.19. Normalized central deflections $w_c / \left( \frac{pL^4}{100D} \right)$ of simply supported circular plate subjected to uniform load using irregular node distribution with $n_g = 5$ .....	56
Table 5.20. Normalized central moments $M_c / \left( \frac{pL^2}{10} \right)$ of simply supported circular plate subjected to uniform load using irregular node distribution with $n_g = 5$ .....	57
Table 6.1. Material properties of laminated composite plates .....	73
Table 6.2. Normalized central deflections $w_c * \left( \frac{100E_2h^3}{qL^4} \right)$ for clamped square plate angle-ply orientation .....	74
Table 6.3. Normalized central deflections $w_c * \left( \frac{100E_2h^3}{qL^4} \right)$ for clamped square plate cross-ply orientation.....	76
Table 6.4. Normalized central stresses $\sigma_c * \left( \frac{h^2}{qL^2} \right)$ in the $x$ direction for clamped square plate cross-ply orientation.....	77
Table 6.5. Normalized central stresses $\sigma_c * \left( \frac{h^2}{qL^2} \right)$ in the $y$ direction for clamped square plate cross-ply orientation.....	78



Table 6.6. Normalized central deflections $w_c * (100E_2h^3 / qL^4)$ for clamped square plate angle-ply orientation .....	80
Table 6.7. Normalized central deflections $w_c * (100E_2h^3 / qL^4)$ according to $h / L = 0.1$ for simply supported square plate cross-ply orientations .....	82
Table 6.8. Normalized central stresses $\sigma_c * (h^2 / qL^2)$ in the $x$ direction according to $h / L = 0.1$ for simply supported square plate cross-ply orientations.....	83
Table 6.9. Normalized central stresses $\sigma_c * (h^2 / qL^2)$ in the $y$ direction according to $h / L = 0.1$ for simply supported square plate cross-ply orientations.....	84
Table 6.10. Normalized central deflections $w_c * (100E_2h^3 / qL^4)$ according to $h / L = 0.05$ for simply supported square plate cross-ply orientations .....	85
Table 6.11. Normalized central stresses $\sigma_c * (h^2 / qL^2)$ in the $x$ direction according to $h / L = 0.05$ for simply supported square plate cross-ply orientations.....	86
Table 6.12. Normalized central stresses $\sigma_c * (h^2 / qL^2)$ in the $y$ direction according to $h / L = 0.05$ for simply supported square plate cross-ply orientations.....	87
Table 6.13. Normalized central deflections $w_c * (100E_2h^3 / qL^4)$ according to $h / L = 0.01$ for simply supported square plate cross-ply orientations .....	88
Table 6.14. Normalized central stresses $\sigma_c * (h^2 / qL^2)$ in the $x$ direction according to $h / L = 0.01$ for simply supported square plate cross-ply orientations.....	89
Table 6.15. Normalized central stresses $\sigma_c * (h^2 / qL^2)$ in the $y$ direction according to $h / L = 0.01$ for simply supported square plate cross-ply orientations.....	90
Table 6.16. Normalized central deflections $w_c * (1000E_2h^3 / qL^4)$ for simply supported square plate asymmetric angle-ply orientations .....	92

Table 6.17. Normalized central deflections $w_c * \left( \frac{D}{qR^4} \right)$ for clamped circular orthotropic plate .....	94
Table 6.18. Normalized central deflections $w_c * \left( \frac{1000E_2h^3}{qL^4} \right)$ for simply supported skew plate angle-ply and cross-ply orientations.....	96
Table 6.19. Normalized central stresses $\sigma_c * \left( \frac{h^2}{qL^2} \right)$ in the $x$ direction for simply supported skew plate angle-ply and cross-ply orientations.....	97

## CHAPTER 1

### INTRODUCTION

#### 1.1. General Introduction

The analysis of a system prior to its production in real life has a crucial importance in engineering applications. Analysis step is one of the most careful parts in engineering design, and in today's world, it is generally performed by using various numerical methods such as Finite Element Method (FEM), Boundary Element Method (BEM), Finite Difference Method (FDM), Meshfree Methods etc. The FEM can be accepted as the most popular and preferred one among these methods due to its successful applications in a wide range of engineering areas. The basic feature of FEM is to divide the whole domain into finite number of simpler small elements. This is called as finite element discretization which is used to create the finite element mesh of the domain.

FEM has several advantages;

- Ability to tackle problems with irregular boundaries,
- Ability to deal with complex boundary conditions,
- Easy modifications to improve solution quality,
- Handling non-linear problems with linear approximations.

Although having these properties, FEM has the following limitations;

- Time consuming remesh procedure requirements for the geometry changes of problem domain
- Reliability problems for the stress evaluations,
- Remarkable accuracy loss for the large deformation problems,
- Discontinuity problems for the derivatives of field variables at the boundaries of elements,
- Mesh quality dependent solution accuracy.

Meshfree methods have been developed as a new numerical approach to overcome above issues and improved remarkably in last decade. The mesh based discretization scheme for the problem domain definition is not found in the solution procedure of meshfree methods. A set of arbitrarily scattered nodes are used to define problem domain and its boundaries in the meshfree methods rather than used mesh in FEM. The local domains are constructed using instantly selected field nodes and the interpolation of field variables are carried out using the nodes of local domains. Meshfree methods suffer from some problems such as stability, singularity etc. In recent years, a lot of research has attempted to solve and improve the meshfree methods.

## **1.2 Research Objectives and Tasks**

The main goals of this thesis are the investigation of effect of the selectable parameters such as weight functions, number of gauss points in a background cell, size of support domain, value of penalty coefficient and number of monomials on the solution accuracy of element-free Galerkin method (EFGM) for the non-layered isotropic plate bending problems, and the analysis of layered orthotropic plate bending problems using EFGM.

The research tasks can be shown as follows;

- I. An overview of some important meshfree methods in the literature.
- II. Detailed review of the element-free Galerkin method in the literature.
- III. Construction of shape functions using the MLS Approximation.
- IV. Implementation of the MLS shape functions to EFGM.
- V. Revising of bending theories of plates.
- VI. Development of MATLAB source codes for the solution of non-layered isotropic and layered orthotropic plate bending problems using EFGM.
- VII. Investigation of effects of the selectable parameters on the solution accuracy of EFGM for the non-layered isotropic plate bending problems.
- VIII. Analysis of layered orthotropic bending problems using EFGM.

## **1.3 Layout of Thesis**

A brief literature survey about meshfree methods and a special review of element-free Galerkin method are presented in chapter two. A short presentation about plate

bending theories are given in chapter three. The main concepts of element-free Galerkin method is summarized in chapter four. In chapter five, solution of some non-layered isotropic plate bending problems using EFGM with different values of selectable parameters and discussions of the results are provided. The EFGM solutions of some layered orthotropic bending problems are presented in chapter six. The conclusions are revealed in chapter seven.

## CHAPTER 2

### LITERATURE SURVEY

#### 2.1 Introduction

There are many types of meshfree methods in the literature such as Smoothed Particle Hydrodynamics (SPH) method [1, 2], Diffuse Element Method (DEM) [3], Element-Free Galerkin Method [4], Reproducing Kernel Particle Method (RKPM) [5], Point Interpolation Method (PIM) [6], Meshless Local Petrov Galerkin (MLPG) Method [7], Natural Element Method (NEM) [8], and Finite Particle Method (FPM) [9]. A short literature review only about the SPH, the DEM, the PIM, the MLPG and the RKPM are mentioned briefly in section 2.2. A detailed literature survey about the EFGM are presented in section 2.3. The EFGM for the solution of isotropic and layered orthotropic plate bending problems are revealed in section 2.4 and 2.5, respectively. The conclusions on literature survey are summarized in section 2.6.

#### 2.2 General Review of Some Meshfree Methods

In this section, some popular meshfree methods (the SPH, the DEM, the PIM, the MLPG and the RKPM) are introduced briefly to acquire important knowledge's about them.

##### 2.2.1 Smoothed Particle Hydrodynamics Method

The smoothed particle hydrodynamics (SPH) method is a meshfree method which used Lagrangian numerical technique, firstly developed to solve gas dynamics problems in astrophysics. The SPH method was introduced by Gingold and Monaghan [1] and Lucy [2] in late 1970s. Its meshless character makes the method very flexible and enables simulations of physical problems which might be difficult to capture by conventional grid-based methods. A set of moving particles are used in this method. These particles do not have any predefined relations and are used to represent physical problem domain. The mathematical model of physical problem is constructed using

partial differential equations which are transformed into selected finite integral form to compute integral over the particles [10]. There are a lot of variations in the original form of the SPH to improve stability and convergence of the method. An alternative approach similar to the approach adopted in Moving Particle Semi-implicit models [11] and was firstly proposed by Cummins and Rudman calling it as Incompressible SPH (ISPH).

The SPH has a constantly evolving application areas such as fluid dynamics [12], explosion [13], large deformations and fracture in solid continuums [14]. However, SPH method is not foolproof; it has stability and consistency problems especially in solid mechanics [15].

### **2.2.2 Diffuse Element Method**

The DEM is considered as first example of meshfree methods based on Galerkin weak form, was developed by B. Nayroles et al [3] in 1992. The main difference between FEM and DEM is about field approximation. Unlike FEM, the field approximation of the DEM is obtained for local domains using Moving Least Squares (MLS) approximation and these local domains contain varying numbers of nodes.

### **2.2.3 Point Interpolation Method**

The Point Interpolation method (PIM) was introduced by G.R. Liu in 2001 [6] as a new meshfree method. The PIM, originally based on the Galerkin method. The field variables are interpolated using point interpolation shape functions. The interpolation functions are constructed using polynomials chosen symmetrically from the Pascal's Triangle. The point interpolation shape functions have the Kronecker Delta property which simplifies the enforcement of the boundary conditions by the elimination of any extra algorithm requirements. This increases the computational efficiency of the PIM.

Despite these features, the PIM has a serious problem that is the singularity of moment matrix which avoids the construction of interpolation functions. To elimination of singularity problems, some algorithms have been proposed to overcome this problem such as diagonal offset algorithm [16], matrix triangularization method [17], and transformation of points in a local domain [18].

Another strategy to overcome singularity problems is the usage of radial basis functions for construction of point interpolation shape functions. This is also called as Radial Point Interpolation Method (RPIM) which was developed by Wang and Liu [19]. It solves the singularity problems but it has some drawbacks. The determination of shape parameters used in the RPIM shape functions are required for the accuracy solution. The RPIM also possess Kronecker Delta property but accuracy of the RPIM is less than accuracy of the PIM.

The several applications of PIM can be found in the literature such as 2D and 3D problems [19], beams and shells [19], composite laminated plates [20], plate bending problems [21], thermoplastic problems [22], buckling [23], static problems [19], elastoplastic problems [24], dynamic response of thin and thick plates [25].

#### **2.2.4 Meshless Local Petrov Galerkin Method**

Meshless Local Petrov Galerkin (MLPG) method is accepted as a truly meshfree method which eliminates the background cell requirement despite of other meshfree methods such as PIM, EFG method etc. The MLPG was proposed by Atluri and Zhu [7]. After this study; Atluri and Shen improved significantly the MLPG [26]. The MLPG method is based on a weak form which is constructed on a local subdomain. Background cells are not required in method. It is adopted the Moving Least Squares (MLS) as well as the augmented Radial Basis Functions (RBF) as the trial functions. Only nodal information is a requirement, element connectivity is not a necessity. This provides to a simple pre-processing.

The MLPG are used in many application areas according to literature examination. Some examples can be given as analysis of thin and thick plates [27], heat transfer problems [28], fluid mechanics problems [29], large deformation problems [30], fracture mechanics [31], analysis of shell deformations [19] etc.

#### **2.2.5 Reproducing Kernel Element Method**

Reproducing Kernel Particle Method (RKPM) was developed by Liu [5] to ensure lack of consistency, especially in the SPH method. Then, RKPM is obtained as a new meshfree method. RKPM has been applied a lot of areas such as problems of solids, structures, fluids etc.



### 2.3 Element Free Galerkin Method

Element Free Galerkin Method (EFGM) is a meshfree method which was proposed by Belytschko et al [4]. The EFGM approximation procedure, is based only on nodes, does not need to any mesh generation or remeshing operations. However, a set of background cells is used to take integral of Galerkin weak form. Additionally, EFGM converges more rapidly than the FEM [32, 33]. It has also more reliable than FEM in stress solutions. Despite of all these features, it has also some drawbacks against the FEM. Since MLS shape functions are used in EFGM, this requires to solve a set of algebraic equations for each sampling point. The computational cost of EFGM is higher than FEM since the requirement of more nodes for the construction of the MLS shape functions lead to larger band width for the resultant system matrix [19].

A set of arbitrary scattered nodes are used to represent problem domain and boundaries in the EFGM. The irregularity of node distribution does not suffer much degradation in accuracy [19]. Because of that, EFGM becomes one of the promising meshfree methods.

The EFGM has lack of Kronecker Delta property since the MLS shape functions are used for interpolations. So, there is no resemblance between the boundary conditions. For implementation of boundary conditions, various special techniques are developed such as the penalty method [33], Lagrange multiplier method [34], coupling with FEM [35] and employment of singular weight functions [36]. However, the benefit of using MLS approximation is to achieve stability in function approximation and use of Galerkin procedure to provide stable and well behaved discretized global system equations.

The EFGM is one of the most widely used meshfree method that can be seen in many engineering applications such as solid mechanics, fluid mechanics, heat transfer, and electromagnetic field problems. According to literature review, plane stress [37], plane strain [38], beams [39], shell [40], plate problems [41], composite laminated plate problems [42], axisymmetric [43] can be given as solid mechanics applications. Fluid mechanics applications are free surface flow [44], incompressible flow problems [45], fluid-structure interaction problems [46]. The simple list of heat transfer applications are axisymmetric heat transfer problems [47], moving heat source problems [48], heat

transfer of composite slabs [49], heat conduction analysis [50]. The applications of electromagnetic field problems can be summarized as 3D electromagnetic field [51], static and quasi-static electromagnetic field [52], 2D electromagnetic wave scattering [53], axisymmetric electromagnetic [54] problems.

The EFGM is one of the best numerical methods to solve fracture mechanics and crack propagation problems because EFGM serves stable solutions, high convergence rates and application flexibility by eliminating mesh requirement. Several examples of fracture mechanics and crack analysis using EFGM [55] are found in the literature.

Additionally, many techniques have been proposed of coupling EFG method with FEM [35] to improve the efficiency in the solution of a related problem. The EFGM is a developed method day by day as a mature and practical computational approach in the computational area of engineering.

#### **2.4 Element Free Galerkin Method in the Solution of Non-Layered Isotropic Plate Problems**

The solution of plate problems holds a very important place in the engineering area since they are used nearly everywhere in the life. Because of this, the analysis of plate problems have gained great significance. Some numerical techniques have been proposed for analysis them such as FEM, BEM and meshfree methods. Unlike FEM and BEM, the mesh-based discretization is not found in the meshfree methods.

The EFGM is one of the commonly used meshfree methods to analyze of plates and is used in the various analysis of plates such as static analysis of thin plates [41], buckling [56], vibration [57], elasto-plastic [58], crack [59], and also bending analysis of Kirchhoff plates [60], Mindlin-Reissner plates [61], and composite plates [62] in the literature.

Despite the EFGM is widely used in several application areas, it has a main issue that named is shear locking problem. To overcome this problem, several techniques are seen used such as using of the higher order basis [63], using of the first derivatives of shape functions as shape functions for rotations [64] in the literature.

## **2.5 Element Free Galerkin Method in the Solution of Composite Plate Problems**

In recent years, composite plates are preferred in many application fields such as automotive industry, aircraft structure, compressed gas containers, sports equipments, marine vehicles etc. Because of this, they must be analyzed correctly. Due to the complex structure of composite plates, several numerical methods, such as FEM, BEM and meshfree methods, have been used for the analyses of composite plates in the literature. Sheikh et al. [65] used FEM on the solution of composite plates having different shapes. Moments and stresses using BEM were examined by Albuquerque and his friends [66]. Haddad et al. [67] applied to Finite Difference Method (FDM) for free vibration analysis of composite plates.

The EFGM is seen as a promising candidate for the analysis of composite plates. It was used by Belinha and Dinis for the analysis of anisotropic plates and laminates [68]. Also, EFGM has been preferred for the various analysis of composite plates such as buckling problems [69], vibration problems [70], bending problems [68], crack analysis [71], fracture analysis [72], etc.

## **2.6 Conclusions on Literature Survey**

The EFGM has some selectable parameters that effect the accuracy of solutions such as size of support domain, order of monomials, type of weight function, number of integration points in a background cell and value of penalty coefficient. Although solutions of several problems are found in the literature, but the literature examination shows that effects of these parameters have not been investigated for bending problems of non-layered isotropic plates in detail.

According to literature survey; many studies are present about bending analysis of layered orthotropic plates using numerical methods such as FEM, BEM. But, the EFGM application is not common in the literature. This can be a new application area to examine reliability of the EFGM solutions.

## CHAPTER 3

### PLATE THEORIES

#### 3.1 Introduction

When a body is bounded by surfaces, flat in geometry, whose lateral dimensions are large compared to the between the surfaces is called as a plate. Plates are generally subjected to transverse lateral loads, as shown in Figure 3.1, and also may be subjected to in-plane loading according to purpose of usage in applications.

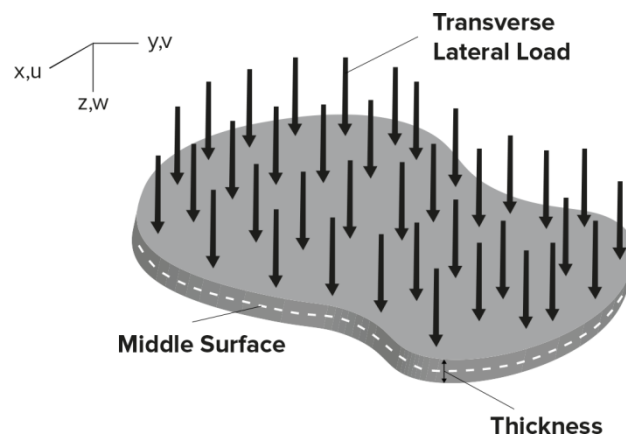


**Figure 3.1.** Plate subjected to transverse lateral loads.

Three main theories are present for bending analysis of plates in the literature. The theories are as follows;

- Higher-Order Shear Deformation Theory,
- Kirchhoff Plate Theory,
- Reissner-Mindlin Plate Theory.

A brief summary about Higher-Order Shear Deformation Theory is given in section 3.2.1. The Kirchhoff Plate Theory is introduced in section 3.2.2 and the Reissner-Mindlin Plate Theory, used in this study, is presented with governing equations for plate bending problems in section 3.2.3.

## 3.2 Review of the Plate Theories

### 3.2.1 Higher-Order Shear Deformation Theory

The Higher-Order Shear Deformation Theory (HSDT) is used for bending analyses of thick plates. The thickness of the plate is bigger than 1/10 ratio when comparing other lateral dimensions [73]. The theory does not need to shear correction factors. The theory can generally guarantee zero transverse shear stress values on the top and bottom surfaces of the plate.

### 3.2.2 Kirchhoff Plate Theory

The Kirchhoff plate theory is also known as the classical plate theory (CPT). It is used for the bending analyses of thin plates. The plates with a ratio of thickness to minimum lateral dimension less than 1/100 is considered as thin plates [73]. The assumptions of the Kirchhoff Plate Theory is based on assumption of the Bernoulli beam analysis. Kirchhoff applied them to plates and shells. Three main assumptions are used [74] as follows;

- Normal to the mid-plane before deformation remain straight and normal to the mid-plane after deformation.
- Transverse direct and shear stress effects are negligible.
- Deflections are small compared with the plate thickness.

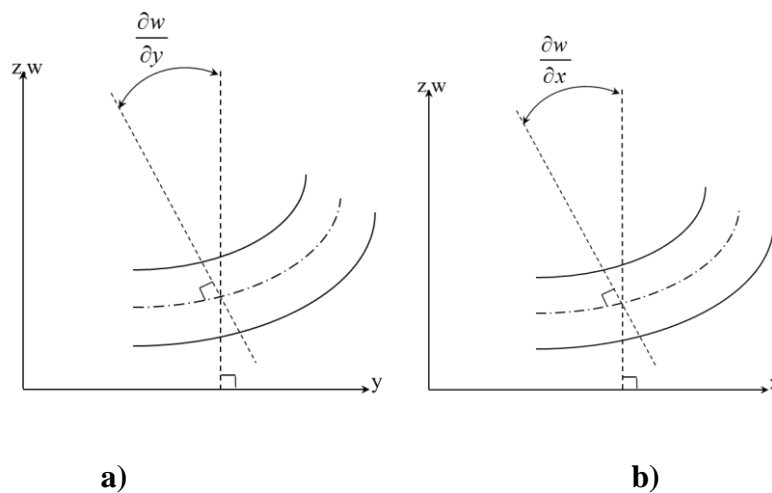


**Figure 3.2.** Deformed geometries of an edge according to Kirchhoff plate theory in plate cross-section **a)**  $y - z$  plane, **b)**  $x - z$  plane

The displacements of lateral axes  $x$  and  $y$  are  $u$  and  $v$ , respectively, and can be expressed as

$$u = -z \frac{\partial w}{\partial x} \quad (3.1)$$

$$v = -z \frac{\partial w}{\partial y} \quad (3.2)$$

where  $z$  is the direction of the plate thickness.

From the assumption of transverse shear effects elimination, the strains can be written as

$$\{ \epsilon_x \ \epsilon_y \ \gamma_{xy} \} = -z \{ \kappa_x \ \kappa_y \ \kappa_{xy} \} \quad (3.3)$$

where  $\kappa$ , is the curvature,

$$\boldsymbol{\kappa}^T = \{ \kappa_x \ \kappa_y \ \kappa_{xy} \} = \left\{ \frac{\partial^2 w}{\partial x^2} \ \frac{\partial^2 w}{\partial y^2} \ 2 \frac{\partial^2 w}{\partial x \partial y} \right\} \quad (3.4)$$

By substituting Eq.(3.3) into equation of  $\boldsymbol{\sigma} = \mathbf{D}\boldsymbol{\epsilon}$ , the plane stress constitutive equation for an isotropic material can be written as

$$\boldsymbol{\sigma} = -z\mathbf{D}\boldsymbol{\kappa} \quad (3.5)$$

in which  $\boldsymbol{\sigma} = \{ \sigma_x \ \sigma_y \ \tau_{xy} \}$  and  $\mathbf{D}$  is the material property matrix,

$$\mathbf{D} = \frac{E}{1 - \nu^2} \begin{bmatrix} 1 & \nu & 0 \\ \nu & 1 & 0 \\ 0 & 0 & \frac{1 - \nu}{2} \end{bmatrix} \quad (3.6)$$

Moments are considered as

$$\mathbf{M} = \int_{-h/2}^{h/2} \boldsymbol{\sigma} z \, dz \quad (3.7)$$

where  $\mathbf{M} = \{ M_x \ M_y \ M_{xy} \}$  and  $h$  is the thickness of plate.

Substituting of Eq. (3.5) into Eq. (3.7),

$$\mathbf{M} = -\mathbf{D}\boldsymbol{\kappa} \quad (3.8)$$

Equilibrium equations are obtained from the free body diagram as shown in Fig. 3.3. Moment equilibriums about the  $y$  – and  $x$  – axes and force equilibrium about the  $z$  – axis, after neglecting higher order terms, can be written as

$$\frac{\partial M_x}{\partial x} + \frac{\partial M_{xy}}{\partial y} - Q_x = 0 \quad (3.9)$$

$$\frac{\partial M_{xy}}{\partial x} + \frac{\partial M_y}{\partial y} - Q_y = 0 \quad (3.10)$$

$$\frac{\partial Q_x}{\partial x} + \frac{\partial Q_y}{\partial y} + p = 0 \quad (3.11)$$

where  $Q_x$  and  $Q_y$  are the shear forces and  $p$  is the distributed pressure load.

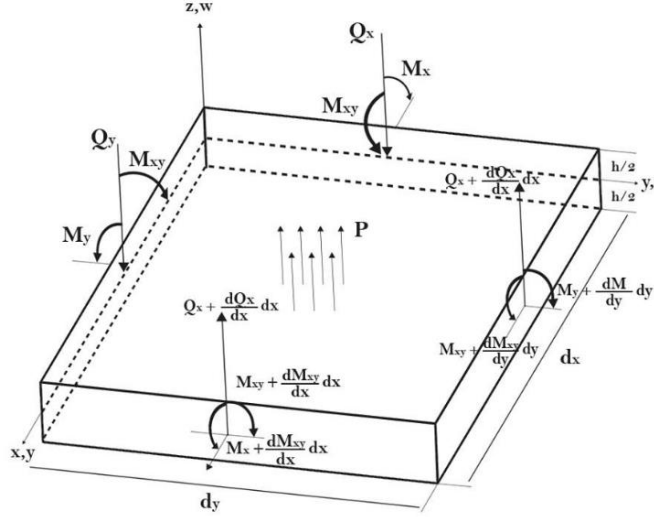


**Figure 3.3.** Free body diagram of the plate element

The shear forces are neglected from Eq. (3.9), Eq. (3.10) and Eq. (3.11) gives

$$\frac{\partial^2 M_x}{\partial x^2} + 2 \frac{\partial^2 M_{xy}}{\partial x \partial y} + \frac{\partial^2 M_y}{\partial y^2} + p = 0 \quad (3.12)$$

When combining of Eq. (3.4), Eq. (3.8) and Eq. (3.12), the governing equation for plate bending is produced in terms of the transverse displacement  $w$ .

$$\frac{\partial^4 w}{\partial x^4} + 2 \frac{\partial^4 w}{\partial x^2 \partial y^2} + \frac{\partial^4 w}{\partial y^4} = \frac{p}{D_r} \quad (3.13)$$

where  $D_r = \frac{Eh^3}{12(1-\nu^2)}$  is the rigidity of the plate.

### 3.2.3 Reissner-Mindlin Plate Theory

Reissner-Mindlin plate theory is also known as the First-Order Shear Deformation Theory (FSDT). It is used for moderately-thick plates that thickness of the plate is between 1/10 and 1/100 ratio comparing to other two dimensions [73]. Unlike Kirchhoff plate theory, the shear effects are considered in the analysis according to Reissner-Mindlin plate theory. The theory has assumptions which are based on Timoshenko beam theory assumptions.

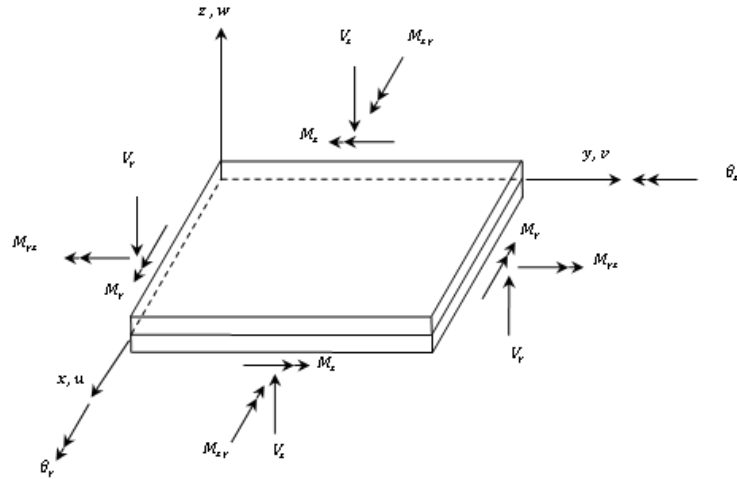


**Figure 3.4.** A typical Reissner-Mindlin plate

The assumptions of the Reissner-Mindlin plate theory as follows [74];

- Normal to the mid-plane before deformation remain straight but not necessarily normal to the mid-plane after deformation.
- Stresses normal to the mid-plane may be neglected.
- Deflections are small compared with the plate thickness.

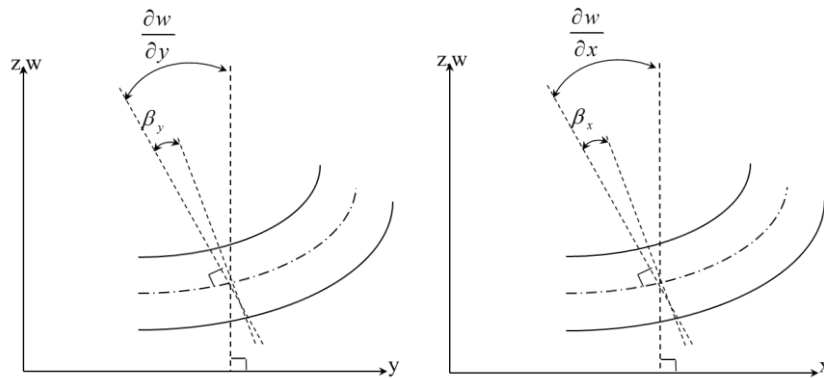


**Figure 3.5.** Deformed geometries of an edge according to Reissner-Mindlin plate theory in plate cross-section **a)**  $y - z$  plane **b)**  $x - z$  plane

The displacements of parallel to the undeformed neutral surface,  $u$  and  $v$ , can be expressed by

$$u = -z\theta_x(x, y) \quad (3.14)$$

$$v = -z\theta_y(x, y) \quad (3.15)$$



where  $\theta_x$  and  $\theta_y$  are the normal rotations of the cross section of the plate about the  $y$  – and  $x$  –axis and can be expressed as

$$\theta_x = \frac{\partial w}{\partial x} - \gamma_{xz} \quad (3.16)$$

$$\theta_y = \frac{\partial w}{\partial y} - \gamma_{yz} \quad (3.17)$$

The transverse displacement can be written as

$$w = w(x, y) \quad (3.18)$$

The strains are expressed as

$$\boldsymbol{\varepsilon} = [ \epsilon_x \quad \epsilon_y \quad \gamma_{xy} \quad \gamma_{xz} \quad \gamma_{yz} ]^T \quad (3.19)$$

where the strains are given as

$$\epsilon_x = -\frac{\partial \theta_x}{\partial x} \quad (3.20)$$

and

$$\epsilon_y = -\frac{\partial \theta_y}{\partial y} \quad (3.21)$$

and the shear strains are expressed as

$$\gamma_{xy} = -\left( \frac{\partial \theta_y}{\partial x} + \frac{\partial \theta_x}{\partial y} \right) \quad (3.22)$$

$$\gamma_{xz} = \left( \frac{\partial w}{\partial x} - \theta_x \right) \quad (3.23)$$

and

$$\gamma_{yz} = \left( \frac{\partial w}{\partial y} - \theta_y \right) \quad (3.24)$$

The constitutive relationships are given in the form

$$\boldsymbol{\sigma} = \mathbf{D} \boldsymbol{\epsilon} \quad (3.25)$$

where

$$\boldsymbol{\sigma} = [M_x \ M_y \ M_{xy} \ Q_x \ Q_y]^T \quad (3.26)$$

in which  $M_x$  and  $M_y$  are the direct bending moments and  $M_{xy}$  is the twisting moment. The quantities  $Q_x$  and  $Q_y$  are the shear forces in the  $x - z$  and  $y - z$  planes.

For an isotropic material,  $\mathbf{D}$  is given as;

$$\mathbf{D} = \begin{bmatrix} D & \nu D & 0 & 0 & 0 \\ \nu D & D & 0 & 0 & 0 \\ 0 & 0 & \frac{(1-\nu)D}{2} & 0 & 0 \\ 0 & 0 & 0 & S & 0 \\ 0 & 0 & 0 & 0 & S \end{bmatrix} \quad (3.27)$$

in which for a plate of thickness,  $t$

$$D = \frac{Et^3}{12(1-\nu^2)} \quad (3.28)$$

and

$$S = \frac{Gt}{1.2} \quad (3.29)$$

where  $G$  is the shear modulus and the factor 1.2 is a correction term.

## CHAPTER 4

### ELEMENT FREE GALERKIN METHOD

#### FOR BENDING PROBLEMS OF REISSNER-MINDLIN PLATE

##### 4.1 Introduction

Nowadays, composite materials have played an important role in the engineering applications that require high strength/weight or stiffness/weight ratios. Because of that, analysis of composite materials have gained great significance. Due to the complex structure of composite materials, several numerical methods, such as FEM, BEM and meshfree methods, have been used for the analysis of composite laminates in the literature. The performances of FEM and BEM depend on mesh quality of the problem model. Meshfree methods have been developed to overcome this limitation.

Element Free Galerkin Method is a popular method in meshfree methods. In meshfree methods, problem domain and its boundaries are defined by using only informations of scattered nodes. Despite its popularity, it has a drawback. The EFGM uses Moving Least Square (MLS) approximation to construct shape functions. The Kronecker delta feature is not provided by the MLS approximation. Because of that, extra algorithms are required to imply boundary conditions. These algorithms generally resulted with an increase in computational load and solution time.

In this chapter, solution procedure of meshfree methods in solid mechanics is mentioned shortly in section 4.2. First-Order Shear Deformation Theory (FSDT) formulations for composite plates are reviewed in section 4.3. In last section 4.4, The EFGM is presented that includes the construction of MLS shape functions and Galerkin weak form for Reissner-Mindlin plate problems.

## **4.2 Short Description of Implementation Procedure for Galerkin Meshfree Methods**

The implementation procedure of Galerkin meshfree methods can be classified into four basic steps as domain representation, field interpolation, formulation of system equations and solution of the system equations for field variables, respectively. In the first step, the problem domain and its boundaries are represented by a set of scattered nodes. There is no any predefined relation between the nodes which is the main difference between discretization of FEM and meshfree methods. After the domain representation, the field variables at any point are interpolated by constructing shape functions (approximation or interpolation functions). Shape functions are constructed using the nodes of local domain constructed for a point of interest. There is no predefined relationship to construct shape functions. In the third step, system equations are formulated for local domains and combined to obtain global system equations. The technique of formulations for system equations can be different for different meshfree methods. The last step includes the solution of the equations. It is similar to the FEM. Any equation solver depends on the problem type can be used for solution.

### **4.2.1 Basic Definitions for Meshfree Methods**

In meshfree methods, terms such as local domain, background cell are mentioned every time. In this part of chapter 4, these terms are presented about what they mean or why they are used in meshfree methods.

#### **4.2.1.1 Local Domains (Support and Influence Domains)**

A local domain is defined as a domain which determines the nodes used for the approximation of field variables. Despite it is similar to the elements in FEM, there are three main differences between local domains in meshfree methods and elements in FEM. Firstly, while local domains are only used for interpolation, elements in FEM are used not only interpolation but also integration purposes. Another difference is their predefined shape conditions. The elements need to be predefined regular shapes, but it is not necessary for the local domains. Last difference is that the local domains don't have any predefined nodes as the elements.

The local domain size is determined by the following equation 4.1.

$$r_s = \alpha_s \times r_c \quad (4.1)$$

where  $r_c$  is the average nodal spacing and  $\alpha_s$  is the dimensionless size of support domain.

#### 4.2.1.2 Background Cells

Background cells are used for the integration process in the Galerkin meshfree methods. These cells have no other use in the problem domain. They just subdivide the domain into either squares, triangles or any other chosen shape. Even if the background cells look like elements in FEM, they are not similar for their usage. There isn't any influence of background cell in the formation of the shape function as is the case with elements in FEM. The background cells and influence domains are shown clearly in Fig 4.1.

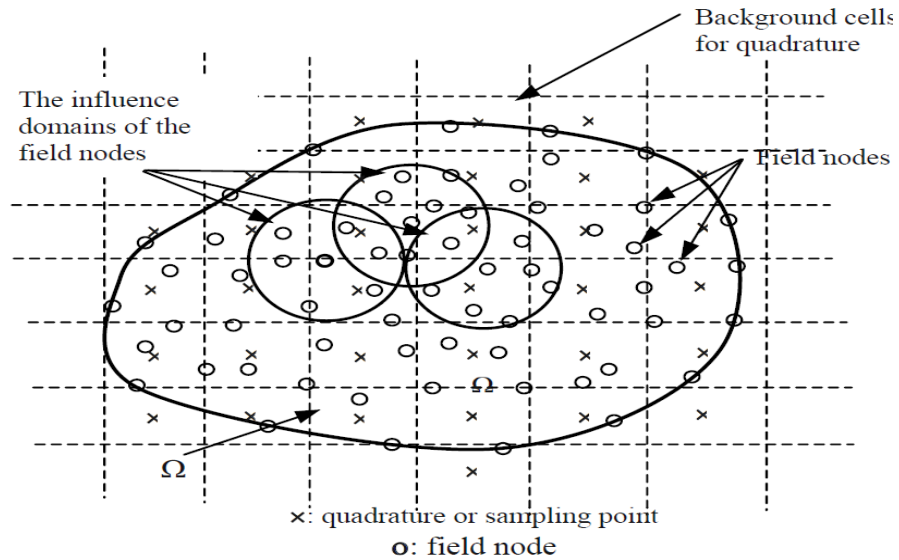


**Figure 4.1.** Support Domain; the centre is a quadrature point

### 4.3 First-Order Shear Deformation Theory (FSDT) for composite plates

A typical Mindlin-Reissner plate with mid-plane lying in the  $x - y$  plane of Cartesian coordinate system is depicted in Fig. 4.2. The displacement field of a point at a distance  $z$  to the mid-plane can be written as [68]

$$\mathbf{u} = \begin{Bmatrix} u \\ v \\ w \end{Bmatrix} = \begin{Bmatrix} -z\theta_x(x, y) \\ -z\theta_y(x, y) \\ w(x, y) \end{Bmatrix} \quad (4.2)$$

where  $(u, v, w)$  are the displacements of the plate in the  $x, y, z$  directions.  $\theta_x$  and  $\theta_y$  are the rotations of cross-section of the plate about  $y$  and  $x$  axes, respectively. The linear strains in the Mindlin-Reissner plate are the strains resulting from bending are obtained in terms of the rotations,  $\theta_x, \theta_y$  and of the mid-surface displacement,  $w$ , as

$$\boldsymbol{\varepsilon} = \begin{Bmatrix} \varepsilon_{xx} \\ \varepsilon_{yy} \\ \gamma_{xy} \\ \gamma_{yz} \\ \gamma_{xz} \end{Bmatrix} = \begin{Bmatrix} -z \frac{\partial \theta_x(x, y)}{\partial x} \\ -z \frac{\partial \theta_y(x, y)}{\partial y} \\ -z \frac{\partial \theta_x(x, y)}{\partial y} - z \frac{\partial \theta_y(x, y)}{\partial x} \\ -\theta_y(x, y) + \frac{\partial w(x, y)}{\partial y} \\ -\theta_x(x, y) + \frac{\partial w(x, y)}{\partial x} \end{Bmatrix} \quad (4.3)$$

Using the generalized Hooke's law for orthotropic linear elastic materials, the stresses for the  $i^{th}$  layer is given as,

$$\boldsymbol{\sigma}^i = \bar{\mathbf{c}}^i \boldsymbol{\varepsilon} \quad (4.4)$$

where

$$\boldsymbol{\sigma}^i = \{\sigma_{xx} \quad \sigma_{yy} \quad \tau_{xy} \quad \tau_{yz} \quad \tau_{xz}\}^T \quad (4.5)$$

$$\bar{\mathbf{c}}^i = \mathbf{T}^T \mathbf{c}^i \mathbf{T} \quad (4.6)$$

where  $\mathbf{c}^i$  is the material matrix of the  $i^{th}$  layer. It includes six independent material properties that are  $E_1, E_2, \nu_{12}, G_{12}, G_{13}$  and  $G_{23}$ . The material matrix of the orthotropic materials can be written as

$$\mathbf{c}^i = \begin{bmatrix} \frac{E_1}{1 - \nu_{12}\nu_{21}} & \frac{E_1\nu_{21}}{1 - \nu_{12}\nu_{21}} & 0 & 0 & 0 \\ \frac{E_1\nu_{12}}{1 - \nu_{12}\nu_{21}} & \frac{E_2}{1 - \nu_{12}\nu_{21}} & 0 & 0 & 0 \\ 0 & 0 & G_{12} & 0 & 0 \\ 0 & 0 & 0 & G_{23} & 0 \\ 0 & 0 & 0 & 0 & G_{31} \end{bmatrix} \quad (4.7)$$

and  $\mathbf{T}$  is the transformation matrix, which has lay-up of the laminae, can be given as

$$\mathbf{T} = \begin{bmatrix} \cos^2\theta & \sin^2\theta & -\sin 2\theta & 0 & 0 \\ \sin^2\theta & \cos^2\theta & \sin 2\theta & 0 & 0 \\ \sin\theta \cos\theta & -\sin\theta \cos\theta & \cos^2\theta - \sin^2\theta & 0 & 0 \\ 0 & 0 & 0 & \cos\theta & -\sin\theta \\ 0 & 0 & 0 & \sin\theta & \cos\theta \end{bmatrix} \quad (4.8)$$

where the  $\theta$  is the lay-up or orientation of fiber on the  $i^{th}$  lamina.

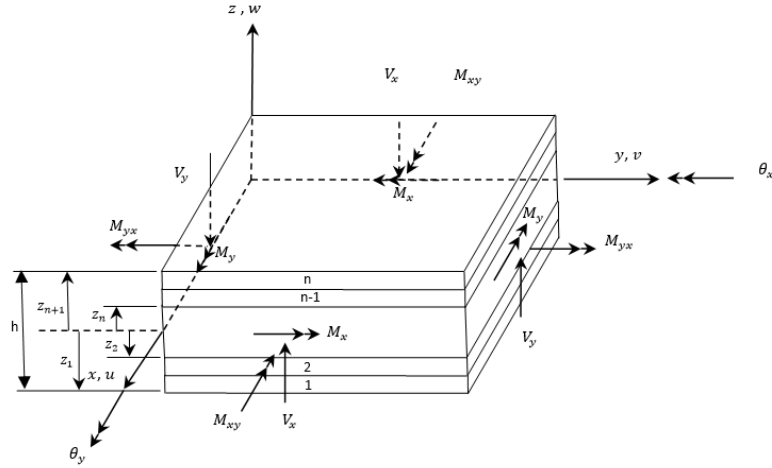


**Figure 4.2.** A typical laminate plate

Considering the  $\{\varepsilon_{xx} \ \varepsilon_{yy} \ \gamma_{xy}\} = z \{\bar{\varepsilon}_{xx} \ \bar{\varepsilon}_{yy} \ \bar{\gamma}_{xy}\}$  the stresses on the top face of layer ( $i$ ) are

$$\begin{aligned} \sigma_{xx}^{z_i+1} &= z_{i+1} [\bar{c}_{11}^i \bar{\varepsilon}_{xx} + \bar{c}_{12}^i \bar{\varepsilon}_{yy} + \bar{c}_{13}^i \bar{\gamma}_{xy}] \\ \sigma_{yy}^{z_i+1} &= z_{i+1} [\bar{c}_{12}^i \bar{\varepsilon}_{xx} + \bar{c}_{22}^i \bar{\varepsilon}_{yy} + \bar{c}_{23}^i \bar{\gamma}_{xy}] \\ \tau_{xy}^{z_i+1} &= z_{i+1} [\bar{c}_{13}^i \bar{\varepsilon}_{xx} + \bar{c}_{23}^i \bar{\varepsilon}_{yy} + \bar{c}_{33}^i \bar{\gamma}_{xy}] \\ \tau_{xz}^{z_i+1} &= [\bar{c}_{44}^i \gamma_{xz} + \bar{c}_{45}^i \gamma_{yz}] \\ \tau_{yz}^{z_i+1} &= [\bar{c}_{45}^i \gamma_{xz} + \bar{c}_{55}^i \gamma_{yz}] \end{aligned} \quad (4.9)$$

The bending moments ( $M_{ij}$ ) and the shear forces ( $V_{ij}$ ) are

$$\begin{aligned} M_{xx} &= \sum_i^n \int_{z_i}^{z_{i+1}} z \sigma_{xx}^i dz \\ M_{yy} &= \sum_i^n \int_{z_i}^{z_{i+1}} z \sigma_{yy}^i dz \\ M_{xy} &= \sum_i^n \int_{z_i}^{z_{i+1}} z \tau_{xy}^i dz \end{aligned} \quad (4.10)$$

and

$$V_{xx} = k_{sh} \sum_i^n \int_{z_i}^{z_{i+1}} \tau_{xz}^i dz \quad (4.11)$$

$$V_{yy} = k_{sh} \sum_i^n \int_{z_i}^{z_{i+1}} \tau_{yz}^i dz$$

where  $k_{sh}$  is the shear correction factor. Substituting the stress values in Eqs. (4.9) into moment in Eqs. (4.10) and shear forces in Eqs. (4.11):

$$\begin{aligned} M_{xx} &= \sum_i^n \left[ \frac{z_{i+1}^3}{3} - \frac{z_i^3}{3} \right] [\bar{c}_{11}^i \bar{\varepsilon}_{xx} + \bar{c}_{12}^i \bar{\varepsilon}_{yy} + \bar{c}_{13}^i \bar{\gamma}_{xy}] \\ M_{yy} &= \sum_i^n \left[ \frac{z_{i+1}^3}{3} - \frac{z_i^3}{3} \right] [\bar{c}_{12}^i \bar{\varepsilon}_{xx} + \bar{c}_{22}^i \bar{\varepsilon}_{yy} + \bar{c}_{23}^i \bar{\gamma}_{xy}] \\ M_{xy} &= \sum_i^n \left[ \frac{z_{i+1}^3}{3} - \frac{z_i^3}{3} \right] [\bar{c}_{13}^i \bar{\varepsilon}_{xx} + \bar{c}_{12}^i \bar{\varepsilon}_{yy} + \bar{c}_{13}^i \bar{\gamma}_{xy}] \\ V_{xx} &= k_{sh} \sum_i^n [z_{i+1} - z_i] [\bar{c}_{44}^i \gamma_{xz} + \bar{c}_{45}^i \gamma_{yz}] \\ V_{yy} &= k_{sh} \sum_i^n [z_{i+1} - z_i] [\bar{c}_{45}^i \gamma_{xz} + \bar{c}_{55}^i \gamma_{yz}] \end{aligned} \quad (4.12)$$

The Eqs. (4.12) can be arranged as in the following form:

$$\mathbf{M} = \begin{bmatrix} M_{xx} \\ M_{yy} \\ M_{xy} \end{bmatrix} = \sum_i^n \mathbf{D}^i \mathbf{L} \Phi \left( \frac{z_{i+1}^3}{3} - \frac{z_i^3}{3} \right) = \left[ \sum_i^n \mathbf{D}^i \left( \frac{z_{i+1}^3}{3} - \frac{z_i^3}{3} \right) \right] \mathbf{L} \Phi \quad (4.13)$$

$$\mathbf{V} = \begin{bmatrix} V_{xx} \\ V_{yy} \end{bmatrix} = k_{sh} \sum_i^n [\mathbf{A}_{sh}^i (\nabla \mathbf{w} - \Phi) (z_{i+1} - z_i)] = k_{sh} \left[ \sum_i^n \mathbf{A}_{sh}^i (z_{i+1} - z_i) \right] (\nabla \mathbf{w} - \Phi)$$

where,

$$\mathbf{L} = \begin{bmatrix} -\frac{\partial}{\partial x} & 0 & -\frac{\partial}{\partial y} \\ 0 & -\frac{\partial}{\partial y} & -\frac{\partial}{\partial x} \end{bmatrix} \quad (4.14)$$



$$\Phi = \{\theta_x \quad \theta_y\}^T \quad (4.15)$$

$$\nabla = \left\{ \frac{\partial}{\partial x} \quad \frac{\partial}{\partial y} \right\}^T \quad (4.16)$$

and  $\mathbf{D}^i$  and  $\mathbf{A}_{sh}^i$  are the material properties related with bending and shear effects. They can be written in the matrix forms, as follows:

$$\mathbf{D}^i = \begin{bmatrix} \bar{c}_{11}^i & \bar{c}_{12}^i & \bar{c}_{13}^i \\ \bar{c}_{12}^i & \bar{c}_{22}^i & \bar{c}_{23}^i \\ \bar{c}_{13}^i & \bar{c}_{23}^i & \bar{c}_{33}^i \end{bmatrix} \quad (4.17)$$

$$\mathbf{A}_{sh}^i = \begin{bmatrix} \bar{c}_{44}^i & \bar{c}_{45}^i \\ \bar{c}_{45}^i & \bar{c}_{55}^i \end{bmatrix} \quad (4.18)$$

In the absence of mass forces, the equilibrium equations obtained using the virtual work principle are given as,

$$\mathbf{L}^T \mathbf{M} - \mathbf{V} = 0 \quad (4.19)$$

$$\nabla^T \mathbf{V} + \mathbf{b} = 0$$

where  $\mathbf{b}$  is the vector of applied external forces. EFGM is used for the solution of this system equations.

## 4.4 Element-Free Galerkin Method

### 4.4.1 Moving-Least Square (MLS) Approximation

The MLS approximation for the function of a field variable  $u(\mathbf{x})$  in a local domain  $\Omega$  is defined at a point  $\mathbf{x}$  as

$$u^h(\mathbf{x}) = \sum_{i=1}^m p_i(\mathbf{x}) a_i(\mathbf{x}) = \mathbf{p}^T(\mathbf{x}) \mathbf{a}(\mathbf{x}) \quad (4.20)$$

where  $m$  is the number of basis terms,  $\mathbf{p}^T(\mathbf{x}) = \{p_1(\mathbf{x}), p_2(\mathbf{x}), p_3(\mathbf{x}), \dots, p_m(\mathbf{x})\}$  is the vector of monomial basis functions,  $\mathbf{a}^T(\mathbf{x}) = \{a_1(\mathbf{x}), a_2(\mathbf{x}), a_3(\mathbf{x}), \dots, a_m(\mathbf{x})\}$  is the vector of unknown coefficients, and  $\mathbf{x}^T = [x, y]$  is the position vector for 2D problems. The monomials are selected from the Pascal triangle with providing minimum

completeness to build the basis function  $\mathbf{p}^T(\mathbf{x})$ . For example, the linear and quadratic basis functions in 2D problems can be given by

$$\mathbf{p}^T(\mathbf{x}) = [1, x, y], \quad m = 3 \quad (4.21)$$

$$\mathbf{p}^T(\mathbf{x}) = [1, x, y, x^2, xy, y^2], \quad m = 6 \quad (4.22)$$

The difference between the function  $u(\mathbf{x})$  and its local approximation  $u^h(\mathbf{x})$  must be minimized by weighted discrete  $L_2$  norm to obtain the vector of coefficients  $\mathbf{a}(\mathbf{x})$ .

$$J = \sum_{i=1}^n w(\mathbf{x} - \mathbf{x}_i) [\mathbf{p}^T(\mathbf{x}_i) \mathbf{a}(\mathbf{x}) - u_i]^2 \quad (4.23)$$

where  $n$  is the number of nodes in the support domain of point  $\mathbf{x}$ ,  $u_i$  is the nodal value of  $u$  at  $\mathbf{x} = \mathbf{x}_i$ ,  $w(\mathbf{x} - \mathbf{x}_i)$  is the weight function associated with the influence domain of node  $i$ . From weight function properties, it must be greater than zero for all nodes in the support domain of point  $\mathbf{x}$ .

The minimization of weighted residual with respect to  $\mathbf{a}(\mathbf{x})$  at any arbitrary point  $\mathbf{x}$  gives

$$\frac{\partial J}{\partial \mathbf{a}} = 0 \quad (4.24)$$

which can be written as a set of linear equations.

$$\mathbf{A}(\mathbf{x}) \mathbf{a}(\mathbf{x}) = \mathbf{B}(\mathbf{x}) \mathbf{U}_s \quad (4.25)$$

where  $\mathbf{U}_s = \{u_1, u_2, u_3, \dots, u_n\}^T$  is the vector of nodal values of field function for the nodes of support domain. The matrices  $\mathbf{A}$  and  $\mathbf{B}$  have the following forms

$$\mathbf{A}(\mathbf{x}) = \sum_{i=1}^n w_i(\mathbf{x}) p(x_i) p^T(x_i), \quad w_i(\mathbf{x}) = w(\mathbf{x} - x_i) \quad (4.26)$$

$$\mathbf{B}(\mathbf{x}) = [w_1(\mathbf{x})p(x_1) \quad w_2(\mathbf{x})p(x_2) \quad \dots \quad w_n(\mathbf{x})p(x_n)] \quad (4.27)$$

The matrix  $\mathbf{A}$  is called as weighted moment matrix of MLS and if it is non-singular  $\mathbf{a}(\mathbf{x})$  can be written as

$$\mathbf{a}(\mathbf{x}) = \mathbf{A}^{-1}(\mathbf{x})\mathbf{B}(\mathbf{x})\mathbf{U}_s \quad (4.28)$$

The local approximation  $u^h(\mathbf{x})$  can be rewritten by substituting Eq. (1)

$$u^h(\mathbf{x}) = \sum_{i=1}^n \phi_i(\mathbf{x})u_i = \mathbf{\Phi}^T(\mathbf{x})\mathbf{U}_s \quad (4.29)$$

where  $\mathbf{\Phi}^T$  is the vector of MLS shape functions and it can be expressed as

$$\mathbf{\Phi}^T(\mathbf{x}) = \{\phi_1(\mathbf{x}) \quad \phi_2(\mathbf{x}) \quad \cdots \quad \phi_n(\mathbf{x})\} = \mathbf{p}^T(\mathbf{x})\mathbf{A}^{-1}(\mathbf{x})\mathbf{B}(\mathbf{x}) \quad (4.30)$$

The partial derivatives of shape function can be achieved by the following equation.

$$\Phi_{,i} = (\mathbf{p}^T\mathbf{A}^{-1}\mathbf{B})_{,i} = \mathbf{p}_{,i}^T\mathbf{A}^{-1}\mathbf{B} + \mathbf{p}^T\mathbf{A}_{,i}^{-1}\mathbf{B} + \mathbf{p}^T\mathbf{A}^{-1}\mathbf{B}_{,i} \quad (4.31)$$

where

$$\mathbf{A}_{,i}^{-1} = -\mathbf{A}^{-1}\mathbf{A}_{,i}\mathbf{A}^{-1} \quad (4.32)$$

The spatial derivative are designated with index  $i$  following a comma. The weight functions are one of the most important points for derivation of MLS shape functions. The continuity and locality features of the MLS approximation are mainly based on weight functions. The weight function must be positive inside the support domain by taking its maximum value at the centre of support domain and must be zero outside the support domain using a monotonically decrease. There are various weight functions in literature [19]. The cubic spline weight function is used in this work and is given by

$$w_i(\mathbf{x} - \mathbf{x}_i) = w(\bar{r}_i) = \begin{cases} 2/3 - 4\bar{r}_i^2 + 4\bar{r}_i^3 & \bar{r}_i \leq 0.5 \\ 4/3 - 4\bar{r}_i + 4\bar{r}_i^2 - 4/3\bar{r}_i^3 & 0.5 < \bar{r}_i \leq 1 \\ 0 & \bar{r}_i > 1 \end{cases} \quad (4.33)$$

For rectangular influence domain in 2-D problems, weight functions can be obtained by

$$w(\bar{r}_i) = w(r_x)w(r_y) = w_x w_y \quad (4.34)$$

$$r_x = \frac{|x - x_i|}{r_{wx}} \quad \text{and} \quad r_y = \frac{|y - y_i|}{r_{wy}} \quad (4.35)$$

where  $r_{wx}$  and  $r_{wy}$  are the size of support domain in the  $x$  and  $y$  direction.

#### 4.4.2 Galerkin Weak Form and Enforcement Boundary Conditions

The Galerkin weak form for Mindlin-Reissner plates can written as

$$\begin{aligned} \int_{\Omega} \delta(\mathbf{L}_d u)^T D L_d u d\Omega - \int_{\Omega} \delta(\mathbf{L}_u u)^T b d\Omega - \int_{\Gamma_t} \delta(\mathbf{L}_u u)^T t_{\Gamma} dS \\ + \delta \int_{\Gamma_u} \frac{1}{2} (u_b - u_{\Gamma})^T \alpha (u_b - u_{\Gamma}) d\Gamma = 0 \end{aligned} \quad (4.36)$$

The discrete system equation can be written as

$$(\mathbf{K} + \mathbf{K}^{\alpha})\mathbf{U} = (\mathbf{F} + \mathbf{F}^{\alpha}) \quad (4.37)$$

where  $\mathbf{K}$  is the global stiffness matrix and is obtained by assembling the point stiffness matrices

$$K_{ij} = \int_{\Omega} \mathbf{B}_i^T \mathbf{D} \mathbf{B}_j d\Omega \quad (4.38)$$

in which

$$\mathbf{B}_i = \begin{bmatrix} 0 & 0 & 0 & \frac{\partial \phi_i}{\partial x} & \frac{\partial \phi_i}{\partial y} \\ \frac{\partial \phi_i}{\partial x} & 0 & \frac{\partial \phi_i}{\partial y} & \phi_i & 0 \\ 0 & \frac{\partial \phi_i}{\partial y} & \frac{\partial \phi_i}{\partial x} & 0 & \phi_i \end{bmatrix}^T \quad (4.39)$$

and

The  $\mathbf{K}^{\alpha}$  is the matrix of penalty factors defined by

$$(\mathbf{K}^{\alpha})_{ij} = \int_{\Gamma_u} \varphi_i^T \alpha \varphi_j d\Gamma \quad (4.40)$$

where  $\varphi_i$  is a diagonal matrix. If the relevant DOF is free, the diagonal elements of  $\varphi_i$  are equal to 0, otherwise equal to 1.

The force vector  $\mathbf{F}$  in Eq. (4.37) is the global force vector assembled using the nodal force vector of

$$F_i = \int_{\Omega} (\mathbf{L}_u \Phi_i)^T b d\Omega + \int_{\Omega} (\mathbf{L}_u \Phi_i)^T t_{\Gamma} dS \quad (4.41)$$

where  $\Phi_i$  is a diagonal matrix of shape functions.

The  $\mathbf{F}^{\alpha}$  vector shows the forces obtained by the implementation of essential boundary conditions and can be obtained as follows

$$F_i^{\alpha} = \int_{\Gamma_u} \varphi_i^T \alpha u_{\Gamma} d\Gamma \quad (4.42)$$

## CHAPTER 5

### NUMERICAL RESULTS AND DISCUSSIONS FOR BENDING ANALYSIS OF NON-LAYERED ISOTROPIC PLATES

#### 5.1 Introduction

Four numerical examples have been performed to investigate the effects of selectable parameters of the EFGM on the solution accuracy of the non-layered isotropic plate bending problems based on Reissner-Mindlin plate theory. The numerical examples are;

- Clamped square plate under transverse centric point load,
- Clamped square plate under uniform transverse load,
- Simply supported circular plate under uniform transverse load,
- Simply supported Morley's skew plate under uniform transverse load.

In this chapter; the obtained EFGM results by using different values of selectable parameters are compared with analytical results in the literature and are discussed effects on the solution accuracy.

Tables and figures are used to represent results of numerical examples. However, invalid/unacceptable results are not given into figures and tables to show more clearly variations of normalized displacements/moments against the values of selectable parameters. The value of penalty coefficient is presented in the form of  $10^{\alpha p}$ . The number of gauss points in a background cell, central deflections and moments of plates are symbolized with  $n_g$ ,  $w_c$ , and  $M_c$  respectively.

#### 5.2 Clamped square plate under transverse centric point load

The square plate has fully clamped boundary condition and is loaded with transverse centric point load as shown in Fig.5.1. The material properties are as follows; Young's modulus  $E$  of material is 10920 Pa and Poisson's ratio is  $\nu = 0.3$ . The thickness and length of the plate are given by  $h = 0.01$  m and  $L = 1$  m, respectively. The value of applied transverse centric point load,  $P$  is 16.3527 N. Due to symmetry, only one

quarter of the plate is modelled for EFGM solutions. The EFGM models used in the solutions are shown in Fig. 5.2. 1089 field nodes and 1024 background cells are used for regular and irregular node distributions in the quarter model of square plate. Quartic spline is considered as weight function in this case. The normalized deflection values at the centre of square plate are used as the critical value for the evaluation of accuracy and are compared exact solution [75].

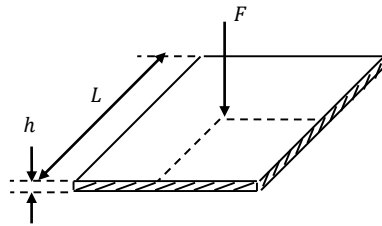


**Figure 5.1.** Clamped square plate under transverse centric point load

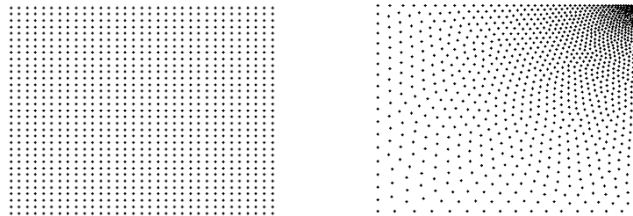


**Figure 5.2.** The EFGM models for a) regular node distributions, b) irregular node distributions

The normalized central displacement results obtained using the different values of selectable parameters values are presented in Table 5.1 to Table 5.4 and variations can be seen in Figure 5.3 to Figure 5.6. Since, the clamped square plate under transverse centric point load has stress singularity problem at the centre of plate, only displacement results are used for accuracy performance investigations. The normalized central displacements against the number of gauss points in a background cell are given in Table 5.1 and Table 5.2. The effect of value of penalty coefficient on the displacement is given in Table 5.3 and Table 5.4.

According to obtained results, it is not observed that any significant accuracy loss for regular node distribution in Fig. 5.3. However, solutions obtained by using irregular node distribution have some fluctuations are seen for value of  $n_{\text{Gauss}} = 4$  and  $n_{\text{Gauss}} = 8$  in Fig. 5.4. From Table 5.3 and 5.4 and Figures 5.5 and 5.6, it can be understood that several variations are found for value of penalty coefficient is bigger

than  $1 \times 10^9$ . If the value of penalty coefficient is selected between  $1 \times 10^6$  and  $1 \times 10^9$ , acceptable results are observed for different values of  $\alpha_s$ . However,  $\alpha_s = 2.5$  and  $mBasis = 10$  results are not shown in figures because they have unacceptable results. Also, it can be observed that the choice of small number of monomials give more accurate results.



**Table 5.1.** Normalized central deflections  $w_c / \left( \frac{pL^4}{100D} \right)$  of clamped square plate under transverse centric point load for regular node distribution with  $\alpha_p = 6$ .

Number of monomials	Number of gauss points	Dimensionless size of support domain ( $\alpha_s$ )					Exact [75]
		2.5	3.0	3.5	4.0	4.5	
<b>3</b>	4×4	0.005629	0.005637	0.005643	0.005644	0.005652	0.005600
	5×5	0.005619	0.005637	0.005641	0.005644	0.005652	
	6×6	0.005622	0.005637	0.005642	0.005644	0.005649	
	7×7	0.005621	0.005637	0.005641	0.005644	0.005650	
	8×8	0.005622	0.005637	0.005642	0.005644	0.005648	
<b>6</b>	4×4	0.005638	0.005641	0.005669	0.005650	0.005666	
	5×5	0.005636	0.005641	0.005668	0.005650	0.005666	
	6×6	0.005636	0.005641	0.005668	0.005650	0.005665	
	7×7	0.005637	0.005641	0.005668	0.005650	0.005665	
	8×8	0.005637	0.005642	0.005668	0.005650	0.005665	
<b>10</b>	4×4	-----	0.005643	0.005672	0.005677	0.005690	
	5×5	-----	0.005643	0.005672	0.005676	0.005687	
	6×6	-----	0.005643	0.005672	0.005676	0.005687	
	7×7	-----	0.005643	0.005672	0.005676	0.005687	
	8×8	-----	0.005643	0.005672	0.005677	0.005687	

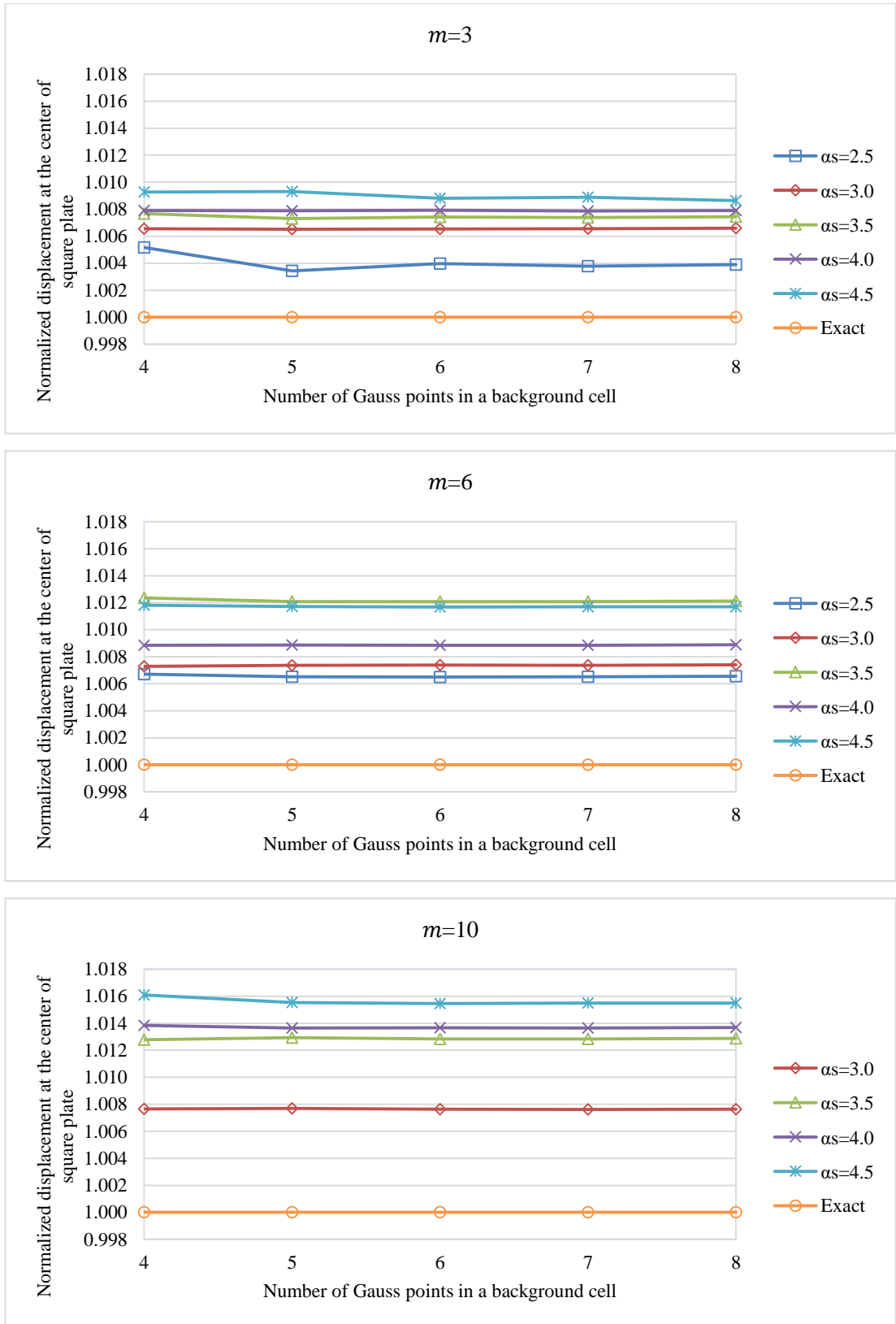


**Figure 5.3.** Variations of normalized central deflections  $w_c/\left(\frac{pL^4}{100D}\right)$  against  $n_g$  for clamped square plate under transverse centric point load and regular node distribution with  $\alpha_p = 6$ .

**Table 5.2.** Normalized central deflections  $w_c / \left( \frac{pL^4}{100D} \right)$  of clamped square plate under transverse centric point load for irregular node distribution with  $\alpha_p = 6$ .

Number of monomials	Number of gauss points	Dimensionless size of support domain ( $\alpha_s$ )					Exact [75]
		2.5	3.0	3.5	4.0	4.5	
<b>3</b>	4×4	0.005686	0.005736	0.005742	0.005801	0.005964	0.005600
	5×5	0.005642	0.005655	0.005664	0.005677	0.005718	
	6×6	0.005640	0.005646	0.005650	0.005654	0.005662	
	7×7	0.005638	0.005644	0.005648	0.005651	0.005654	
	8×8	0.005639	0.005636	0.005643	0.005686	0.005622	
<b>6</b>	4×4	0.005698	0.005714	0.005794	0.005801	0.005834	
	5×5	0.005649	0.005651	0.005661	0.005665	0.005676	
	6×6	0.005647	0.005650	0.005653	0.005656	0.005660	
	7×7	0.005646	0.005648	0.005650	0.005648	0.005648	
	8×8	0.005661	0.005628	0.005613	0.005551	0.006354	
<b>10</b>	4×4	-----	0.005812	0.005922	0.005995	0.005909	
	5×5	-----	0.005662	0.005665	0.005672	0.005675	
	6×6	-----	0.005658	0.005657	0.005664	0.005665	
	7×7	-----	0.005651	0.005656	0.005671	0.005658	
	8×8	-----	0.005694	0.005692	0.005804	0.005534	

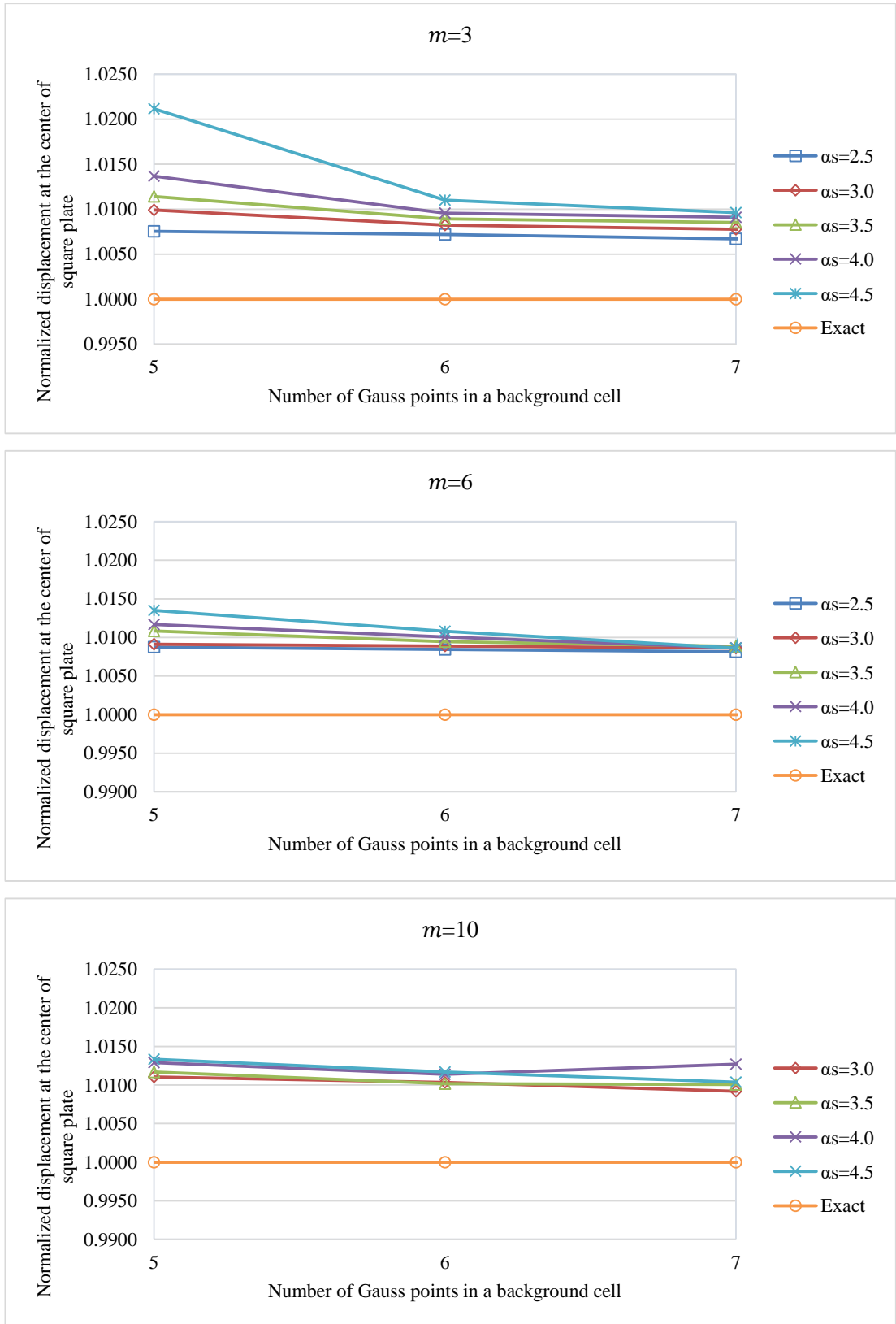


**Figure 5.4.** Variations of normalized central deflections  $w_c/\left(\frac{pL^4}{100D}\right)$  against  $n_g$  for clamped square plate under transverse centric point load using and irregular node distribution with  $\alpha_p = 6$ .

**Table 5.3.** Normalized central deflections  $w_c / \left( \frac{pL^4}{100D} \right)$  of clamped square plate under transverse centric point load using regular node distribution with  $n_g = 5$ .

Number of monomials	Value of penalty coefficient	Dimensionless size of support domain ( $\alpha_s$ )					Exact [75]
		2.5	3.0	3.5	4.0	4.5	
<b>3</b>	6	0.005619	0.005637	0.005641	0.005644	0.005652	0.005600
	7	0.005619	0.005637	0.005642	0.005650	0.005663	
	8	0.005619	0.005636	0.005639	0.005655	0.005641	
	9	0.005619	0.005636	0.005636	0.005639	0.005634	
	10	0.005619	0.005627	0.005633	0.005071	0.005596	
	11	0.005661	0.005658	0.009021	0.006120	0.007032	
<b>6</b>	6	0.005636	0.005641	0.005668	0.005650	0.005666	
	7	0.005636	0.005641	0.005667	0.005650	0.005665	
	8	0.005636	0.005641	0.005668	0.005639	0.005716	
	9	0.005637	0.005641	0.005667	0.005634	0.005693	
	10	0.005639	0.005641	0.005601	0.005950	0.006067	
	11	0.005605	0.006694	0.004530	0.001139	0.006195	
<b>10</b>	6	0.000280	0.005643	0.005672	0.005676	0.005687	
	7	0.000214	0.005643	0.005673	0.005676	0.005688	
	8	0.000465	0.005643	0.005672	0.005676	0.005672	
	9	0.000261	0.005642	0.005651	0.005680	0.005738	
	10	-0.000048	0.005665	0.005267	0.005862	0.011795	
	11	0.002589	0.005491	0.005560	0.003655	0.004805	

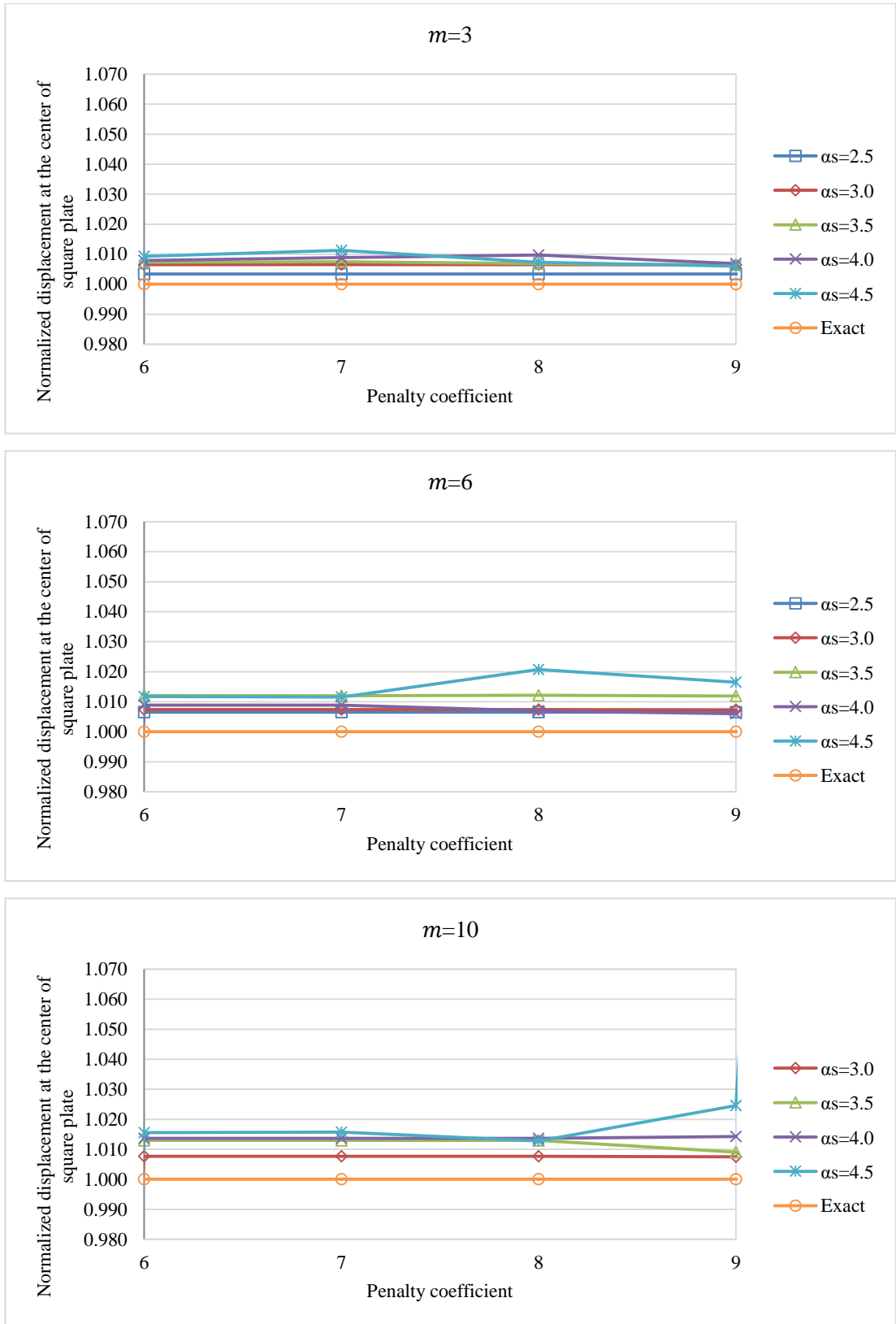


**Figure 5.5.** Variations of normalized central deflections  $w_c/\left(\frac{pL^4}{100D}\right)$  against  $\alpha_p$  for clamped square plate under transverse centric point load and regular node distribution with  $n_g = 5$ .

**Table 5.4.** Normalized central deflections  $w_c / \left( \frac{pL^4}{100D} \right)$  of clamped square plate under transverse centric point load using irregular node distribution with  $n_g = 5$ .

Number of monomials	Value of penalty coefficient	Dimensionless size of support domain ( $\alpha_s$ )					Exact [75]
		2.5	3.0	3.5	4.0	4.5	
<b>3</b>	6	0.005642	0.005655	0.005664	0.005676	0.005716	0.005600
	7	0.005642	0.005655	0.005664	0.005677	0.005718	
	8	0.005642	0.005656	0.005664	0.005676	0.005681	
	9	0.005642	0.005656	0.005654	0.005664	0.005583	
	10	0.005642	0.005550	0.005709	0.005680	0.005726	
	11	0.005788	0.005278	0.005612	0.005255	0.004676	
<b>6</b>	6	0.005649	0.005651	0.005661	0.005665	0.005675	
	7	0.005649	0.005651	0.005661	0.005665	0.005676	
	8	0.005649	0.005651	0.005661	0.005666	0.005676	
	9	0.005651	0.005650	0.005646	0.005665	0.005682	
	10	0.005655	0.005640	0.005079	0.005499	0.007328	
	11	0.005680	0.002720	-0.000739	0.012371	0.005607	
<b>10</b>	6	-0.005153	0.005662	0.005665	0.005672	0.005675	
	7	-0.000328	0.005662	0.005665	0.005672	0.005675	
	8	0.000337	0.005662	0.005666	0.005669	0.005675	
	9	0.000058	0.005663	0.005671	0.005661	0.005700	
	10	0.000397	0.005666	0.005497	0.005652	0.004943	
	11	0.000060	0.004912	0.060423	0.005582	0.005901	

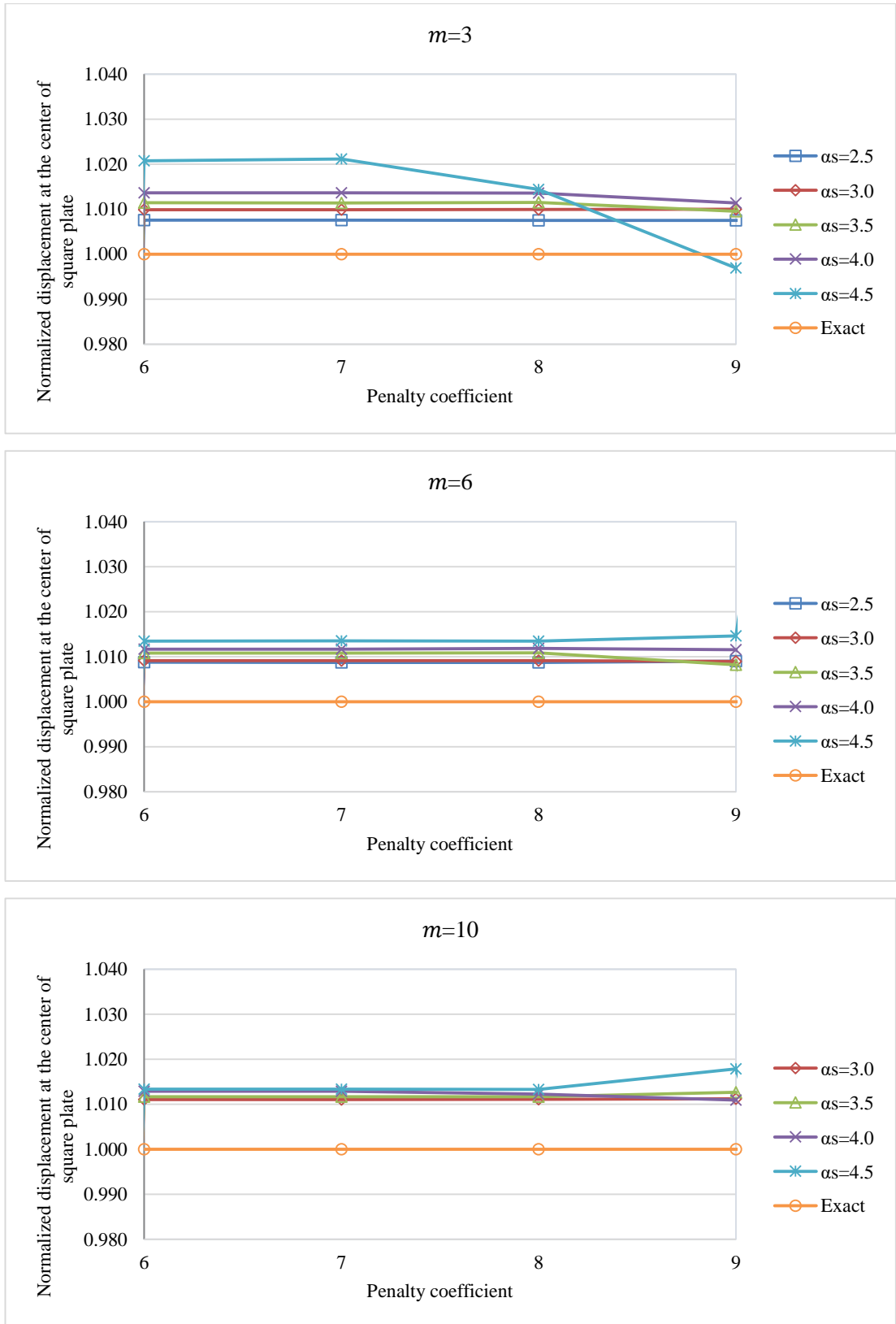


**Figure 5.6.** Variations of normalized central deflections  $w_c/\left(\frac{\rho L^4}{100D}\right)$  against  $\alpha_p$  for clamped square plate under transverse centric point load and irregular node distribution with  $n_g = 5$



### 5.3 Clamped square plate under uniform transverse load

A clamped square plate under uniform transverse load, shown in Fig. 5.7, is analysed by using different values for the selectable parameters [83]. The thickness and length of the plate are given by  $h = 0.01 \text{ m}$  and  $L = 1 \text{ m}$ , respectively. The Young's modulus  $E$  of material is  $10920 \text{ Pa}$  and Poisson's ratio is  $\nu = 0.3$ . Because of the symmetry, one quarter of the plate is modelled in EFGM solutions. In the model of square plate, 1089 field nodes and 1024 background cells are used for regular and irregular node distributions. The value of applied uniform transverse load  $P$  is  $1 \text{ Pa}$ . The normalized deflection and normalized moment values at the center of square plate are taken as the critical value for assessment of accuracy. Cubic spline is used as weight function in this example. The results obtained using different values for the selectable parameters are presented and compared with exact solutions [76] in Table 5.5 to Table 5.12.

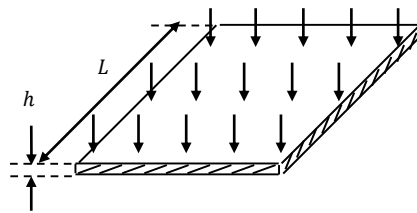


**Figure 5.7.** Clamped square plate under uniform load.

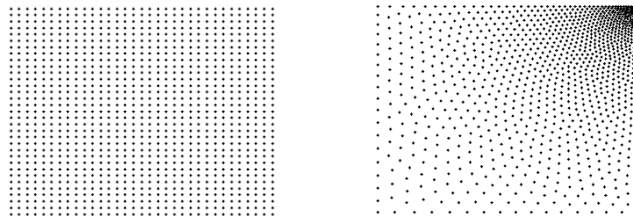


**Figure 5.8.** The EFGM models for **a)** regular node distributions, **b)** irregular node distributions

The normalized central displacements/moments against the number of gauss points in a background cell are given in Table 5.5 and Table 5.8. The effect of value of penalty coefficient on the displacement is given in Table 5.9 and Table 5.12. From the results in Table 5.5 to 5.12, it can be observed that irregularity of node distribution does not show any accuracy loss. The results of small domains seem to be more stable and more accurate. Also, it can be found that an increase for the number of gauss points results

an increase in the accuracy for the irregular node distributions and the accuracy of smaller penalty coefficients are higher than the bigger ones.

**Table 5.5.** Normalized central deflections  $w_c / \left( \frac{pL^4}{100D} \right)$  of clamped square plate subjected to uniform load for regular node distribution with  $\alpha_p = 6$ .

Number of monomials	Number of gauss points	Dimensionless size of support domain ( $\alpha_s$ )					Exact [76]
		2.5	3.0	3.5	4.0	4.5	
<b>3</b>	4×4	0.126440	0.126780	0.126909	0.126852	0.126836	0.126532
	5×5	0.126433	0.126763	0.126794	0.126826	0.126905	
	6×6	0.126439	0.126767	0.126808	0.126848	0.126778	
	7×7	0.126434	0.126766	0.126013	0.123538	0.126812	
	8×8	0.126437	0.126766	0.126839	0.126695	0.127163	
<b>6</b>	4×4	0.126770	0.126770	0.126868	0.127450	0.128110	
	5×5	0.126756	0.126771	0.126859	0.126768	0.126887	
	6×6	0.126760	0.126771	0.126860	0.127049	0.127118	
	7×7	0.126758	0.126770	0.126861	0.126915	0.126957	
	8×8	0.126759	0.126770	0.126859	0.127089	0.127085	
<b>10</b>	4×4	0.007554	0.126791	0.126879	0.127113	0.127235	
	5×5	0.001913	0.126790	0.126873	0.127169	0.127226	
	6×6	0.000925	0.126790	0.126874	0.127357	0.127214	
	7×7	-0.069174	0.126790	0.126873	0.127301	0.127217	
	8×8	0.003803	0.126790	0.126875	0.127215	0.127226	

**Table 5.6.** Normalized central moments  $M_c / \left( \frac{pL^2}{10} \right)$  of clamped square plate subjected to uniform load for regular node distribution using with  $\alpha_p = 6$ .

Number of monomials	Number of gauss points	Dimensionless size of support domain ( $\alpha_s$ )					Exact [76]
		2.5	3.0	3.5	4.0	4.5	
<b>3</b>	4×4	0.220273	0.226801	0.233437	0.234838	0.228536	0.22905
	5×5	0.220256	0.226747	0.228009	0.224284	0.230803	
	6×6	0.220309	0.226746	0.233083	0.229562	0.227977	
	7×7	0.220251	0.226761	0.160449	0.058100	0.228516	
	8×8	0.220282	0.226748	0.232194	0.213945	0.232311	
<b>6</b>	4×4	0.228807	0.227187	0.226751	0.283487	0.357014	
	5×5	0.227876	0.227075	0.226848	0.230692	0.241907	
	6×6	0.228263	0.227122	0.226788	0.247138	0.244159	
	7×7	0.228126	0.227101	0.226860	0.237759	0.237510	
	8×8	0.228147	0.227107	0.226696	0.256088	0.242944	
<b>10</b>	4×4	11.66488	0.2264135	0.2209203	0.212290	0.264404	
	5×5	-9.673737	0.2261617	0.222392	0.267805	0.269976	
	6×6	1.138023	0.2256435	0.2216954	0.317124	0.267672	
	7×7	23.62524	0.2253575	0.2220767	0.282098	0.267732	
	8×8	4.410360	0.2253424	0.2220136	0.288722	0.270582	

**Table 5.7.** Normalized central deflections  $w_c / \left( \frac{pL^4}{100D} \right)$  of clamped square plate subjected to uniform load for irregular node distribution with  $\alpha_p = 6$ .

Number of monomials	Number of gauss points	Dimensionless size of support domain ( $\alpha_s$ )					Exact [76]
		2.5	3.0	3.5	4.0	4.5	
<b>3</b>	4×4	0.126526	0.127108	0.129390	0.131393	0.132356	0.126532
	5×5	0.126468	0.126901	0.127498	0.128500	0.128037	
	6×6	0.126448	0.126819	0.127041	0.127481	0.127414	
	7×7	0.126437	0.126763	0.126898	0.127183	0.127198	
	8×8	0.126437	0.126731	0.126864	0.127017	0.127015	
<b>6</b>	4×4	0.126791	0.126832	0.127033	0.127750	0.128852	
	5×5	0.126760	0.126800	0.126878	0.127062	0.127299	
	6×6	0.126755	0.126794	0.126855	0.126968	0.127109	
	7×7	0.126753	0.126791	0.126842	0.126935	0.127027	
	8×8	0.126752	0.126791	0.126837	0.126929	0.127005	
<b>10</b>	4×4	-0.004057	0.126944	0.127063	0.127537	0.128154	
	5×5	-0.001433	0.126862	0.126888	0.127072	0.127260	
	6×6	-0.009520	0.126857	0.126870	0.127013	0.127149	
	7×7	-0.000343	0.126841	0.126864	0.126975	0.127096	
	8×8	0.017142	0.126838	0.126862	0.126968	0.127080	

**Table 5.8.** Normalized central moments  $M_c / \left( \frac{pL^2}{10} \right)$  of clamped square plate subjected to uniform load for irregular node distribution with  $\alpha_p = 6$ .

Number of monomials	Number of gauss points	Dimensionless size of support domain ( $\alpha_s$ )					Exact [76]
		2.5	3.0	3.5	4.0	4.5	
<b>3</b>	4×4	0.021998	0.021107	0.027677	0.036261	0.057237	0.22905
	5×5	0.023409	0.023524	0.026204	0.024145	0.026202	
	6×6	0.021854	0.022761	0.022327	0.023133	0.022873	
	7×7	0.022754	0.022726	0.022813	0.023184	0.023526	
	8×8	0.022403	0.022833	0.022672	0.023118	0.022976	
<b>6</b>	4×4	0.022811	0.023237	0.019257	0.016366	0.043108	
	5×5	0.023369	0.023341	0.023096	0.023736	0.025337	
	6×6	0.021578	0.022464	0.022991	0.022190	0.022951	
	7×7	0.023468	0.023040	0.022567	0.023212	0.023480	
	8×8	0.022241	0.022730	0.022987	0.022804	0.023120	
<b>10</b>	4×4	-0.026270	0.017281	0.021681	0.027778	0.029866	
	5×5	-0.032685	0.022477	0.023398	0.024282	0.018642	
	6×6	1.274110	0.020917	0.022219	0.022354	0.024074	
	7×7	-1.330267	0.023630	0.022338	0.023230	0.022410	
	8×8	0.361232	0.021181	0.023202	0.022355	0.022603	

**Table 5.9.** Normalized central deflections  $w_c / \left( \frac{pL^4}{100D} \right)$  of clamped square plate subjected to uniform load using regular node distribution with  $n_g = 5$ .

Number of monomials	Value of penalty coefficient	Dimensionless size of support domain ( $\alpha_s$ )					Exact [76]
		2.5	3.0	3.5	4.0	4.5	
<b>3</b>	6	0.126433	0.126763	0.126794	0.126826	0.126905	0.126532
	7	0.126433	0.126763	0.126214	0.126764	0.126848	
	8	0.126433	0.126764	0.126737	0.127082	0.126776	
	9	0.126436	0.126801	0.126729	0.126834	0.126565	
	10	0.126432	0.126248	0.127530	0.129988	0.126057	
	11	0.126278	0.126041	0.111635	0.134735	0.131717	
<b>6</b>	6	0.126756	0.126771	0.126859	0.126768	0.126887	
	7	0.126756	0.126771	0.126865	0.126999	0.126907	
	8	0.126756	0.126772	0.129389	0.126375	0.126852	
	9	0.126758	0.126783	0.127891	0.125890	0.127375	
	10	0.126951	0.124576	0.129112	0.125334	0.129903	
	11	0.127008	0.123518	0.129367	0.124725	0.062518	
<b>10</b>	6	0.001913	0.126790	0.126873	0.127169	0.127226	
	7	0.017516	0.126790	0.126869	0.127334	0.127305	
	8	-0.001358	0.126787	0.126941	0.127336	0.127672	
	9	0.011062	0.126802	0.126606	0.126857	0.145203	
	10	0.001619	0.126975	0.132896	0.124583	0.131461	
	11	-0.191121	0.129141	0.135977	0.073397	0.145359	

**Table 5.10.** Normalized central moments  $M_c / \left( \frac{pL^2}{10} \right)$  of clamped square plate subjected to uniform load using regular node distribution with  $n_g = 5$ .

Number of monomials	Value of penalty coefficient	Dimensionless size of support domain ( $\alpha_s$ )					Exact [76]
		2.5	3.0	3.5	4.0	4.5	
<b>3</b>	6	0.222778	0.228234	0.229455	0.225712	0.231116	0.22905
	7	0.222778	0.228235	0.197497	0.229492	0.226305	
	8	0.222779	0.228273	0.228941	0.231400	0.229474	
	9	0.222796	0.228899	0.246187	0.228458	0.226305	
	10	0.223014	0.225801	0.205424	0.233262	0.228310	
	11	0.222326	0.227809	0.219824	0.284981	0.215284	
<b>6</b>	6	0.228165	0.227480	0.227903	0.231240	0.241860	
	7	0.228163	0.227482	0.228011	0.248146	0.233347	
	8	0.228159	0.227547	0.214909	0.188005	0.228315	
	9	0.228170	0.227141	0.250154	0.316561	0.109148	
	10	0.229887	0.509683	0.185733	0.199848	0.422719	
	11	0.213197	0.240821	0.669066	0.364602	0.802180	
<b>10</b>	6	-----	0.226334	0.223033	0.286704	0.270394	
	7	-----	0.226322	0.223115	0.259484	0.252641	
	8	-----	0.226397	0.223542	0.252302	0.247275	
	9	-----	0.226106	0.240292	0.003620	0.748420	
	10	-----	0.233004	0.237098	1.836826	1.056695	
	11	-----	0.320446	1.895828	0.460924	6.398777	



**Table 5.11.** Normalized central deflections  $w_c / \left( \frac{pL^4}{100D} \right)$  of clamped square plate subjected to uniform load using irregular node distribution with  $n_g = 5$ .

Number of monomials	Value of penalty coefficient	Dimensionless size of support domain ( $\alpha_s$ )					Exact [76]
		2.5	3.0	3.5	4.0	4.5	
<b>3</b>	6	0.126468	0.126901	0.127498	0.128500	0.128037	0.126532
	7	0.126468	0.126901	0.127496	0.128494	0.128307	
	8	0.126467	0.126901	0.127485	0.128406	0.127735	
	9	0.126479	0.126895	0.126604	0.128657	0.127684	
	10	0.126330	0.126486	0.128813	0.130046	0.126236	
	11	0.125608	0.059782	0.130317	0.118880	0.164985	
<b>6</b>	6	0.126760	0.126800	0.126878	0.127062	0.127299	
	7	0.126760	0.126800	0.126878	0.127060	0.127293	
	8	0.126759	0.126797	0.126881	0.127047	0.127288	
	9	0.126777	0.126796	0.126869	0.126914	0.126754	
	10	0.127332	0.126829	0.126812	0.145521	0.121012	
	11	0.133478	0.129931	0.137213	0.141025	0.141995	
<b>10</b>	6	-0.001433	0.126862	0.126888	0.127072	0.127260	
	7	-0.012535	0.126862	0.126891	0.127075	0.127266	
	8	0.147390	0.126869	0.126895	0.127055	0.127272	
	9	-0.000455	0.126922	0.127046	0.126714	0.111222	
	10	-0.000074	0.126081	0.128956	0.130919	0.159409	
	11	0.000004	0.133288	-0.058304	0.043413	0.044011	

**Table 5.12.** Normalized central moments  $M_c / \left(\frac{pL^2}{10}\right)$  of clamped square plate subjected to uniform load using irregular node distribution with  $n_g = 5$ .

Number of monomials	Value of penalty coefficient	Dimensionless size of support domain ( $\alpha_s$ )					Exact [76]
		2.5	3.0	3.5	4.0	4.5	
<b>3</b>	6	0.231408	0.235186	0.262691	0.231896	0.259817	0.22905
	7	0.231402	0.235174	0.262759	0.234450	0.252804	
	8	0.231328	0.235297	0.265312	0.217930	0.222152	
	9	0.230140	0.230743	0.210371	0.124551	0.238444	
	10	0.235161	0.357763	3.927675	0.271700	0.198007	
	11	0.234608	1.875189	0.224397	0.698783	0.378160	
<b>6</b>	6	0.233808	0.232184	0.231906	0.235700	0.253998	
	7	0.233808	0.232174	0.231761	0.235217	0.246653	
	8	0.233962	0.231705	0.232194	0.236094	0.210382	
	9	0.225913	0.246280	0.242021	0.222640	0.277255	
	10	0.197897	0.242759	0.245568	2.687105	0.146298	
	11	0.271154	4.881884	0.357481	1.502087	0.586453	
<b>10</b>	6	0.130951	0.243652	0.233719	0.244129	0.188343	
	7	0.198299	0.243399	0.231613	0.237502	0.191071	
	8	0.215736	0.235826	0.236902	0.245416	0.091169	
	9	-0.752781	0.320773	0.263018	0.287695	0.102685	
	10	0.342614	0.565406	0.707094	2.294113	0.512227	
	11	1.063893	4.553931	3.670624	4.143685	0.762874	

#### 5.4 Simply supported circular plate under uniform load

A simply supported circular plate under uniform transverse load, shown in Fig. 5.29, is examined as a third numerical example [83]. The thickness, radius, Young's modulus and Poisson's ratio are  $h = 1\text{ m}$ ,  $R = 5\text{ m}$ ,  $10.92\text{ Pa}$ , and  $\nu = 0.3$ , respectively. Due to the symmetry, one quarter of the plate is modelled. In the model of quarter circular plate, 817 field nodes and 768 background cells are used for regular and irregular node distributions. The value of applied uniform transverse load  $P$  is  $1\text{ Pa}$ . Table 5.13 to Table 5.20 provide normalized deflection and moment and comparison with exact solutions [76] using different values of the selectable parameters by using quartic spline weight function.

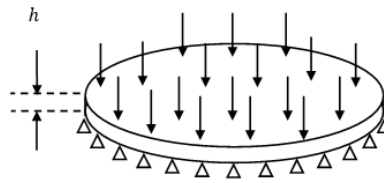


**Figure 5.9.** Simply supported circular plate under uniform load.

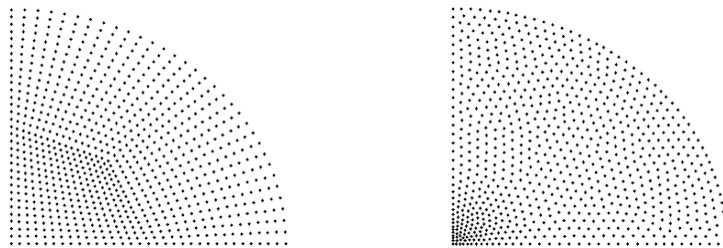


**Figure 5.10.** The EFGM models for **a)** regular node distributions, **b)** irregular node distributions

The normalized central displacements/moments against the number of gauss points in a background cell are given in Table 5.13 and Table 5.16. The effect of value of penalty coefficient on the displacement is given in Table 5.17 and Table 5.20. It can be found from the results in Table 5.13-5.20 that irregularity of node distribution shows small fluctuations for moments, an increase for the order of monomials does not always result an increase in accuracy, the smaller penalty coefficients increase the accuracy of results.

**Table 5.13.** Normalized central deflections  $w_c / \left( \frac{pL^4}{100D} \right)$  of simply supported circular plate subjected to uniform load for regular node distribution with  $\alpha_p = 6$ .

Number of monomials	Number of gauss points	Dimensionless size of support domain ( $\alpha_s$ )					Exact [76]
		2.5	3.0	3.5	4.0	4.5	
<b>3</b>	4×4	0.665931	0.666042	0.666102	0.666105	0.666254	0.665600
	5×5	0.665933	0.666047	0.666121	0.666100	0.666272	
	6×6	0.665932	0.666047	0.666106	0.666098	0.666267	
	7×7	0.665932	0.666046	0.666116	0.666101	0.666265	
	8×8	0.665931	0.666046	0.666108	0.666098	0.666323	
<b>6</b>	4×4	0.665871	0.665972	0.666509	0.666368	0.666552	
	5×5	0.665870	0.665971	0.666495	0.666368	0.666520	
	6×6	0.665871	0.665971	0.666505	0.666368	0.666533	
	7×7	0.665870	0.665971	0.666499	0.666368	0.666527	
	8×8	0.665869	0.665970	0.666502	0.666367	0.666526	
<b>10</b>	4×4	0.004753	0.085714	0.666467	0.667353	0.667174	
	5×5	-0.027194	-0.038747	0.666436	0.667324	0.667152	
	6×6	0.026288	0.080240	0.666416	0.667322	0.667153	
	7×7	-0.001611	-0.031465	0.666419	0.667325	0.667147	
	8×8	0.001901	0.012682	0.666414	0.667318	0.667147	

**Table 5.14.** Normalized central moments  $M_c / \left(\frac{pL^2}{10}\right)$  of simply supported circular plate subjected to uniform load for regular node distribution with  $\alpha_p = 6$ .

Number of monomials	Number of gauss points	Dimensionless size of support domain ( $\alpha_s$ )					Exact [76]
		2.5	3.0	3.5	4.0	4.5	
<b>3</b>	4×4	2.005078	2.029307	2.049496	2.053753	2.071245	2.062344
	5×5	2.005447	2.029614	2.049892	2.053702	2.071104	
	6×6	2.005517	2.029666	2.049522	2.053578	2.071281	
	7×7	2.005341	2.029566	2.049800	2.053667	2.071092	
	8×8	2.005548	2.029562	2.049635	2.053637	2.071519	
<b>6</b>	4×4	2.040578	1.974229	2.056917	2.050842	2.086076	
	5×5	2.032278	1.973078	2.055204	2.052620	2.086334	
	6×6	2.037076	1.973751	2.056129	2.052318	2.085494	
	7×7	2.033614	1.973492	2.056071	2.052388	2.085883	
	8×8	2.036204	1.973332	2.055370	2.052219	2.085808	
<b>10</b>	4×4	-2305.325	216.5278	2.040810	2.418292	2.311396	
	5×5	602.6892	-208.0641	2.041055	2.382921	2.290838	
	6×6	-935.5124	-12.22692	2.033994	2.377163	2.298903	
	7×7	22.12304	165.3259	2.038753	2.388402	2.294604	
	8×8	760.4520	12.31105	2.039714	2.384878	2.295134	

**Table 5.15.** Normalized central deflections  $w_c / \left( \frac{pL^4}{100D} \right)$  of simply supported circular plate subjected to uniform load for irregular node distribution with  $\alpha_p = 6$ .

Number of monomials	Number of gauss points	Dimensionless size of support domain ( $\alpha_s$ )					Exact [76]
		2.5	3.0	3.5	4.0	4.5	
<b>3</b>	4×4	0.665990	0.666097	0.666268	0.666176	0.666300	0.665600
	5×5	0.665970	0.666008	0.666088	0.666062	0.666143	
	6×6	0.665974	0.665983	0.666033	0.666025	0.666049	
	7×7	0.665970	0.665989	0.666020	0.666022	0.666048	
	8×8	0.665970	0.665983	0.666013	0.666015	0.666048	
<b>6</b>	4×4	0.666006	0.665990	0.666038	0.666084	0.666165	
	5×5	0.665993	0.665987	0.665990	0.666038	0.666067	
	6×6	0.665992	0.665986	0.665987	0.666039	0.666048	
	7×7	0.665992	0.665985	0.665987	0.666023	0.666051	
	8×8	0.665991	0.665985	0.665985	0.666028	0.666048	
<b>10</b>	4×4	0.678353	0.666031	0.666020	0.666090	0.666225	
	5×5	0.670335	0.665991	0.666002	0.666043	0.666106	
	6×6	0.669178	0.665982	0.665992	0.666030	0.666092	
	7×7	0.668574	0.665979	0.665991	0.666022	0.666068	
	8×8	0.667464	0.665977	0.665989	0.666024	0.666073	

**Table 5.16.** Normalized central moments  $M_c / \left(\frac{pL^2}{10}\right)$  of simply supported circular plate subjected to uniform load for irregular node distribution with  $\alpha_p = 6$ .

Number of monomials	Number of gauss points	Dimensionless size of support domain ( $\alpha_s$ )					Exact [76]
		2.5	3.0	3.5	4.0	4.5	
<b>3</b>	4×4	2.059970	2.044946	2.000748	2.039810	2.052553	2.062344
	5×5	2.047096	2.060184	2.071364	2.051118	2.057045	
	6×6	2.051420	2.052160	2.057042	2.063346	2.058350	
	7×7	2.049566	2.051656	2.052576	2.052570	2.059945	
	8×8	2.049352	2.052420	2.057177	2.057336	2.060921	
<b>6</b>	4×4	2.053699	2.059687	2.027205	1.998922	2.018057	
	5×5	2.065549	2.058194	2.064023	2.080776	2.050086	
	6×6	2.079550	2.057942	2.048976	2.060772	2.047013	
	7×7	2.084744	2.056180	2.047976	2.053766	2.049384	
	8×8	2.070313	2.055901	2.049883	2.057525	2.047272	
<b>10</b>	4×4	40.86512	2.137203	2.068406	1.939528	2.043022	
	5×5	13.32584	2.091290	1.959436	2.076705	2.086221	
	6×6	6.295620	2.054560	2.016260	2.011183	2.043642	
	7×7	3.465794	2.069183	2.000256	2.025050	2.055499	
	8×8	2.296053	2.044456	2.011382	2.021311	2.045132	

**Table 5.17.** Normalized central deflections  $w_c / \left( \frac{pL^4}{100D} \right)$  of simply supported circular plate subjected to uniform load using regular node distribution with  $n_g = 5$ .

Number of monomials	Value of penalty coefficient	Dimensionless size of support domain ( $\alpha_s$ )					Exact [76]
		2.5	3.0	3.5	4.0	4.5	
<b>3</b>	6	0.665933	0.666047	0.666121	0.666100	0.666272	0.665600
	7	0.665933	0.666048	0.666121	0.666100	0.666272	
	8	0.665933	0.666048	0.666121	0.666100	0.666272	
	9	0.665933	0.666047	0.666121	0.666100	0.666272	
	10	0.665934	0.666048	0.666121	0.666096	0.666297	
	11	0.665935	0.666031	0.666110	0.666279	0.665609	
<b>6</b>	6	0.665870	0.665971	0.666495	0.666368	0.666520	
	7	0.665870	0.665971	0.666495	0.666368	0.666520	
	8	0.665870	0.665971	0.666495	0.666368	0.666520	
	9	0.665870	0.665971	0.666495	0.666368	0.666519	
	10	0.665870	0.665968	0.666499	0.666368	0.666514	
	11	0.665837	0.665958	0.666534	0.666385	0.666624	
<b>10</b>	6	-0.027194	-0.038747	0.666436	0.667324	0.667152	
	7	0.000307	0.379188	0.666436	0.667324	0.667152	
	8	-0.021853	0.080286	0.666436	0.667324	0.667152	
	9	0.035885	-0.312649	0.666436	0.667324	0.667152	
	10	-0.059948	-0.001439	0.666435	0.667329	0.667151	
	11	0.017107	-0.215847	0.666451	0.667153	0.667138	



**Table 5.18.** Normalized central moments  $M_c / \left( \frac{pL^2}{10} \right)$  of simply supported circular plate subjected to uniform load using regular node distribution with  $n_g = 5$ .

Number of monomials	Value of penalty coefficient	Dimensionless size of support domain ( $\alpha_s$ )					Exact [76]
		2.5	3.0	3.5	4.0	4.5	
<b>3</b>	6	2.038665	2.051753	2.062857	2.062440	2.074044	2.062344
	7	2.038666	2.051753	2.062857	2.062441	2.074045	
	8	2.038664	2.051759	2.062858	2.062439	2.074070	
	9	2.038621	2.051762	2.062860	2.062476	2.074317	
	10	2.038768	2.052071	2.062705	2.062607	2.075679	
	11	2.037018	2.049616	2.063898	2.060986	2.045592	
<b>6</b>	6	2.038260	1.990853	2.067618	2.059376	2.092070	
	7	2.038259	1.990852	2.067619	2.059379	2.092067	
	8	2.038254	1.990833	2.067594	2.059388	2.092056	
	9	2.038096	1.991126	2.067880	2.059279	2.091862	
	10	2.039576	1.991938	2.068262	2.060470	2.095709	
	11	2.038165	1.983722	-----	2.061213	2.150306	
<b>10</b>	6	40.31616	34.00839	2.047673	2.384500	2.290476	
	7	28.69866	59.78704	2.047688	2.384441	2.290471	
	8	13.01323	1211.134	2.047688	2.384977	2.290531	
	9	46.24900	70.77776	2.047242	2.383174	2.290936	
	10	15.95353	127.5712	2.049562	2.398362	2.290834	
	11	6.116528	39.44529	2.042506	2.289148	2.298392	

**Table 5.19.** Normalized central deflections  $w_c / \left( \frac{pL^4}{100D} \right)$  of simply supported circular plate subjected to uniform load using irregular node distribution with  $n_g = 5$ .

Number of monomials	Value of penalty coefficient	Dimensionless size of support domain ( $\alpha_s$ )					Exact [76]
		2.5	3.0	3.5	4.0	4.5	
<b>3</b>	6	0.665978	0.666024	0.666042	0.666043	0.666058	0.665600
	7	0.665978	0.666024	0.666042	0.666043	0.666058	
	8	0.665978	0.666024	0.666042	0.666043	0.666058	
	9	0.665978	0.666024	0.666042	0.666043	0.666058	
	10	0.665977	0.666024	0.666043	0.666042	0.666059	
	11	0.665978	0.666028	0.666044	0.666039	0.666054	
<b>6</b>	6	0.665994	0.665996	0.666032	0.666055	0.666078	
	7	0.665994	0.665996	0.666032	0.666055	0.666078	
	8	0.665994	0.665996	0.666032	0.666055	0.666078	
	9	0.665994	0.665996	0.666032	0.666055	0.666078	
	10	0.665995	0.665995	0.666032	0.666053	0.666082	
	11	0.665993	0.665980	0.666015	0.666053	0.666065	
<b>10</b>	6	0.671484	0.666017	0.666065	0.666102	0.666131	
	7	0.671495	0.666017	0.666065	0.666102	0.666131	
	8	0.671422	0.666017	0.666065	0.666102	0.666131	
	9	0.671423	0.666018	0.666065	0.666102	0.666131	
	10	0.672539	0.666017	0.666062	0.666111	0.666132	
	11	0.705717	0.666027	0.666156	0.666131	0.666201	

**Table 5.20.** Normalized central moments  $M_c / \left(\frac{pL^2}{10}\right)$  of simply supported circular plate subjected to uniform load using irregular node distribution with  $n_g = 5$ .

Number of monomials	Value of penalty coefficient	Dimensionless size of support domain ( $\alpha_s$ )					Exact [76]
		2.5	3.0	3.5	4.0	4.5	
<b>3</b>	6	2.059636	2.060674	2.059273	2.056814	2.060339	2.062344
	7	2.059636	2.060674	2.059273	2.056814	2.060339	
	8	2.059650	2.060674	2.059276	2.056816	2.060339	
	9	2.059532	2.060759	2.059229	2.056857	2.060350	
	10	2.059328	2.060444	2.059252	2.056824	2.060097	
	11	2.055589	2.060238	2.059215	2.056537	2.062454	
<b>6</b>	6	2.055047	2.036481	2.034838	2.063106	2.048245	
	7	2.055046	2.036486	2.034840	2.063098	2.048245	
	8	2.054987	2.036496	2.034741	2.063091	2.048287	
	9	2.055207	2.037036	2.035031	2.062719	2.048693	
	10	2.056375	2.034727	2.035754	2.063723	2.046757	
	11	2.052038	2.038904	2.033516	2.068601	2.061346	
<b>10</b>	6	17.86555	2.076705	1.855043	2.064847	2.046155	
	7	17.84520	2.076680	1.855018	2.064868	2.046150	
	8	18.73009	2.076745	1.855431	2.064868	2.046170	
	9	7.851396	2.075146	1.854292	2.060386	2.047742	
	10	4.338912	2.070534	1.857914	2.046806	2.049600	
	11	530.4940	2.168797	1.892390	2.195134	2.134634	

### 5.5 Simply supported Morley's skew plate under uniform transverse load

The Morley's skew plate has simply supported boundary conditions with all edge and is loaded with uniform transverse load as shown in Fig.5.1. The material properties are as follows; Young's modulus  $E$  of material is 1092000 Pa and Poisson's ratio is  $\nu = 0.3$ . The thickness and length of the plate are given by  $h = 20$  m and  $L = 50$  m, respectively. Due to the asymmetry, the whole plate is modelled. In the model of whole skew plate, 289 field nodes and 256 background cells are used for regular and irregular node distributions. The value of applied uniform transverse load  $P$  is 1 Pa. Figure 5.13 to Figure 5.24 provide variations of normalized deflection, normalized maximum and minimum moments with different values of the selectable parameters by using cubic spline weight function, respectively.

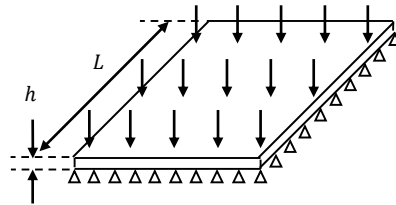


**Figure 5.11.** Simply supported Morley's skew plate under uniform load



**Figure 5.12.** The EFGM models for **a)** regular node distributions, **b)** irregular node distributions

The variations according to obtained results of normalized displacements, maximum and minimum moments using the different values of selectable parameters values are presented and compared with exact solutions [77] in Figure 5.13 to Table 5.24. The variations against the number of gauss points in a background cell are given in Table 5.13 to Table 5.18. The effect of value of penalty coefficient on the displacement is given in Table 5.19 and Table 5.24.

According to displacement results, it is observed that obtained results by using irregular node distribution are closer to exact solutions than regular ones. There is no significant difference between regularity and irregularity for maximum and moment results. It can be said that 3 monomials are enough to get acceptable results for different values of  $\alpha_s$ . However, some fluctuations are seen for value of nGauss = 8 and penalty coefficient is  $1 \times 10^{11}$ .

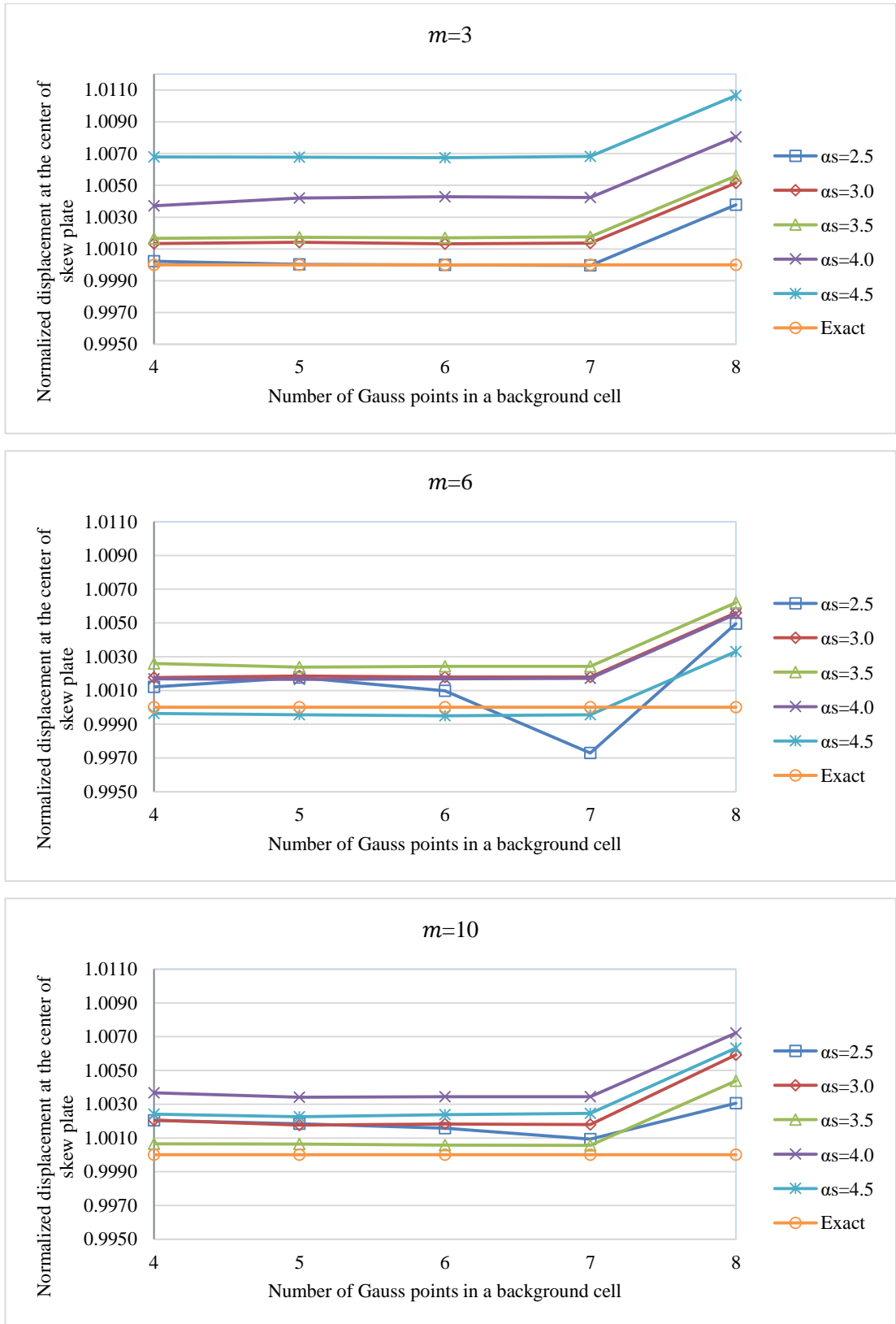


**Figure 5.13.** Variations of normalized central deflections  $w_c / \left( \frac{pL^4}{100D} \right)$  against  $n_g$  for simply supported skew plate subjected to uniform load and regular node distribution with  $\alpha_p = 6$ .

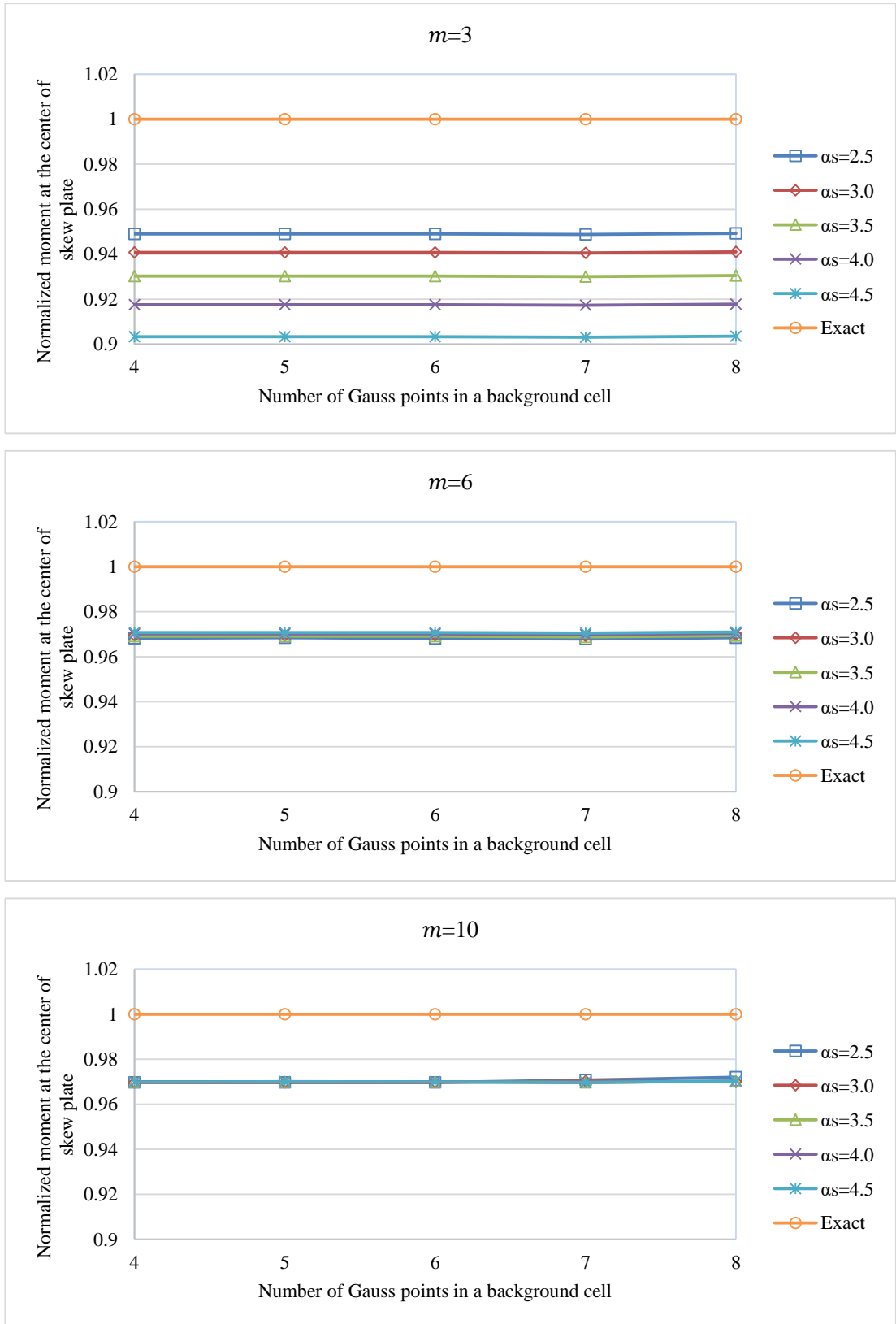


**Figure 5.14.** Variations of normalized central maximum moments  $M_c / \left( \frac{pL^2}{10} \right)$  against  $n_g$  for simply supported skew plate subjected to uniform load and regular node distribution with  $\alpha_p = 6$ .

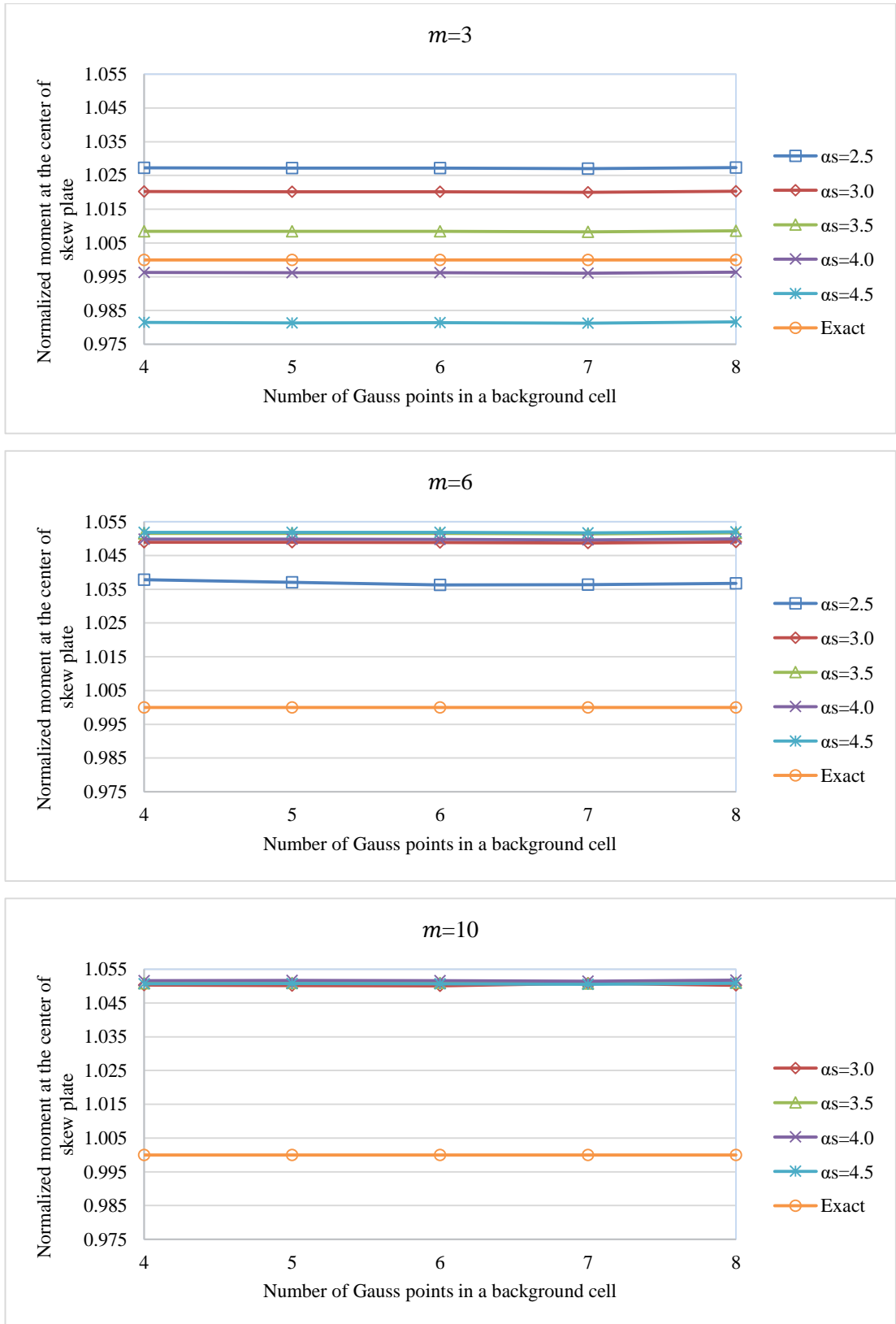


**Figure 5.15.** Variations of normalized central minimum moments  $M_c / \left( \frac{pL^2}{10} \right)$  against  $n_g$  for simply supported skew plate subjected to uniform load and regular node distribution with  $\alpha_p = 6$ .



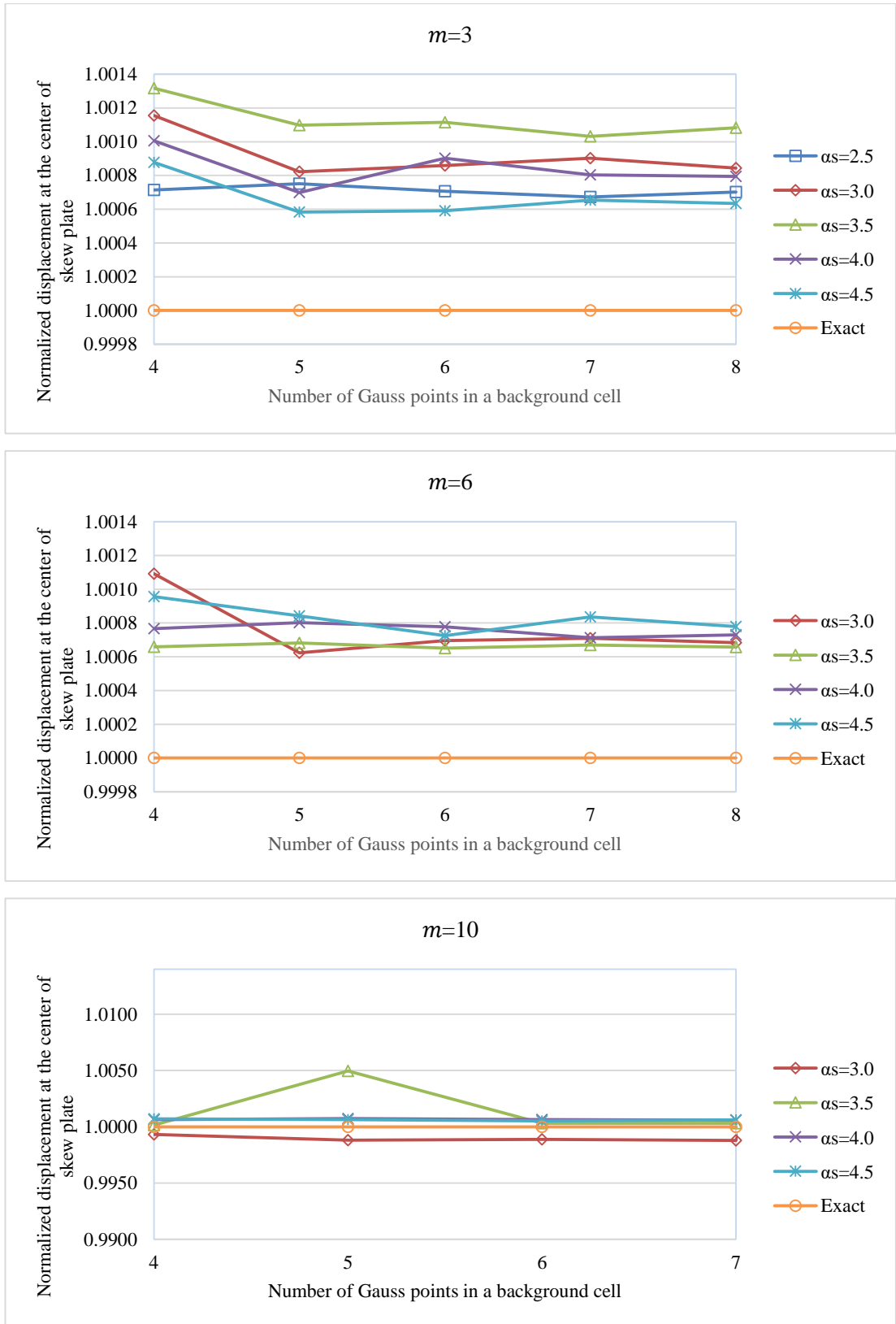


**Figure 5.16.** Variations of normalized central deflections  $w_c / \left( \frac{pL^4}{100D} \right)$  against  $n_g$  for simply supported skew plate subjected to uniform load and irregular node distribution with  $\alpha_p = 6$ .

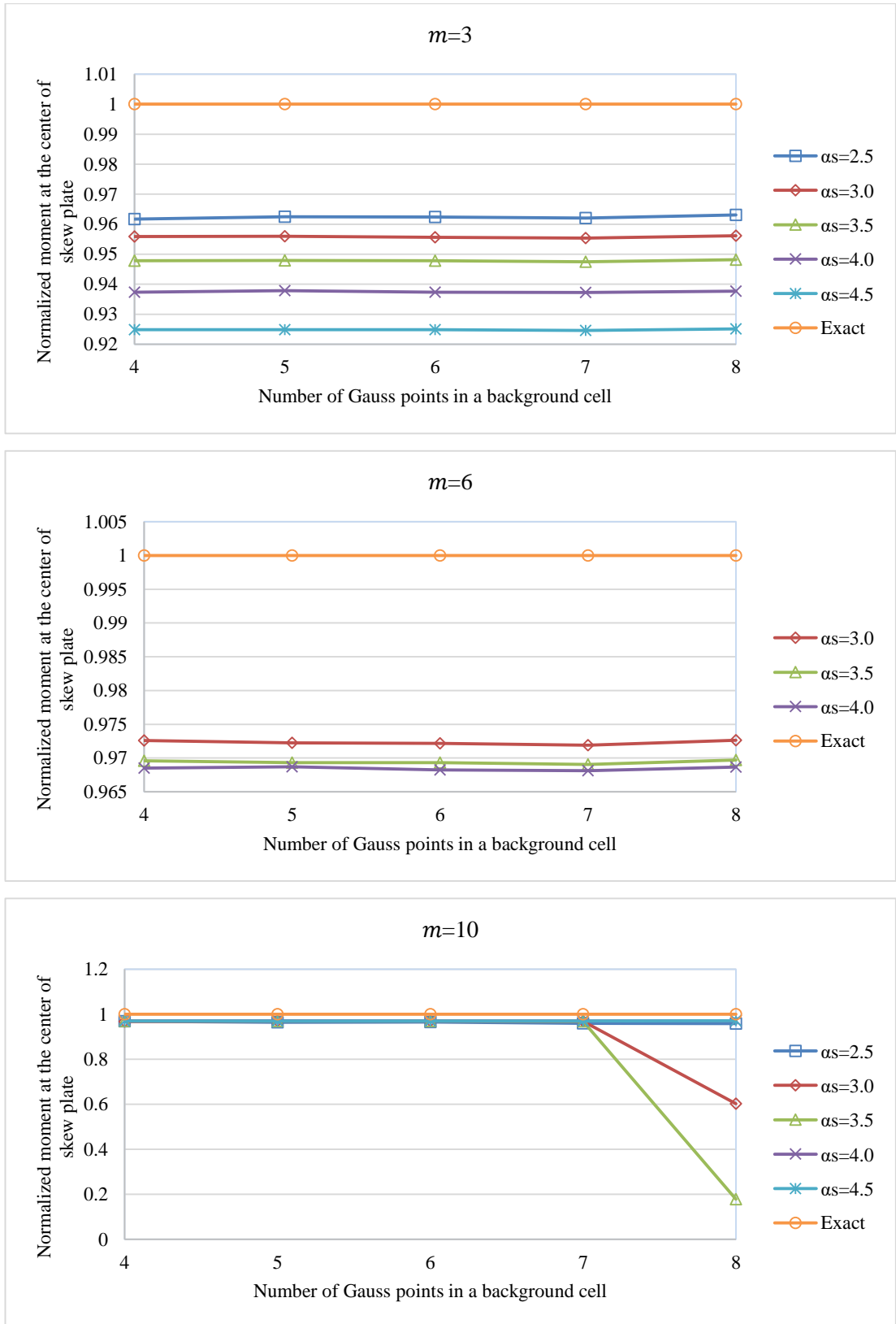


**Figure 5.17.** Variations of normalized central maximum moments  $M_c / \left( \frac{pL^2}{10} \right)$  against  $n_g$  for simply supported skew plate subjected to uniform load and irregular node distribution with  $\alpha_p = 6$ .

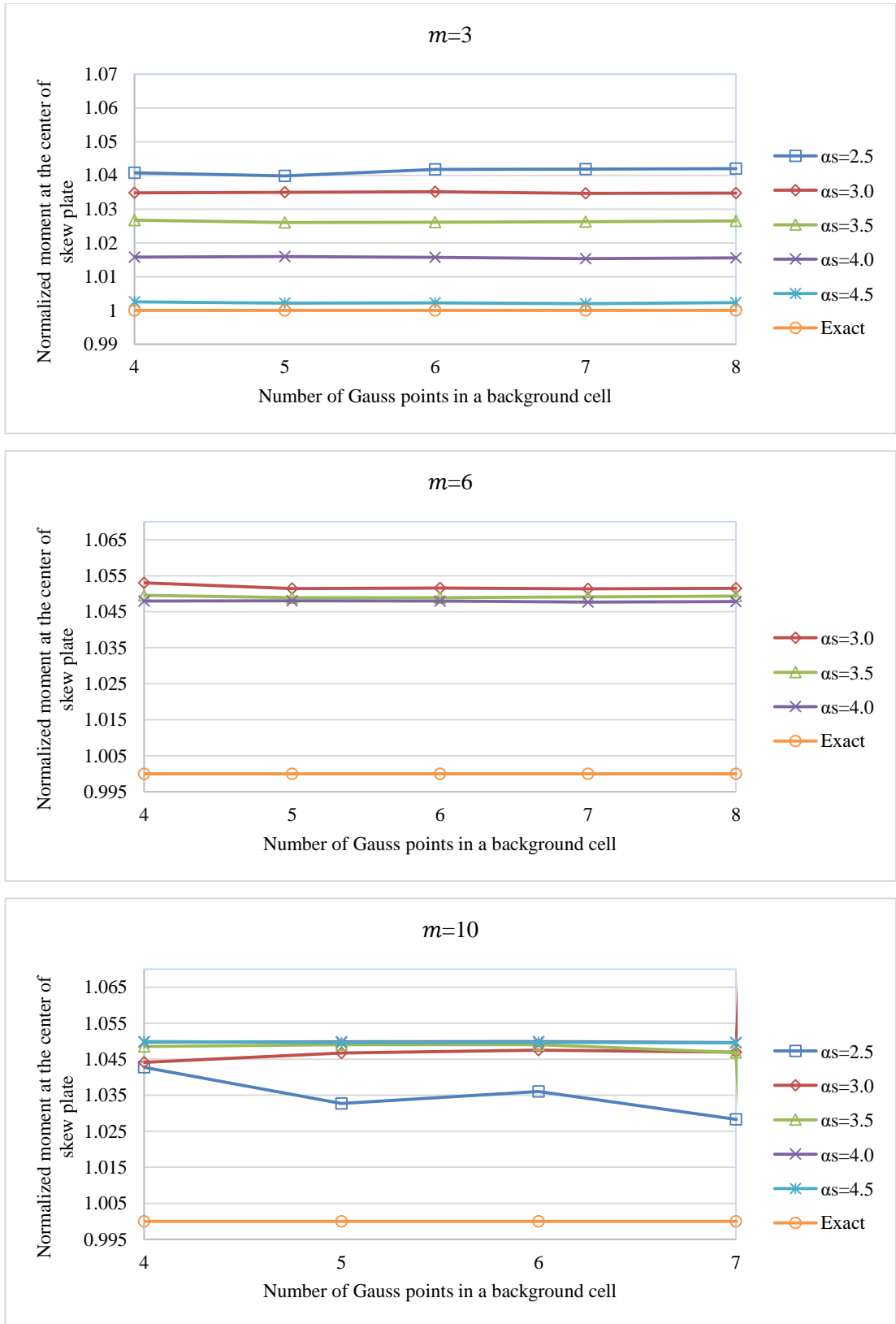


**Figure 5.18.** Variations of normalized central minimum moments  $M_c / \left( \frac{pL^2}{10} \right)$  against  $n_g$  for simply supported skew plate subjected to uniform load and irregular node distribution with  $\alpha_p = 6$ .

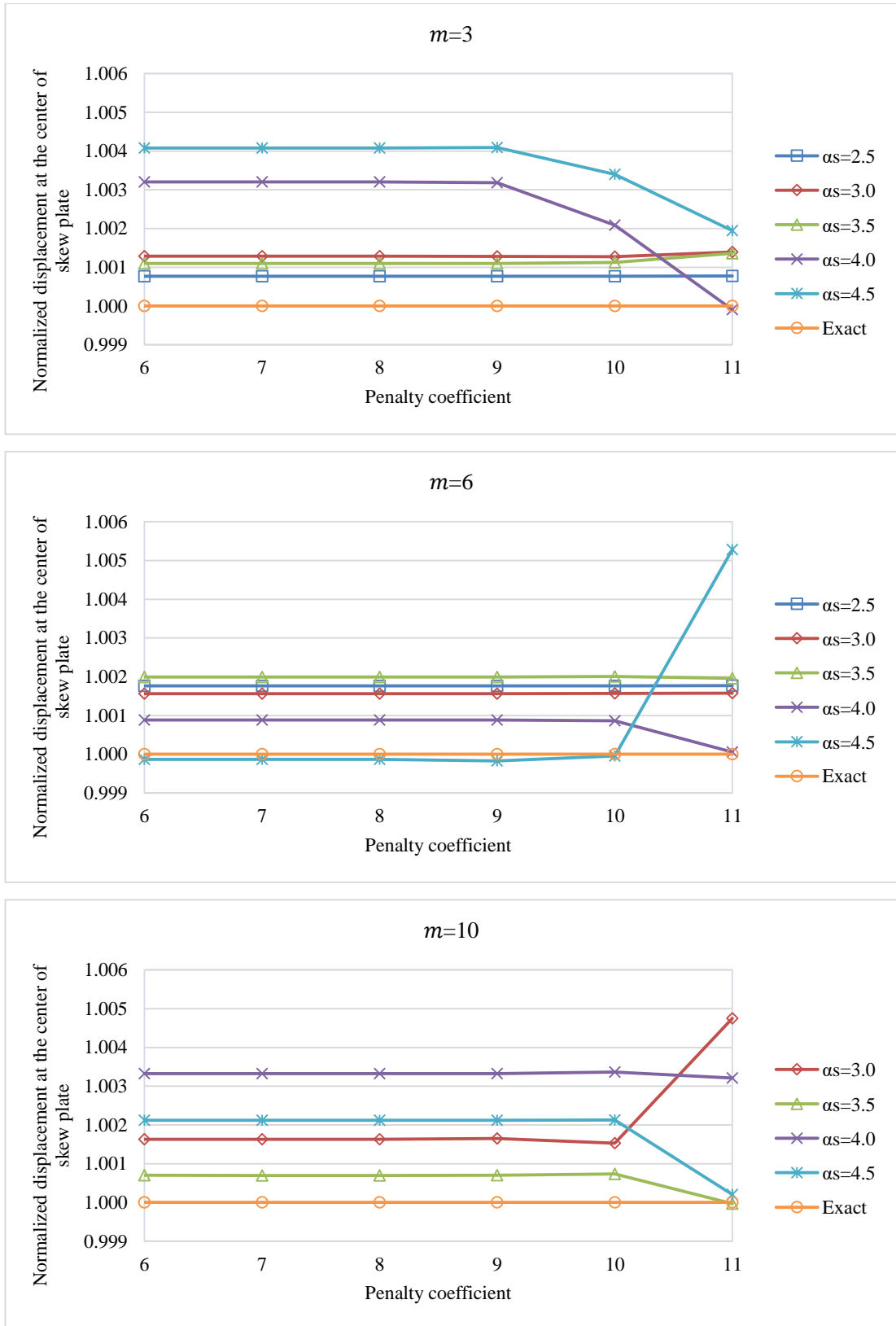


**Figure 5.19.** Variations of normalized central deflections  $w_c / \left( \frac{\rho L^4}{100D} \right)$  against  $\alpha_p$  for simply supported skew plate subjected to uniform load and regular node distribution with  $n_g = 5$ .

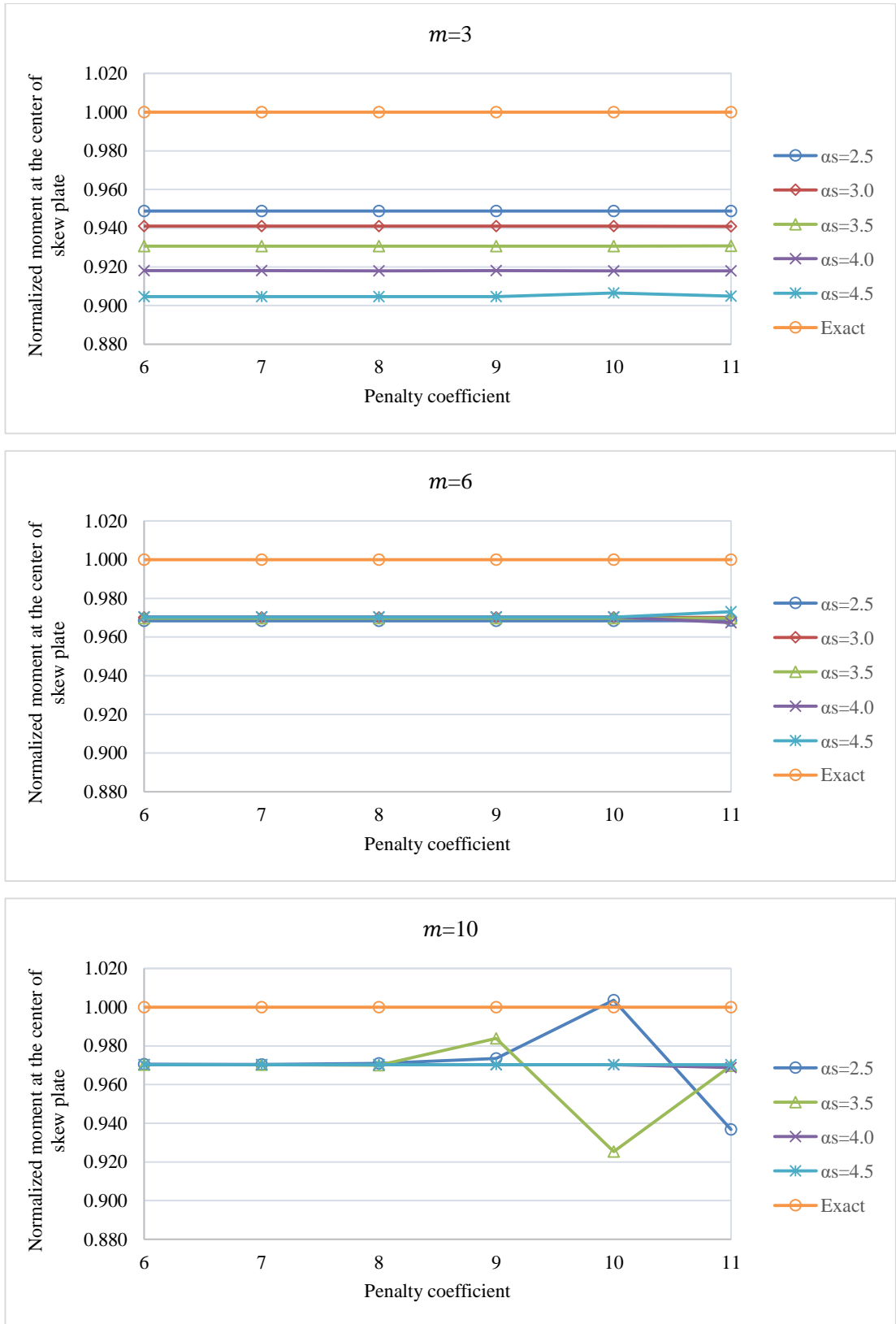


**Figure 5.20.** Variations of normalized central maximum moments  $M_c / \left( \frac{\rho L^2}{10} \right)$  against  $\alpha_p$  for simply supported skew plate subjected to uniform load and regular node distribution with  $n_g = 5$ .

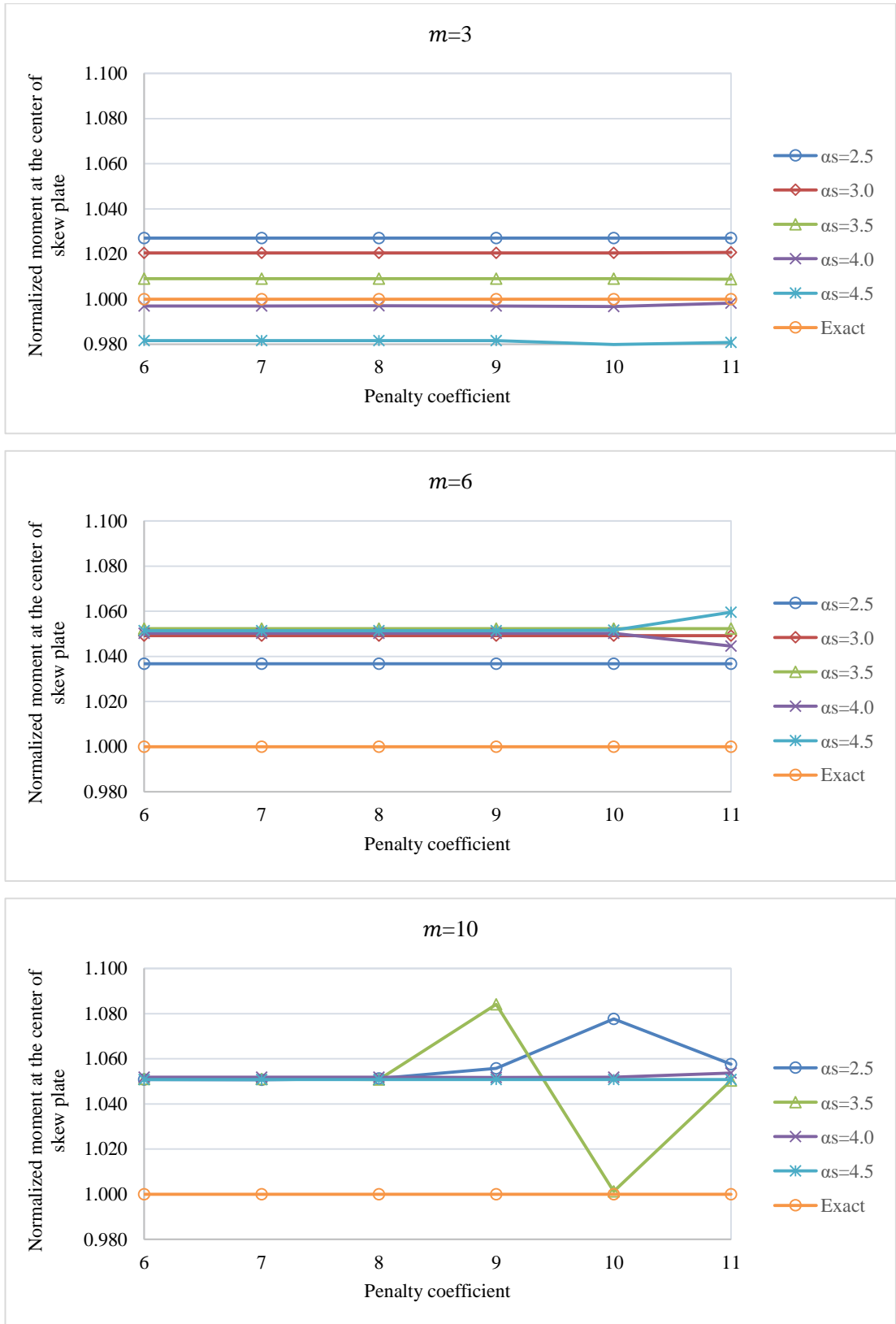


**Figure 5.21.** Variations of normalized central minimum moments  $M_c / \left( \frac{pL^2}{10} \right)$  against  $\alpha_p$  for simply supported skew plate subjected to uniform load and regular node distribution with  $n_g = 5$ .

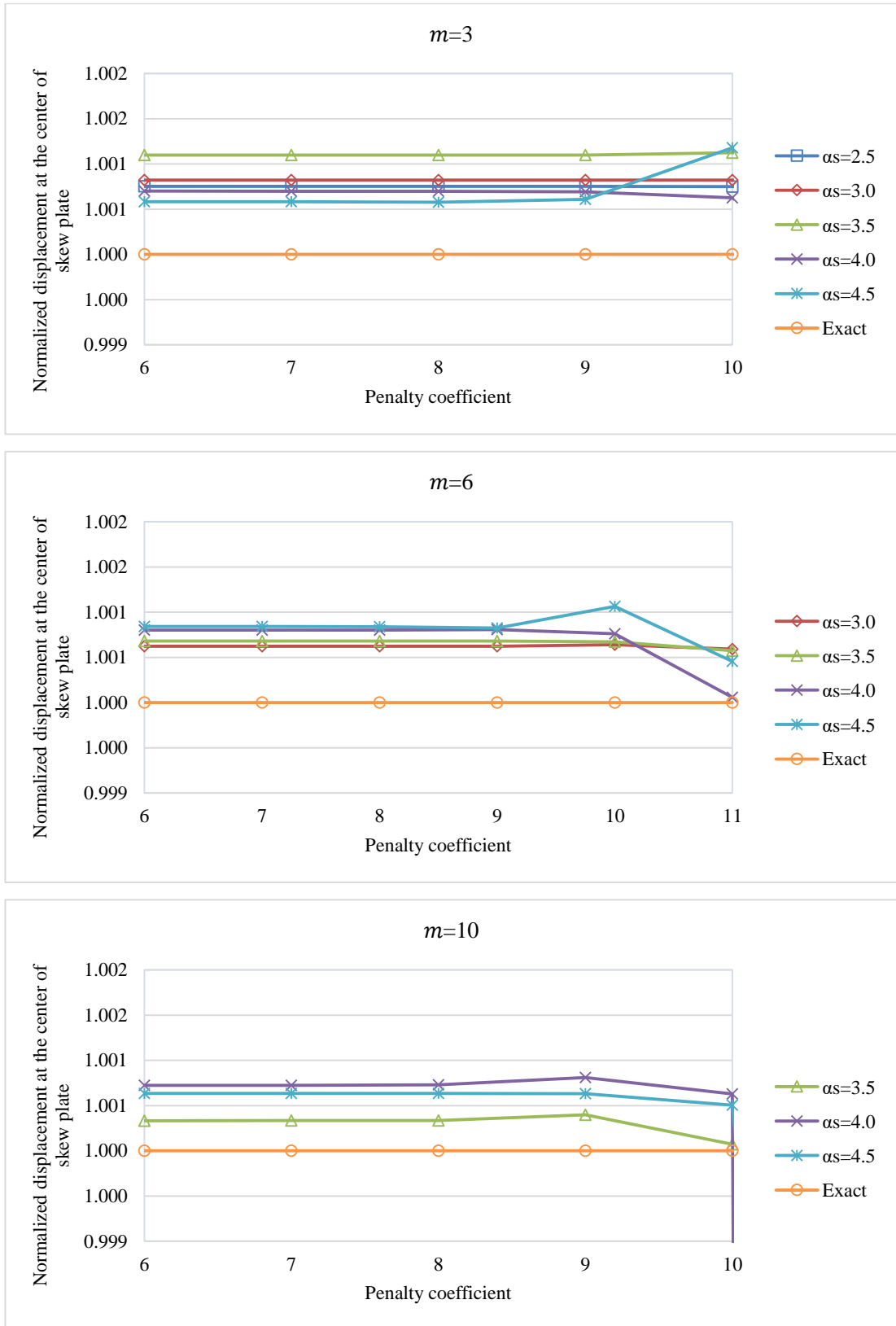


**Figure 5.22.** Variations of normalized central deflections  $w_c / \left( \frac{\rho L^4}{100D} \right)$  against  $\alpha_p$  for simply supported skew plate subjected to uniform load and irregular node distribution with  $n_g = 5$ .

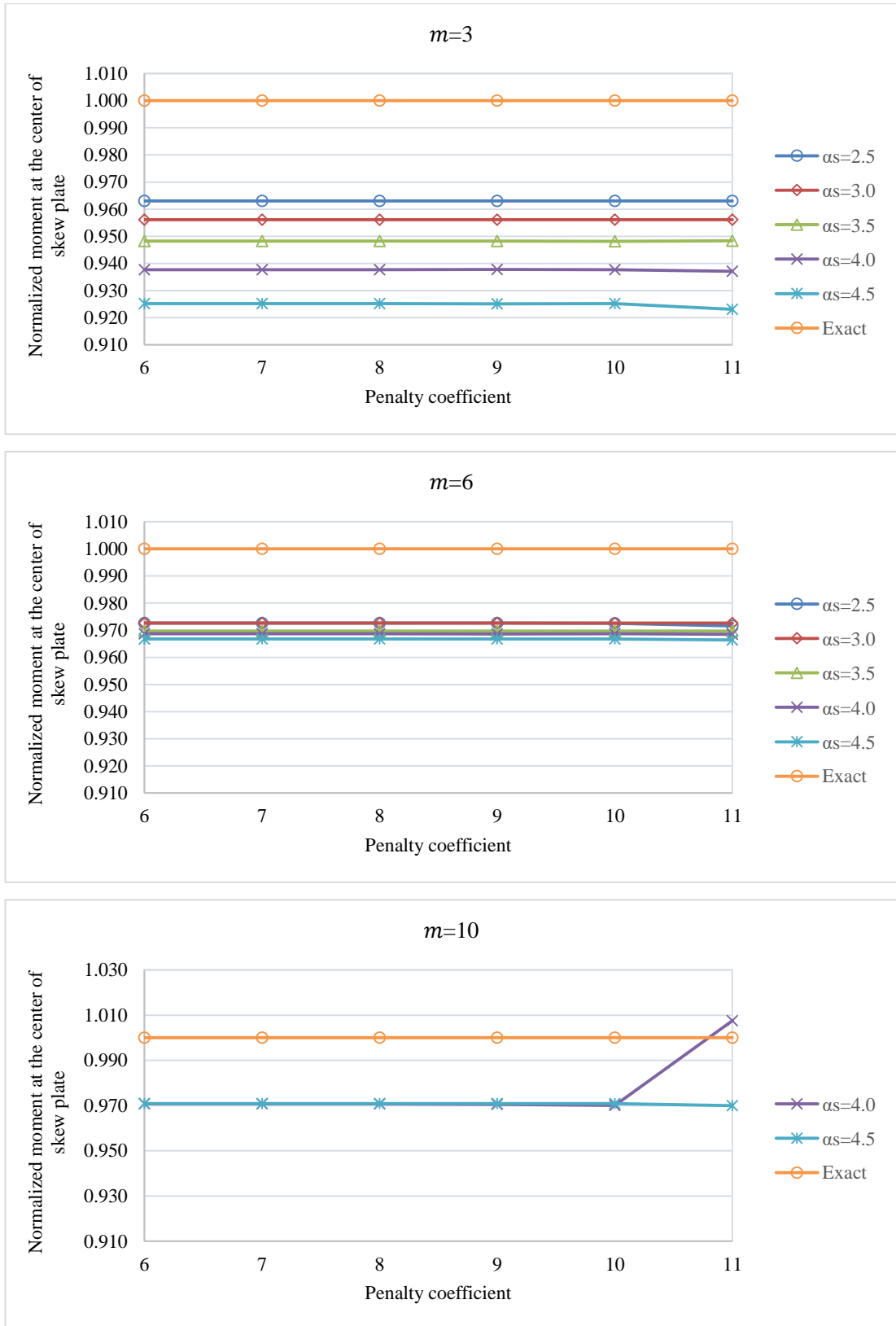


**Figure 5.23.** Variations of normalized central maximum moments  $M_c / \left( \frac{\rho L^2}{10} \right)$  against  $\alpha_p$  for simply supported skew plate subjected to uniform load and irregular node distribution with  $n_g = 5$ .



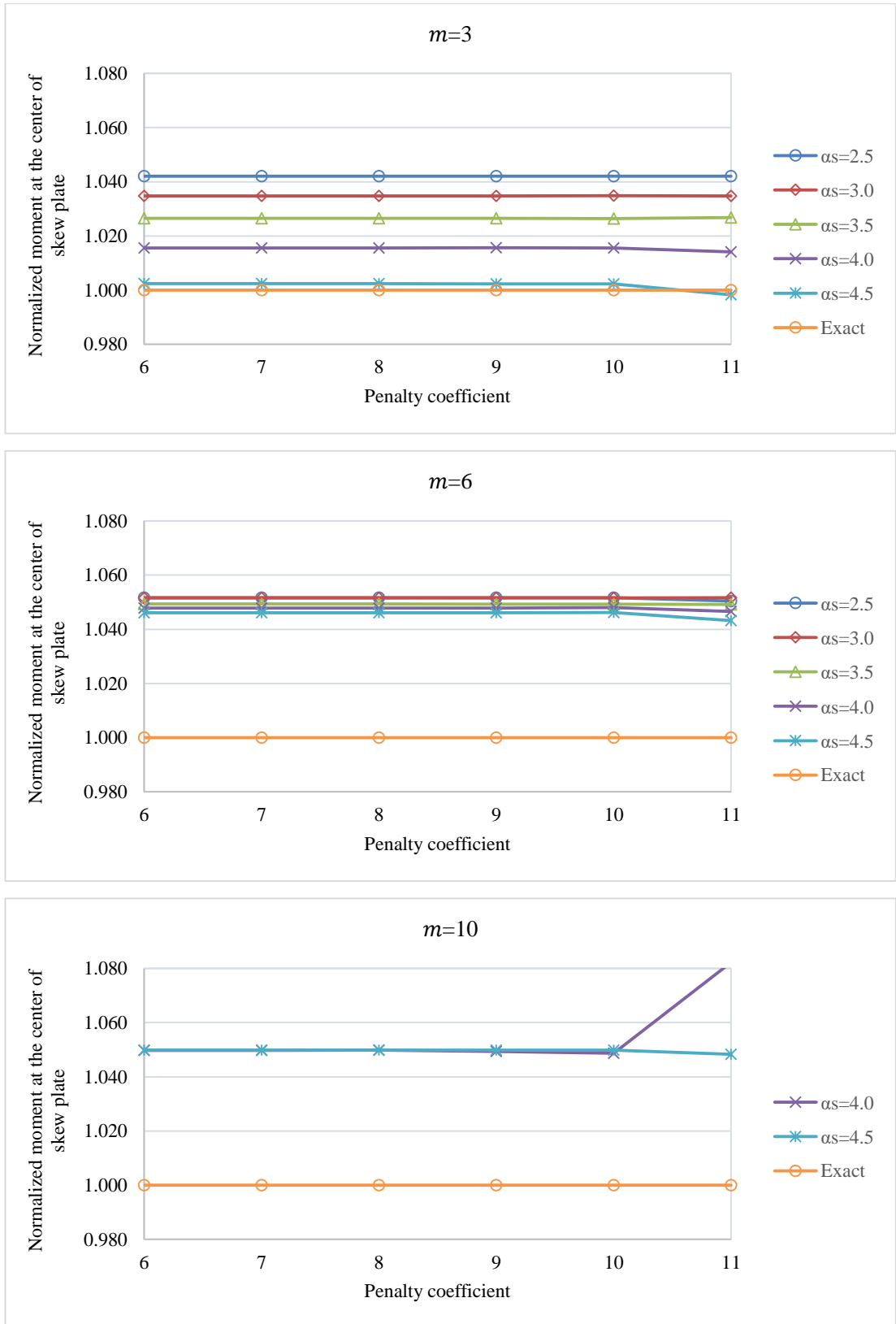


**Figure 5.24.** Variations of normalized central minimum moments  $M_c / \left( \frac{pL^2}{10} \right)$  against  $\alpha_p$  for simply supported skew plate subjected to uniform load and irregular node distribution with  $n_g = 5$ .

## CHAPTER 6

### NUMERICAL RESULTS AND DISCUSSIONS FOR BENDING ANALYSIS OF LAMINATED COMPOSITE PLATES

#### 6.1 Introduction

Seven numerical examples have been performed to apply EFGM and FEM solutions on bending analyses of laminated composite plates. The numerical examples are;

- Clamped square plate angle-ply orientation,
- Clamped square plate cross-ply orientation,
- Simply supported square plate angle-ply orientation,
- Simply supported square plate cross-ply orientation,
- Simply supported square plate asymmetric orientation,
- Clamped circular orthotropic plate,
- Simply supported skew plate cross-ply and angle-ply orientation,

In this chapter; the obtained EFGM using regular and irregular node distributions and FEM results are compared with analytical or reference results in the literature and are discussed on the solution accuracy.

Various number of nodes in the problem domain are used for EFGM and FEM solutions. Tables are used to represent the obtained central normalized displacements and stresses of numerical examples. The 4-node quadrilateral displacement based linear element is considered in the FEM solutions. The selectable parameters are chosen the best ones in the solution of isotropic plate bending problems. The value of penalty coefficient, the number of gauss integration points, support domain size are used as  $10^6$ ,  $5 \times 5$  and 3.0 in the EFGM solutions, respectively. Also, cubic spline is used as weight function in examples. Shear correction factor is given as  $5/6$  in all solutions. The properties of materials used in the examples are given in Table 6.1. The deflections of the laminated composite plates are obtained on the midpoint of the first

layer and are symbolized with  $w_c$ . The stresses of laminated composite plates are obtained on first layer for the  $x$  component and second layer for the  $y$  component and are symbolized with  $\sigma_c$ .

**Table 6.1** Material properties of laminated composite plates

	<b>M1</b>	<b>M2</b>	<b>M3</b>	<b>M4</b>	<b>M5</b>	<b>M6</b>
$E_1, Pa$	$40 \times 10^6$	$30 \times 10^9$	$250 \times 10^9$	$40 \times 10^6$	$5.6 \times 10^6$	$25 \times 10^6$
$E_2, Pa$	$1.0 \times 10^6$	$1.2 \times 10^9$	$10 \times 10^9$	$1.0 \times 10^6$	$1.2 \times 10^6$	$1.0 \times 10^6$
$G_{12}, Pa$	$0.5 \times 10^6$	$0.6 \times 10^9$	$5 \times 10^9$	$0.6 \times 10^6$	$0.6 \times 10^6$	$0.5 \times 10^6$
$G_{13}, Pa$	$0.5 \times 10^6$	$0.6 \times 10^9$	$5 \times 10^9$	$0.6 \times 10^6$	$0.6 \times 10^6$	$0.5 \times 10^6$
$G_{23}, Pa$	$0.5 \times 10^6$	$0.24 \times 10^9$	$2 \times 10^9$	$0.5 \times 10^6$	$0.6 \times 10^6$	$0.2 \times 10^6$
$\nu_{12}$	0.25	0.25	0.25	0.25	0.26	0.25

## 6.2 Clamped square plate angle-ply orientation

The clamped square plate has two layers having  $[-\theta^\circ/\theta^\circ]$  fiber orientation. The material is considered as M1, presented in Table 6.1, with length,  $L$  is 10 and the thickness,  $t$  is 0.02. The applied uniform load,  $q$  is 1.0. Due to asymmetry, whole plate is modelled using 9, 25, 81, 289 and 1089 number of nodes in problem domain for EFGM and FEM solutions. The normalized central deflection results obtained from EFGM and FEM solutions are presented and compared with exact solutions [78] in Table 6.2.

According to results in Table 6.2, there is no significant difference between EFGM solutions using regular and irregular node distributions. However, it is observed that stability of FEM solutions occurs earlier than EFGM solutions. The closer results are obtained at the fiber orientations of  $[-25^\circ/+25^\circ]$ ,  $[-35^\circ/+35^\circ]$  and  $[-45^\circ/+45^\circ]$  than  $[-5^\circ/+5^\circ]$  and  $[-15^\circ/+15^\circ]$  ones. Also, it is seen that an increase in number of node gives more accurate results as expected.

**Table 6.2.** Normalized central deflections  $w_c * (100E_2h^3/qL^4)$  for clamped square plate angle-ply orientation.

Fiber orientation	Method	Number of nodes in the problem domain					Exact [78]
		9	25	81	289	1089	
$-5^\circ/+5^\circ$	FEM	0.000120	0.107109	0.100520	0.103496	0.104289	0.0946
	EFGM (regular)	0.000077	0.045024	0.099546	0.103130	0.103451	
	EFGM (irregular)	0.000077	0.010272	0.096953	0.102832	0.103492	
$-15^\circ/+15^\circ$	FEM	0.000120	0.196349	0.193969	0.197657	0.198648	0.1691
	EFGM (regular)	0.000077	0.053431	0.175606	0.194078	0.196739	
	EFGM (irregular)	0.000077	0.010694	0.164672	0.190876	0.196273	
$-25^\circ/+25^\circ$	FEM	0.000120	0.256195	0.254440	0.257632	0.258483	0.2355
	EFGM (regular)	0.000077	0.056140	0.216774	0.249666	0.254993	
	EFGM (irregular)	0.000077	0.010809	0.199583	0.243300	0.253976	
$-35^\circ/+35^\circ$	FEM	0.000120	0.290350	0.285876	0.287706	0.288222	0.2763
	EFGM (regular)	0.000077	0.057086	0.234245	0.276630	0.283658	
	EFGM (irregular)	0.000077	0.010845	0.214170	0.268053	0.282325	
$-45^\circ/+45^\circ$	FEM	0.000120	0.302215	0.295981	0.297075	0.297407	0.2890
	EFGM (regular)	0.000077	0.057338	0.239247	0.284894	0.292472	
	EFGM (irregular)	0.000077	0.010855	0.218913	0.275591	0.291049	

### 6.3 Clamped square plate cross-ply orientation

The clamped laminated square plate with four different aspect ratios of  $h / L = 0.1$ ,  $h / L = 0.05$ ,  $h / L = 0.02$  and  $h / L = 0.01$  are analyzed [84] to determine deformations under the uniformly distributed transverse load  $q = 1.0$ . The unidirectional laminate of material M2, presented in Table 6.1, is used with four layer of  $[0^\circ/90^\circ/90^\circ/0^\circ]$  orientation. Due to the symmetry, only a quarter of plate is modelled using 9, 25, 81, 289 and 1089 number of nodes in the EFGM and FEM solutions. The dimensionless central normalized deflections and stresses of plate are presented and compared with reference solutions [79] in Table 6.3 to 6.5.

Although some stability problems can be observed in solutions, acceptable results, especially in the usage of 81, 289 and 1089 number of nodes in the problem domain, have been obtained at all thickness/span ratios. The FEM solutions and EFGM solutions using regular node distribution are similar characteristics in the usage of higher number of nodes. The EFGM solutions using irregular node distribution is not reliable for this example since it has not stability even usage of 1089 number of nodes in the problem domain.

**Table 6.3.** Normalized central deflections  $w_c * (\frac{100E_2h^3}{qL^4})$  for clamped square plate cross-ply orientation.

$h/L$	Method	Number of nodes in the problem domain					Umasree (2009)
		9	25	81	289	1089	
<b>0.1</b>	FEM	0.486870	0.469849	0.466177	0.465328	0.468663	0.4651
	EFGM (regular)	0.456036	0.465089	0.464637	0.463908	0.465349	
	EFGM (irregular)	0.445830	0.464201	0.467845	0.465675	0.464425	
<b>0.05</b>	FEM	0.234835	0.234359	0.234190	0.234183	0.237496	0.2342
	EFGM (regular)	0.193383	0.232024	0.233620	0.233264	0.234940	
	EFGM (irregular)	0.191572	0.233289	0.236746	0.234754	0.233618	
<b>0.02</b>	FEM	0.149961	0.156778	0.158426	0.158866	0.161679	0.1590
	EFGM (regular)	0.057701	0.152424	0.158020	0.158000	0.159474	
	EFGM (irregular)	0.059125	0.156465	0.160390	0.159137	0.158332	
<b>0.01</b>	FEM	0.136678	0.144799	0.146825	0.147355	0.149549	0.1475
	EFGM (regular)	0.017597	0.136933	0.146091	0.146423	0.147563	
	EFGM (irregular)	0.018312	0.142701	0.147528	0.147233	0.146796	

**Table 6.4.** Normalized central stresses  $\sigma_c * (h^2/qL^2)$  in the  $x$  direction for clamped square plate cross-ply orientation.

$h/L$	Method	Number of nodes in the problem domain					Umasree (2009)
		9	25	81	289	1089	
<b>0.1</b>	FEM	0.108627	0.062883	0.216119	0.222794	0.232011	0.2251
	EFGM (regular)	0.099846	0.178515	0.198981	0.203050	0.209034	
	EFGM (irregular)	0.099846	0.186854	0.207505	0.211147	0.233421	
<b>0.05</b>	FEM	0.112652	0.077509	0.254294	0.262198	0.267739	0.2649
	EFGM (regular)	0.094862	0.213884	0.237190	0.241519	0.245117	
	EFGM (irregular)	0.096575	0.221354	0.243390	0.249630	0.276463	
<b>0.02</b>	FEM	0.101138	0.088500	0.274363	0.282196	0.284693	0.2848
	EFGM (regular)	0.043443	0.229565	0.260819	0.262963	0.263241	
	EFGM (irregular)	0.000077	0.238793	0.264331	0.268755	0.297891	
<b>0.01</b>	FEM	0.091784	0.091487	0.277866	0.285492	0.287689	0.2880
	EFGM (regular)	0.045234	0.226709	0.267798	0.270234	0.267989	
	EFGM (irregular)	0.015135	0.240894	0.269076	0.271158	0.303518	

**Table 6.5.** Normalized central stresses  $\sigma_c * (h^2/qL^2)$  in the  $y$  direction for clamped square plate cross-ply orientation.

$h/L$	Method	Number of nodes in the problem domain					Umasree (2009)
		9	25	81	289	1089	
<b>0.1</b>	FEM	0.267717	0.220471	0.258811	0.257558	0.259777	0.2572
	EFGM (regular)	0.129153	0.222633	0.241980	0.245497	0.247761	
	EFGM (irregular)	0.096998	0.228414	0.251496	0.243411	0.225320	
<b>0.05</b>	FEM	0.191338	0.152727	0.164716	0.162881	0.166876	0.1623
	EFGM (regular)	0.072665	0.143834	0.154623	0.155121	0.157609	
	EFGM (irregular)	0.119044	0.148857	0.161135	0.153765	0.142673	
<b>0.02</b>	FEM	0.144280	0.114994	0.113172	0.111746	0.115308	0.1113
	EFGM (regular)	0.023768	0.096981	0.107927	0.107015	0.108132	
	EFGM (irregular)	0.023910	0.107721	0.109018	0.104416	0.098836	
<b>0.01</b>	FEM	0.135831	0.108403	0.103895	0.102656	0.105220	0.1012
	EFGM (regular)	0.007345	0.086856	0.099850	0.099632	0.099703	
	EFGM (irregular)	0.005977	0.104334	0.096759	0.095059	0.091261	



#### 6.4 Simply supported square plate angle-ply orientation

The simply supported square plate has two layers with  $[-\theta^o/\theta^o]$  fiber orientation. The material is considered as M1, presented in Table 6.1, having length,  $L$  is 10 and the thickness,  $t$  is 0.02. The applied uniform load,  $q$  is 1.0. Due to asymmetry, whole plate is modelled using 9, 25, 81, 289 and 1089 number of nodes in problem domain for EFGM and FEM solutions. The normalized central deflection results obtained from EFGM and FEM solutions are presented and compared with exact solutions [78] in Table 6.6.

From the results of this example, it seems that FEM solutions have better results than EFGM solutions on the solution accuracy. It is observed that stability of FEM solutions occurs after the usage 25 number of node. However, 289 or 1089 number of node must be used to get acceptable results in the EFGM solutions. Also, the EFGM solutions using regular node distribution has the closer results than irregular ones.

**Table 6.6.** Normalized central deflections  $w_c * (100E_2h^3/qL^4)$  for simply supported square plate angle-ply orientation.

Fiber orientation	Method	Number of nodes in the problem domain					Exact [78]
		9	25	81	289	1089	
$-5^\circ/+5^\circ$	FEM	0.367679	0.475091	0.476975	0.473006	0.473607	0.4736
	EFGM (regular)	0.092492	0.337607	0.466782	0.475550	0.472790	
	EFGM (irregular)	0.059945	0.120580	0.445527	0.465969	0.472620	
$-15^\circ/+15^\circ$	FEM	0.548045	0.704311	0.720024	0.713363	0.714243	0.7142
	EFGM (regular)	0.099539	0.429831	0.677921	0.713447	0.713486	
	EFGM (irregular)	0.062914	0.131511	0.637184	0.691953	0.711491	
$-25^\circ/+25^\circ$	FEM	0.618079	0.772782	0.789009	0.786093	0.787070	0.7870
	EFGM (regular)	0.100583	0.448338	0.731024	0.779325	0.781995	
	EFGM (irregular)	0.063377	0.133251	0.684872	0.753283	0.779058	
$-35^\circ/+35^\circ$	FEM	0.608697	0.744053	0.754794	0.755206	0.756085	0.7561
	EFGM (regular)	0.100037	0.435543	0.698472	0.744468	0.747576	
	EFGM (irregular)	0.063135	0.132015	0.656412	0.720478	0.744752	
$-45^\circ/+45^\circ$	FEM	0.598153	0.723813	0.729709	0.731630	0.732267	0.7322
	EFGM (regular)	0.099687	0.426204	0.674919	0.718336	0.721392	
	EFGM (irregular)	0.062970	0.131122	0.635699	0.696859	0.718744	

## 6.5 Simply supported square plate cross-ply orientation

The deformation and stresses of a simply supported square laminated plate subjected to a uniformly distributed transverse load,  $q = 10^5$  is analysed [84] using different lamination schemes with thickness/span ratios of  $h / L = 0.1$ ,  $h / L = 0.05$  and  $h / L = 0.01$  where length,  $L$  is 20. The laminates used are symmetric cross-ply with three, four, five and seven layers of  $[0^\circ/90^\circ/0^\circ]$ ,  $[0^\circ/90^\circ/90^\circ/0^\circ]$ ,  $[0^\circ/90^\circ/0^\circ/90^\circ/0^\circ]$  and  $[0^\circ/90^\circ/90^\circ/0^\circ/90^\circ/90^\circ/0^\circ]$  orientations, respectively. The material M3, presented in Table 6.1, is used in this example.

Due to the symmetry, only a quarter of plate is modelled using 9, 25, 81, 289 and 1089 number of nodes in the EFGM and FEM solutions. The normalized central deflections and stresses according to thickness/span ratios of  $h / L = 0.1$ ,  $h / L = 0.05$  and  $h / L = 0.01$  are presented and compared with exact solutions [80] in Tables 6.7 to 6.15, respectively.

According to results in Tables 6.7 to 6.15, stability problem, especially in the stress solutions, has been occurred in the usage of EFGM using irregular node distribution. It is seen that there is no significant difference between EFGM solutions using regular and the FEM solutions. While all solutions have acceptable results, FEM ones are closer to exact solution.

**Table 6.7.** Normalized central deflections  $w_c * (100E_2h^3/qL^4)$  according to  $h / L = 0.1$  for simply supported square plate cross-ply orientations.

Fiber orientation	Method	Number of nodes in the problem domain					Exact [80]
		9	25	81	289	1089	
<b>0°/90°/0°</b>	FEM	1.052046	1.027597	1.023212	1.022245	1.023610	1.0219
	EFGM (regular)	1.019537	1.024719	1.027076	1.027261	1.027900	
	EFGM (irregular)	1.025495	1.023276	1.027458	1.028617	1.029729	
<b>0°/90°/90°/0°</b>	FEM	1.043563	1.028626	1.025836	1.025218	1.026448	1.025
	EFGM (regular)	1.015265	1.026491	1.029009	1.029220	1.029748	
	EFGM (irregular)	1.015072	1.025677	1.029085	1.030162	1.031657	
<b>0°/90°/0°/90°/0°</b>	FEM	0.982837	0.974351	0.973075	0.972823	0.973888	0.9727
	EFGM (regular)	0.960644	0.972762	0.975322	0.975547	0.976021	
	EFGM (irregular)	0.957094	0.972063	0.975205	0.976301	0.978003	
<b>0°/90°/90°/0°/90°/90°/0°</b>	FEM	0.963368	0.957785	0.957160	0.957065	0.957963	0.9643
	EFGM (regular)	0.943319	0.956100	0.958683	0.958912	0.959291	
	EFGM (irregular)	0.937504	0.955692	0.958369	0.959280	0.961339	

**Table 6.8.** Normalized central stresses  $\sigma_c * (h^2/qL^2)$  in the  $x$  direction according to  $h / L = 0.1$  for simply supported square plate cross-ply orientations.

Fiber orientation	Method	Number of nodes in the problem domain					Exact [80]
		9	25	81	289	1089	
<b>0°/90°/0°</b>	FEM	0.455712	0.699143	0.754124	0.767498	0.768027	0.7719
	EFGM (regular)	0.588401	0.689606	0.708955	0.714686	0.716178	
	EFGM (irregular)	0.621959	0.713637	0.709024	0.732600	0.828454	
<b>0°/90°/90°/0°</b>	FEM	0.438888	0.678911	0.738171	0.752911	0.754095	0.7577
	EFGM (regular)	0.574024	0.675832	0.695763	0.701527	0.703096	
	EFGM (irregular)	0.605755	0.698983	0.696232	0.717860	0.802960	
<b>0°/90°/0°/90°/0°</b>	FEM	0.445260	0.684957	0.744964	0.759976	0.761259	0.7649
	EFGM (regular)	0.581295	0.683995	0.703838	0.709503	0.711006	
	EFGM (irregular)	0.611138	0.706117	0.704118	0.724417	0.801022	
<b>0°/90°/90°/0°/90°/90°/0°</b>	FEM	0.441579	0.678758	0.739410	0.754657	0.756418	0.7605
	EFGM (regular)	0.582100	0.682405	0.702175	0.707655	0.709171	
	EFGM (irregular)	0.610859	0.702878	0.702214	0.719248	0.777554	

**Table 6.9.** Normalized central stresses  $\sigma_c * (h^2/qL^2)$  in the  $y$  direction according to  $h / L = 0.1$  for simply supported square plate cross-ply orientations.

Fiber orientation	Method	Number of nodes in the problem domain					Exact [80]
		9	25	81	289	1089	
<b>0°/90°/0°</b>	FEM	0.365614	0.321747	0.310837	0.308275	0.308222	0.3072
	EFGM (regular)	0.297402	0.304159	0.302031	0.300357	0.300022	
	EFGM (irregular)	0.273055	0.309793	0.306789	0.294096	0.280569	
<b>0°/90°/90°/0°</b>	FEM	0.527118	0.508839	0.502772	0.501253	0.501335	0.5006
	EFGM (regular)	0.424910	0.473583	0.481821	0.483237	0.483861	
	EFGM (irregular)	0.385739	0.485263	0.494260	0.478467	0.443306	
<b>0°/90°/0°/90°/0°</b>	FEM	0.556814	0.555030	0.553237	0.552757	0.553031	0.5525
	EFGM (regular)	0.452208	0.514081	0.525689	0.528306	0.529363	
	EFGM (irregular)	0.407074	0.529067	0.542938	0.527897	0.480935	
<b>0°/90°/90°/0°/90°/90°/0°</b>	FEM	0.612591	0.627640	0.630344	0.630974	0.631402	0.6016
	EFGM (regular)	0.497607	0.292863	0.592466	0.596438	0.598035	
	EFGM (irregular)	0.445966	0.596988	0.616957	0.603219	0.537153	

**Table 6.10.** Normalized central deflections  $w_c * (100E_2h^3/qL^4)$  according to  $h / L = 0.05$  for simply supported square plate cross-ply orientations.

Fiber orientation	Method	Number of nodes in the problem domain					Exact [80]
		9	25	81	289	1089	
<b>0°/90°/0°</b>	FEM	0.755446	0.756019	0.756870	0.757149	0.757642	0.7572
	EFGM (regular)	0.728314	0.754624	0.759073	0.759642	0.760014	
	EFGM (irregular)	0.736906	0.755724	0.759163	0.759996	0.762093	
<b>0°/90°/90°/0°</b>	FEM	0.757584	0.766561	0.768664	0.769201	0.769706	0.7694
	EFGM (regular)	0.730094	0.766916	0.771171	0.771757	0.772103	
	EFGM (irregular)	0.737088	0.768028	0.771197	0.771974	0.774128	
<b>0°/90°/0°/90°/0°</b>	FEM	0.741153	0.754184	0.757161	0.757901	0.758386	0.7581
	EFGM (regular)	0.714957	0.755265	0.759489	0.760104	0.760437	
	EFGM (irregular)	0.717356	0.756522	0.759386	0.760239	0.762470	
<b>0°/90°/90°/0°/90°/90°/0°</b>	FEM	0.736030	0.751419	0.754906	0.755767	0.756227	0.7575
	EFGM (regular)	0.711101	0.752913	0.757100	0.757720	0.758028	
	EFGM (irregular)	0.712384	0.754398	0.756882	0.757703	0.760053	

**Table 6.11.** Normalized central stresses  $\sigma_c * (h^2/qL^2)$  in the  $x$  direction according to  $h / L = 0.05$  for simply supported square plate cross-ply orientations.

Fiber orientation	Method	Number of nodes in the problem domain					Exact [80]
		9	25	81	289	1089	
<b>0°/90°/0°</b>	FEM	0.473739	0.725602	0.780732	0.793989	0.796477	0.7983
	EFGM (regular)	0.596434	0.722359	0.739139	0.741852	0.743464	
	EFGM (irregular)	0.619996	0.740241	0.741644	0.759162	0.856243	
<b>0°/90°/90°/0°</b>	FEM	0.465016	0.720489	0.783723	0.799353	0.802557	0.8045
	EFGM (regular)	0.592680	0.725962	0.744277	0.747626	0.749387	
	EFGM (irregular)	0.616515	0.743711	0.747176	0.763910	0.852101	
<b>0°/90°/0°/90°/0°</b>	FEM	0.465563	0.720982	0.786327	0.802638	0.806114	0.8080
	EFGM (regular)	0.593268	0.730405	0.749015	0.752065	0.753702	
	EFGM (irregular)	0.615019	0.746891	0.751720	0.766781	0.845646	
<b>0°/90°/90°/0°/90°/90°/0°</b>	FEM	0.462390	0.715284	0.781688	0.798381	0.802090	0.8059
	EFGM (regular)	0.593226	0.728932	0.747714	0.750886	0.752470	
	EFGM (irregular)	0.614915	0.744439	0.749829	0.762226	0.822120	



**Table 6.12.** Normalized central stresses  $\sigma_c * (h^2/qL^2)$  in the  $y$  direction according to  $h / L = 0.05$  for simply supported square plate cross-ply orientations.

Fiber orientation	Method	Number of nodes in the problem domain					Exact [80]
		9	25	81	289	1089	
<b>0°/90°/0°</b>	FEM	0.276912	0.235296	0.225788	0.223643	0.223068	0.2227
	EFGM (regular)	0.223186	0.223362	0.219464	0.216176	0.214897	
	EFGM (irregular)	0.208076	0.228098	0.219466	0.211058	0.204767	
<b>0°/90°/90°/0°</b>	FEM	0.421400	0.404673	0.398828	0.397404	0.397003	0.3968
	EFGM (regular)	0.332215	0.378395	0.382963	0.381740	0.381293	
	EFGM (irregular)	0.307634	0.386027	0.389491	0.377257	0.351861	
<b>0°/90°/0°/90°/0°</b>	FEM	0.488002	0.487295	0.485234	0.484693	0.484511	0.4844
	EFGM (regular)	0.384084	0.453642	0.462247	0.462369	0.462492	
	EFGM (irregular)	0.352561	0.464066	0.474268	0.461200	0.421963	
<b>0°/90°/90°/0°/90°/90°/0°</b>	FEM	0.569393	0.586553	0.589014	0.589571	0.589692	0.5475
	EFGM (regular)	0.447311	0.543069	0.556096	0.557375	0.558111	
	EFGM (irregular)	0.409070	0.557759	0.576017	0.562786	0.502377	

**Table 6.13.** Normalized central deflections  $w_c * (100E_2h^3/qL^4)$  according to  $h / L = 0.01$  for simply supported square plate cross-ply orientations.

Fiber orientation	Method	Number of nodes in the problem domain					Exact [80]
		9	25	81	289	1089	
<b>0°/90°/0°</b>	FEM	0.656733	0.666003	0.668731	0.669453	0.669659	0.6697
	EFGM (regular)	0.520528	0.657996	0.669175	0.670721	0.671185	
	EFGM (irregular)	0.418022	0.662874	0.668804	0.670672	0.673310	
<b>0°/90°/90°/0°</b>	FEM	0.660659	0.678133	0.682027	0.682989	0.683248	0.6833
	EFGM (regular)	0.520692	0.671283	0.682956	0.684610	0.685088	
	EFGM (irregular)	0.423705	0.674744	0.682860	0.684545	0.687101	
<b>0°/90°/0°/90°/0°</b>	FEM	0.661104	0.681476	0.685918	0.687001	0.687287	0.6874
	EFGM (regular)	0.518291	0.674850	0.686934	0.688664	0.689156	
	EFGM (irregular)	0.422738	0.677858	0.686871	0.688596	0.691118	
<b>0°/90°/90°/0°/90°/90°/0°</b>	FEM	0.661661	0.684081	0.688948	0.690129	0.690435	0.6896
	EFGM (regular)	0.517722	0.677895	0.690063	0.691814	0.692308	
	EFGM (irregular)	0.430155	0.680875	0.690034	0.691719	0.694232	

**Table 6.14.** Normalized central stresses  $\sigma_c * (h^2/qL^2)$  in the  $x$  direction according to  $h / L = 0.01$  for simply supported square plate cross-ply orientations.

Fiber orientation	Method	Number of nodes in the problem domain					Exact [80]
		9	25	81	289	1089	
<b>0°/90°/0°</b>	FEM	0.480457	0.735678	0.789847	0.802902	0.806122	0.8072
	EFGM (regular)	0.487330	0.736080	0.774068	0.768696	0.758989	
	EFGM (irregular)	0.399531	0.186854	0.768303	0.765377	0.871963	
<b>0°/90°/90°/0°</b>	FEM	0.474142	0.737063	0.801675	0.817564	0.821512	0.8420
	EFGM (regular)	0.487286	0.747363	0.787459	0.782647	0.773416	
	EFGM (irregular)	0.403905	0.766157	0.784718	0.779292	0.875919	
<b>0°/90°/0°/90°/0°</b>	FEM	0.472071	0.736030	0.803958	0.820840	0.825046	0.8264
	EFGM (regular)	0.485274	0.749629	0.791820	0.787939	0.778372	
	EFGM (irregular)	0.404007	0.768735	0.788764	0.781890	0.870299	
<b>0°/90°/90°/0°/90°/90°/0°</b>	FEM	0.469797	0.731247	0.800707	0.818130	0.822481	0.8260
	EFGM (regular)	0.484705	0.748021	0.790451	0.787169	0.778090	
	EFGM (irregular)	0.410243	0.766784	0.787761	0.778841	0.847160	

**Table 6.15.** Normalized central stresses  $\sigma_c * (h^2/qL^2)$  in the  $y$  direction according to  $h / L = 0.01$  for simply supported square plate cross-ply orientations.

Fiber orientation	Method	Number of nodes in the problem domain					Exact [80]
		9	25	81	289	1089	
<b>0°/90°/0°</b>	FEM	0.243989	0.203523	0.195223	0.193337	0.192860	0.1925
	EFGM (regular)	0.162723	0.192208	0.192325	0.190778	0.187996	
	EFGM (irregular)	0.122505	0.209076	0.175232	0.180446	0.181997	
<b>0°/90°/90°/0°</b>	FEM	0.379438	0.362880	0.357645	0.356406	0.356087	0.3558
	EFGM (regular)	0.244080	0.336190	0.349673	0.349371	0.345107	
	EFGM (irregular)	0.185587	0.353280	0.335124	0.335138	0.319635	
<b>0°/90°/0°/90°/0°</b>	FEM	0.459420	0.458635	0.456658	0.456164	0.456033	0.4559
	EFGM (regular)	0.291493	0.422876	0.444394	0.444107	0.438923	
	EFGM (irregular)	0.222590	0.440500	0.432956	0.430284	0.400028	
<b>0°/90°/90°/0°/90°/90°/0°</b>	FEM	0.550848	0.568400	0.570794	0.571334	0.571463	0.5241
	EFGM (regular)	0.346518	0.523138	0.553082	0.552396	0.545728	
	EFGM (irregular)	0.268718	0.540908	0.546767	0.540762	0.488047	

## 6.6 Simply supported square plate asymmetric angle-ply orientation

The deformation of an angle-ply simply supported square plate subjected to a uniformly distributed transverse load,  $q = 1$  is examined [84] using four layers  $[\theta^\circ / -\theta^\circ / \theta^\circ / -\theta^\circ]$ . The solutions are presented with a constant thickness-to-span ratio,  $h / L$ , of 0.1. The material M4 is used, presented in Table 6.1, in this example.

Because of the asymmetry, the whole plate is modelled using 9, 25, 81, 289 and 1089 number of nodes in the EFGM and FEM solutions. Table 6.16 presents the normalized center deflection of plate and comparison of FEM, EFGM and reference [80] solutions.

It is visible that the accuracy of FEM solutions is more accurate than the EFGM. Also, EFGM solutions have some stability problems that can be seen fluctuations in Table 6.16.

**Table 6.16.** Normalized central deflections  $w_c * (\frac{1000E_2h^3}{qL^4})$  for simply supported square plate asymmetric angle-ply orientation.

Fiber orientation	Method	Number of nodes in the problem domain					Reddy (1997)
		9	25	81	289	1089	
$+5^\circ - 5^\circ / +5^\circ / -5^\circ$	FEM	7.472839	7.114253	6.795589	6.757223	6.745030	6.741
	EFGM (regular)	6.411681	6.926699	6.764587	6.749272	6.746870	
	EFGM (irregular)	6.431757	6.775039	6.758258	6.732890	6.757196	
$+15^\circ - 15^\circ / +15^\circ / -15^\circ$	FEM	6.689615	6.354364	6.118003	6.113182	6.093797	6.086
	EFGM (regular)	5.932476	6.265513	6.112581	6.080432	6.070224	
	EFGM (irregular)	5.914719	6.123560	6.100832	6.080572	6.079005	
$+30^\circ - 30^\circ / +30^\circ / -30^\circ$	FEM	5.454464	5.040349	4.858959	4.868983	4.836944	4.825
	EFGM (regular)	5.010505	5.080280	4.878929	4.818350	4.795679	
	EFGM (irregular)	4.949157	4.959900	4.862130	4.863859	4.803643	
$+45^\circ - 45^\circ / +45^\circ / -45^\circ$	FEM	5.070192	4.622783	4.462457	4.466135	4.436225	4.426
	EFGM (regular)	4.673825	4.674571	4.484520	4.419934	4.395635	
	EFGM (irregular)	4.605979	4.571114	4.485889	4.472319	4.400596	

## 6.7 Clamped circular orthotropic plate

The clamped circular plate has one layer with  $[0^\circ]$  fiber orientation. The orthotropic material is considered as M5, presented in Table 6.1, having radius,  $R$  is 5. The plate have six different aspect ratios of  $R / h = 1000$ ,  $R / h = 100$ ,  $R / h = 50$ ,  $R / h = 25$ ,  $R / h = 16.67$  and  $R / h = 10$  are analyzed to determine deformations under the uniformly distributed transverse load  $q = 1.0$ .

Due to symmetry, only one quarter of the plate is modelled using 37, 127, 271 and 817 number of nodes in problem domain for EFGM and FEM solutions. The normalized central deformations of the circular plate in all solutions is  $w = w_c * \frac{D}{qR^4}$  with  $D = 3(D_{11} + D_{22}) + 2(D_{12} + 2D_{66})$  where  $D_{11}$ ,  $D_{22}$ ,  $D_{12}$ ,  $D_{66}$  are bending rigidity coefficients of the laminate. The normalized central deflection results obtained from EFGM and FEM solutions are presented and compared with reference solution [81] in Table 6.17.

From the results in Table 6.17, the EFGM solutions have better solution accuracy than FEM solutions. It is observed that various radius/thickness,  $R / h$  ratios did not cause any problem and acceptable results have been achieved in solutions. Also, it can be seen that increasing the usage of number of node in the problem domain gives more accurate results.

**Table 6.17.** Normalized central deflections  $w_c * \left(\frac{D}{qR^4}\right)$  for clamped circular orthotropic plate.

<b><math>R/h</math></b>	<b>Method</b>	<b>Number of nodes in the problem domain</b>				<b>Nguyen (2007)</b>
		<b>37</b>	<b>127</b>	<b>271</b>	<b>817</b>	
<b>1000</b>	FEM	0.121796	0.123743	0.124564	0.124927	0.1258
	EFGM (regular)	0.029822	0.085802	0.101390	0.116942	
	EFGM (irregular)	0.025682	0.075350	0.096190	0.112665	
<b>100</b>	FEM	0.122014	0.124431	0.124832	0.125065	0.1259
	EFGM (regular)	0.121879	0.125882	0.126018	0.126057	
	EFGM (irregular)	0.118743	0.125751	0.125961	0.125998	
<b>50</b>	FEM	0.122536	0.124887	0.125260	0.125483	0.1264
	EFGM (regular)	0.126078	0.127049	0.126805	0.126582	
	EFGM (irregular)	0.125585	0.127093	0.126813	0.126563	
<b>25</b>	FEM	0.124307	0.126562	0.126925	0.127144	0.1280
	EFGM (regular)	0.129426	0.129049	0.128632	0.128300	
	EFGM (irregular)	0.130160	0.129045	0.128629	0.128286	
<b>16.67</b>	FEM	0.127092	0.129309	0.129671	0.282196	0.1308
	EFGM (regular)	0.133001	0.131939	0.131454	0.129890	
	EFGM (irregular)	0.133768	0.131891	0.131441	0.131074	
<b>10</b>	FEM	0.135734	0.137943	0.138310	0.138530	0.1394
	EFGM (regular)	0.142633	0.140774	0.140220	0.139829	
	EFGM (irregular)	0.143118	0.140684	0.140199	0.139815	



### **6.8 Simply supported skew plate cross-ply and angle-ply orientations**

The simply supported skew plates have three layers with  $[0^\circ/90^\circ/0^\circ]$  and  $[45^\circ/-45^\circ/45^\circ]$  fiber orientations. The material is considered as M6, presented in Table 6.1, having length,  $L$  is 10 and the thickness,  $t$  is 0.1. The applied uniform load,  $q$  is 1.0.

Due to asymmetry, whole plate is modelled using 9, 25, 81, 289 and 1089 number of nodes in problem domain for EFGM and FEM solutions. Table 6.18 and 6.19 show that the normalized central deflection and stress results obtained from EFGM and FEM solutions for angle-ply and cross-ply orientation. All results are considered with two various skew angle  $15^\circ$  and  $30^\circ$  which are relative to vertical axis of the plate, and are compared with reference solutions [82] in Table 6.18 and 6.19.

According to obtained results, it seems that FEM and EFGM solutions show similar characteristics in deflection results, but FEM solutions have better solution accuracy than EFGM solutions for stress results. It is observed that 289 or 1089 number of node must be used to get acceptable results in the FEM and EFGM solutions.

**Table 6.18.** Normalized central deflections  $w_c * (\frac{1000E_2h^3}{qL^4})$  for simply supported skew plate angle-ply and cross-ply orientations.

Fiber orientation	Skew Angle	Method	Number of nodes in the problem domain					Chakrabarti (2004)
			9	25	81	289	1089	
<b>+45°/−45°/+45°</b>	<b>15°</b>	FEM	5.840285	6.429780	6.467096	6.521025	6.546342	6.4332
		EFGM (regular)	1.122156	5.474735	6.249868	6.382581	6.457338	
	<b>30°</b>	FEM	5.842700	5.836345	5.820975	5.837574	5.846956	5.7904
		EFGM (regular)	0.431166	5.159519	5.686199	5.774858	5.806842	
<b>0°/90°/0°</b>	<b>15°</b>	FEM	5.192128	6.358929	6.404640	6.426853	6.434468	6.4321
		EFGM (regular)	1.140922	5.944378	6.420126	6.439451	6.452504	
	<b>30°</b>	FEM	4.718031	5.426954	5.448885	5.476687	5.485953	5.4654
		EFGM (regular)	0.400004	4.951664	5.413463	5.487663	5.510602	

**Table 6.19.** Normalized central stresses  $\sigma_c * (h^2/qL^2)$  in the  $x$  direction for simply supported skew plate angle-ply and cross-ply orientations.

Fiber orientation	Skew Angle	Method	Number of nodes in the problem domain					Chakrabarti (2004)
			9	25	81	289	1089	
$+45^\circ/-45^\circ/+45^\circ$	$15^\circ$	FEM	0.111112	0.265031	0.270111	0.271836	0.273139	0.2693
		EFGM (regular)	0.026613	0.184604	0.245983	0.257516	0.261057	
	$30^\circ$	FEM	0.147447	0.253191	0.257896	0.264100	0.265602	0.2651
		EFGM (regular)	0.011362	0.179738	0.237999	0.251119	0.254626	
$0^\circ/90^\circ/0^\circ$	$15^\circ$	FEM	0.261322	0.641146	0.743913	0.767035	0.772915	0.7812
		EFGM (regular)	0.055785	0.488790	0.697461	0.751603	0.766647	
	$30^\circ$	FEM	0.238854	0.547272	0.633941	0.653867	0.659471	0.6634
		EFGM (regular)	0.019955	0.405482	0.588878	0.638208	0.652156	

## CHAPTER 7

### CONCLUSIONS

In the first part of the study, the effects of selectable parameters such as size of support domain, number of monomials, type of weight function, number of integration points in a background cell and value of penalty coefficient, on the accuracy of the EFGM solutions of the isotropic Reissner-Mindlin plate bending have been investigated. Four numerical examples as benchmark problems are solved using regular and irregular node distributions. According to obtained results, the regularity and irregularity do not so much effects in the solutions. The number of integration points in a background cell has some fluctuations for the value of 4 and 8 at the examined range. Also, the value of penalty coefficient does not exhibit any accuracy loss or fluctuation up to  $1 \times 10^9$ . Finally, the smaller support domain size gives more accurate results. These assessments are valid for both displacement and moment.

From the results of isotropic plate solutions, 3.0,  $5 \times 5$ ,  $1 \times 10^6$  for an isotropic plate bending problem can be suggested as size of support domain, number of gauss points in a background cell, and value of penalty coefficient, respectively. These values may not be the optimum values for every situation, however, in general, give the results with sufficient accuracy.

In the second part of the study, the EFGM reliability on the solution accuracy of bending analysis of laminated composite plates has been examined by comparing FEM solutions and exact solutions in the literature. Seven numerical examples have been performed to apply EFGM and FEM solutions. According to obtained results, the usage of small number of nodes in the solutions is not sufficient accuracy since laminated plates have a complex structure. 289 and 1089 number of nodes must be used to get acceptable results in general. However, the EFGM solutions obtained by using regular and irregular node distributions have close results to exact solutions and show higher convergency rate than FEM solutions in some numerical examples. Also, there is no significant difference between solutions of regular and irregular node

distributions. In conclusion, the EFGM is a reliable method in the bending analyses of laminated composite plates.

## REFERENCES

- [1] Lucy, L. B. (1977). A numerical approach to the testing of the fission hypothesis. *Astronomical Journal*, **82**(12), 1013–1024.
- [2] Gingold, R. A. and Monaghan, J. J. (1977). Smoothed particle hydrodynamics - Theory and application to non-spherical stars. *Monthly notices of the royal astronomical society*, **181**,375-389.
- [3] Breitkopf, P. et al. (2004). Integration constraint in diffuse element method. *Computer methods in applied mechanics and engineering*, **193**, 1203-1220.
- [4] Belytschko, T. et al. (1996). Meshless Methods An Overview and Recent Developments. *International Journal for Numerical Methods in Engineering*, **38**, 1655-1679.
- [5] Memar Ardestani, M. et al. (2014). Analysis of functionally graded stiffened plates based on FSDT utilizing reproducing kernel particle method. *Elsevier journal*, **112**, 231–240.
- [6] Liu, G.R. and Gu, Y.T. (2003). A matrix triangularization algorithm for the polynomial point interpolation method. *Computer methods in applied mechanics and engineering*, **192**, 2269–2295.
- [7] Atluri, S. N. and Zhu, T. (1998). A new meshless local petrov-galerkin (mlpg) approach in computational mechanics, *Computational Mechanics*. **22**, 117–127.
- [8] Shahrokhbabadi, Sh.et al. (2014). Hybrid of Natural Element Method (NEM) with Genetic Algorithm (GA) to find critical slip surface. *Alexandria Engineering Journal*, **53**, 373–383.
- [9] Yu, Y. et al. (2013). Multi-snap-through and dynamic fracture based on Finite Particle Method. *Journal of Constructional Steel Research*, **82**, 142–152.

- [10] William E. B. and Richard C. D. (2001). Elementary Differential Equations and Boundary Value Problems. *Library of Congress Cataloging in Publication Data*, 0-47.
- [11] Cummins, S. J., & Rudman, M. (1999). An SPH projection method. *Journal of computational physics*, **152(2)**, 584-607.
- [12] PEDLEY, T.J. (1977). Introduction to Fluid Dynamics. *Scientia marina*, **61**, (Supl. 1): 7-24.
- [13] Liu, M. B. et al. (2003). Smoothed particle hydrodynamics for numerical simulation of underwater explosion. *Springer-Verlag*, 106–118.
- [14] Li, SH. and Liu, W.K. (2002). Meshfree and particle methods and their applications. *American Society of Mechanical Engineers*, **55**, 10.1115
- [15] Sticks, S. (2013). Smooth Particle Hydrodynamics Applied to Fracture Mechanics. *Uppsala university*, 1401-5757.
- [16] Kanber, B. and Bozkurt, O. Y. (2008). A diagonal offset algorithm for the polynomial point interpolation method, *Numerical method in biomedical engineering*, **24(12)**, 1909-1922.
- [17] Liu R. and Gu. Y.T. (2003). A matrix triangularization algorithm for the polynomial point interpolation method. *Proceedings of the Asia-Pacific Vibration Conference*, **192(19)**, 2269–2295.
- [18] BOYD, J. P. (1985). Complex Coordinate Methods for Hydrodynamic instabilities and Sturm-Liouville Eigen problems with an Interior Singularity. *Journal of computational physics*, **57**, 454-471.
- [19] Liu, G.R. and GU, Y.T. (2005). An Introduction to Meshfree Methods and Their Programming. *Springer Dordrecht*, **10**, 1-4020-3228-5.
- [20] Liu, G.R. et al. (2008). Static and free vibration analysis of laminated composite plates using the conforming radial point interpolation method. *Journal of Elsevier*, **68(2)**, 354–366.

- [21] Sladek, V. et al. (2013). Physical decomposition of thin plate bending problems and their solution by mesh-free methods. *Slovakia engineering analysis with boundary elements*, **37(2)**, 348–365.
- [22] Lear, M.H. (2003). Numerical Simulation of Adiabatic Shear Bands and Crack Propagation in Thermoviscoplastic Materials. *Engineering Mechanics*.
- [23] Singh, S. et al. (2012). Buckling of laminated composite plates subjected to mechanical and thermal loads using meshless collocations. *Journal of mechanical science and technology*, **27**, 327-336.
- [24] Wang, J. G., Liu, G. R. (2000). Radial point interpolation method for elastoplastic problems. 1 st Structural Conference on Structural Stability and Dynamics. p. 703-708.
- [25] Zhu, P. and Liew, K.M. (2011). Free vibration analysis of moderately thick functionally graded plates by local Kriging meshless method, *Journal of Elsevier*, **93(13)**, 2925–2944.
- [26] Atluri, S. N. and Shen, SH. (2002). The Meshless Local Petrov-Galerkin (MLPG) Method: A Simple & Less-costly Alternative to the Finite Element and Boundary Element Methods. *Tech Science Press*. **3**, 1.11-51.
- [27] Li, Q., Soric, J., Jarak, T., & Atluri, S. N. (2005). A locking-free meshless local Petrov–Galerkin formulation for thick and thin plates. *Journal of Computational Physics*, **208(1)**, 116-133.
- [28] Shibahara, M., & Atluri, S. N. (2011). The meshless local Petrov-Galerkin method for the analysis of heat conduction due to a moving heat source, in welding. *International Journal of Thermal Sciences*, **50(6)**, 984-992.
- [29] Lin, H. and Atluri, S.N. (2001). The Meshless Local Petrov-Galerkin (MLPG) Method for Solving Incompressible Navier-Stokes Equations. *Tech Science Press*, **2(2)**, 117-142.
- [30] Batra, R.C. and Porfir, M. (2008). Analysis of rubber-like materials using meshless local Petrov–Galerkin (MLPG) method. *Wiley InterScience*, **24**, 1781-1804.



- [31] Batra, R.C. and Ching, H.K. (2002). Analysis of Elastodynamic Deformations near a Crack/Notch Tip by the Meshless Local Petrov-Galerkin (MLPG). *Tech Science Press*, **3(6)**, 717-730.
- [32] Yu, SH. T. et al. (2013). An element-free Galerkin (EFG) method for generalized Fisher equations (GFE). *China Phys*, **22(6)**, 060210
- [33] Byrd, R. H. et al. (2007). Steering Exact Penalty Methods for Nonlinear Programming. Optimization Technology Center Northwestern University.
- [34] Trench, W.F. (2013). The method of lagrange multipliers. Department of Mathematics Trinity University.
- [35] Fries, T.P. and Matthies, H.G. (2004). Stabilized and Coupled FEM/EFG Approximations for Fluid Problems. *Computational Mechanics*, **65**, D-38106.
- [36] Shyan, Ch. and Ping, W. (2000). New boundary condition treatments in meshfree computation of contact problems. *Computer methods in applied mechanics and engineering*, **187**, 441±468.
- [37] Beissel S, Belytschko T. (1996). Nodal integration of the element-free Galerkin method. *Computer Methods in Applied Mechanics and Engineering*. 139, 49–74.
- [38] Samimi, S. and Pak, A. (2012). Three-dimensional simulation of fully coupled hydro-mechanical behavior of saturated porous media using Element Free Galerkin (EFG) method. *Computers and Geotechnics*, **46**, 75–83.
- [39] Ansari, R., Ali, S. F., Soudbakhsh, A., Rahmdel, K., & Saberi, N. H. (2008). Applying Element-Free Galerkin Method on Beams.
- [40] Krysl, P., & Belytschko, T. (1996). Analysis of thin shells by the element-free Galerkin method. *International Journal of Solids and Structures*, **33(20)**, 3057-3080.
- [41] Liu, G. R. and Chen, X. L. (2001). A Mesh-free Method For Static And Free Vibration Analyses Of Thin Plates Of Complicated Shape. *Journal of Sound and vibration*, **241**, 839-855.

- [42] Kumar, S. K. (2013). Analysis of composite plates using element free galerkin method (Doctoral dissertation, National Institute of Technology, Rourkela).
- [43] Hayati, A. N., Ahmadi, M. M., & Sadrnejad, S. A. (2012). Analysis of Axisymmetric Problems by Element-Free Galerkin Method. *International Journal of Modeling and Optimization*, **2(6)**, 712.
- [44] Park, Y. and Leap, D. (2000). Modeling groundwater flow with a free and moving boundary using the element-free Galerkin (EFG) method. *Springer link journal*, **4(3)**, 243-249.
- [45] Zhang, L. et al. (2011). The coupling of element-free Galerkin method and molecular dynamics for the incompressible flow problems. *Springer link journal*, **10(4)**, 809-820.
- [46] Froehle, B. and Persson, P. (2014). A high order discontinuous Galerkin method for fluid–structure interaction with efficient implicit–explicit time stepping. *Journal of Computational Physics*, **272**, 455–470.
- [47] Jing, C., Kai-wei, Z., Tong-chun, L., & Wei, Z. (2013). Application of Element-Free Galerkin Method for Axis-Symmetric Heat Transfer Problems. *Digital Manufacturing and Automation (ICDMA), 2013 Fourth International Conference*, pp. 287-290.
- [48] Pham, X. T. (2012). Modeling of Moving Heat Sources Using Meshless Element Free Galerkin Method. In 9th International Conference on Trends in Welding Research.
- [49] Singh, I. V. (2006). Heat transfer analysis of composite slabs using meshless element free Galerkin method. *Computational Mechanics*, **38(6)**, 521-532.
- [50] Singh, I. V., Sandeep, K., & Prakash, R. (2002). The element free Galerkin method in three dimensional steady state heat conduction. *International Journal of Computational Engineering Science*, **3(3)**, 291-303.
- [51] Miyamoto, N. and Yamashita, H. (2002). Element-free Galerkin method for electromagnetic field computations, *Browse Journals & Magazines*. **34(5)**, 3236-3239.

- [52] Louaï, F.Z. and et al. (2007). Implementation of an efficient element-free Galerkin method for electromagnetic computation. *Engineering Analysis with Boundary Elements*, **31**, 191–199.
- [53] Cheng, R.J. and Liew, K.M. (2012). Analyzing modified equal width (MEW) wave equation using the improved element-free Galerkin method. *Engineering Analysis with Boundary Elements*, **36**, 1322–1330.
- [54] Louaï, F. et al. (2006). Numerical Analysis Of Electromagnetic Axisymmetric Problems Using Element Free Galerkin Method. *Journal of Electrical Engineering*, **57(2)**:9–104.
- [55] Rao, B.N. and Rahman, S. (2000). An efficient meshless method for fracture analysis of cracks. *Computational Mechanics*, **26**, 398–408.
- [56] Swaminathan, K. et al. (2014). Stress, vibration and buckling analyses of FGM plates - A state-of-the-art Review. *Composite Structures*, **120**, 10–31.
- [57] Tinh Quoc, B. et al. (2011). An efficient meshfree method for vibration analysis of laminated composite plates. *Computer Mechanic*, **48**:175–193.
- [58] Li, D.M. et al. (2014). An improved complex variable element-free Galerkin method for two-dimensional large deformation elastoplasticity problems. *Journal of Elsevier*, **269**, 72–86.
- [59] Goudarzi, M. and Mohammadi, S. (2014). Analysis of cohesive cracking in saturated porous media using an extrinsically enriched EFG method. *Computers and Geotechnics*, **63**, 183–198.
- [60] Liew, K.M. et al. (2011). A review of meshless methods for laminated and functionally graded plates and shells. *Composite Structures*, **93**, 2031–2041.
- [61] Bui, T.Q. et al. (2011). Buckling analysis of Reissner–Mindlin plates subjected to in-plane edge loads using a shear-locking-free and meshfree method. *Engineering Analysis with Boundary Elements*, **35**, 1038–1053.

- [62] Liew, K. M. et al. (2002). Analysis of laminated composite beams and plates with piezoelectric patches using the element-free Galerkin method. *Computational Mechanics(Springer)*, **29**, 486–497.
- [63] Kiasat, A. et al. (2006). Application Of High Order Basis Functions In Solid Mechanics By Element Free Galerkin (EFG) Method. *Computaitional methods*, 1453-1457.
- [64] Emre Erkmen, R. and Bradford, M. (2010). Elimination of slip-locking in composite beam-column analysis by using the element-free Galerkin method. *Computational Mechanics*, **46**,911–924.
- [65] Sheikh, A. H., Haldar, S., Sengupta, D., (2002). A high precision shear deformable element for the analysis of laminated composite plates of different shapes. *Composite Structures*, **55(3)**, 329-336.
- [66] Reis, A., Albuquerque, E. L., Torsani, F. L., Junior, L. P., Sollero P, (2010). Computation of moments and stresses in laminated composite plates by the boundary element method. *Engineering Analysis with Boundary Elements*, **35**, 105-113.
- [67] Numayr, K. S., Haddad, R. H., Haddad, M.A. (2004). Free vibration of composite plates using the finite difference method. *Thin-Walled Structures*, **42**, 399-414.
- [68] Belinha, J., Dinis L. M. J. S. (2006). Analysis of plates and laminates using the element-free Galerkin method. *Computers and Structures*, **84**, 1547-1559.
- [69] Arani, A.G., Maghamikia, Sh., Mohammadimehr, M., Arefmanesh, A. (2011). Buckling analysis of laminated composite rectangular plates reinforced by SWCNTs using analytical and finite element methods. *Journal of Mechanical Science and Technology*, **25(3)**, 809-820.
- [70] Aagaah, M. R., Mahinfalah, M., Jazar, G. N. (2006). Natural frequencies of laminated composite plates using third order shear deformation theory. *Composite Structures*, **72**, 273-279.

- [71] Ghorashi, S. Sh., Sabbagh-Yazdi, S. R., Mohammadi, S. (2010). Element free Galerkin method for crack analysis of orthotropic plates. *Computational Methods in Civil Engineering*, **1**, 1-13.
- [72] Ghorashi, S. S., Mohammadi, S., Sabbagh-Yazdi, S. R. (2011). Orthotropic enriched element free Galerkin method for fracture analysis of composites. *Engineering Fracture Mechanics*, **78**, 1906-1927.
- [73] Altenbach, H., & Eremeyev, V. A. (2011). Shell-like Structures: Non-classical Theories and Applications (Vol. 15), Springer Science & Business Media.
- [74] Owen D.R., and Hinton E. (1980). Finite Elements in Plasticity, Swensea, Pineridge Pres Limited.
- [75] Timoshenko, S., & Woinowsky-Krieger, S. (1959). Theory of plates and shells (Vol. 2, p. 120). New York: McGraw-hill.
- [76] Taylor, R. L., & Auricchio, F. (1993). Linked interpolation for Reissner-Mindlin plate elements: Part II-a simple triangle. *International Journal for Numerical Methods in Engineering*, **36(18)**, 3057-3066.
- [77] Morley L. S. D. (1963). Skew plates and structures, Pergamon Press, Oxford.
- [78] Whitney, J. M. (1970). The effect of boundary conditions on the response of laminated composites. *Journal of Composite Materials*, **4(2)**, 192-203.
- [79] Umasree, P., & Bhaskar, K. (2005). Accurate flexural analysis of clamped moderately thick cross-ply rectangular plates by superposition of exact untruncated infinite series solutions. *Journal of reinforced plastics and composites*, **24(16)**, 1723-1736.
- [80] Reddy, J. N. (1997). Mechanics of laminated composite plates: theory and analysis. CRC press.
- [81] Nguyen-Van, H., Mai-Duy, N., & Tran-Cong, T. (2007). A simple and accurate four-node quadrilateral element using stabilized nodal integration for laminated plates. *CMC: Computers, Materials and Continua*, **6(3)**, 159-176.

[82] Chakrabarti, A., Sengupta, S. K., & Sheikh, A. H. (2004). Analysis of skew composite plates using a new triangular element based on higher order shear deformation theory. *Journal of the Institution of Engineers. India. Civil Engineering Division*, **85**, 77-83.

[83] Bozkurt, Ö. Y., Özbek, Ö. (2014). Study of Selectable Parameters in Element-Free Galerkin Method for Bending Analysis of Mindlin-Reissner Plates. *3<sup>rd</sup> International Eurasian Conference on Mathematical Sciences and Applications*, 25-28 August 2014, **476**, Vienna, Austria.

[84] Özbek, Ö. Bozkurt, Ö. Y. (2015). Analysis of laminated composite plates by using element-free Galerkin method. *1<sup>st</sup> International Conference on Engineering and Naturel Sciences*, 15-19 May 2015, **150**, Skopje, Macedonia.

## PUBLICATIONS

[1] Bozkurt, Ö. Y., Özbek, Ö. (2014). Study of Selectable Parameters in Element-Free Galerkin Method for Bending Analysis of Mindlin-Reissner Plates. *3<sup>rd</sup> International Eurasian Conference on Mathematical Sciences and Applications*, 25-28 August 2014, **476**, Vienna, Austria.

[2] Bozkurt, Ö. Y., Barbar M. O. E., Özbek, Ö. (2014). Investigation of Effects of Parameters in Element-Free Galerkin Method for Bending analysis of Mindlin-Reissner Plates. *1<sup>st</sup> International Conference on Computational and Experimental Science and Engineering*, 25-29 October 2014, **316**, Antalya, Turkey.

[3] Özbek, Ö., Bozkurt, Ö. Y. (2015). Analysis of laminated composite plates by using element-free Galerkin method. *1<sup>st</sup> International Conference on Engineering and Naturel Sciences*, 15-19 May 2015, **150**, Skopje, Macedonia.